Biophysical Chemistry of Lipopolysaccharide Specific Bacteriophages

Kumulative Dissertation

zur Erlangung des akademischen Grades

"doctor rerum naturalium" (Dr. rer. nat.)

in der Wissenschaftsdisziplin "Biochemie"

eingereicht an der

Mathematisch-Naturwissenschaftlichen Fakultät der Universität Potsdam

Institut für Biochemie und Biologie

Physikalische Biochemie

von

Dipl. Biochem. Dorothee Andres

Potsdam, den 15.11.2011

Published online at the
Institutional Repository of the University of Potsdam:
URL http://opus.kobv.de/ubp/volltexte/2012/5926/
URN urn:nbn:de:kobv:517-opus-59261
http://nbn-resolving.de/urn:nbn:de:kobv:517-opus-59261

1 Index

2 Figure and table legend

3 Abbreviations

9NA	*Sipho*virus 9NA
Å	Ångström
Abe	Abequose
Amp	Ampicillin
cm	Chloramphenicol
CMC	Critical micellar concentration
DNase	Deoxyribonuklease I
DNSA	3,5 dinitrosalicylic acid
E_A	Arrhenius barrier
E. coli	*Escherichia coli*
EDTA	Ethylendiamintetraacetate
endoNF	Tailspikes of capsule recognizing podovirus K1F
Gal	α-D-Galactose
Glc	D-Glucose
gp	gene product
ΔH	Enthalpy change
HK620	Podovirus HK620
HK620TSP	Bacteriophage HK620 Tailspike Protein
InvA	Invasion protein A
IPTG	Isopropyl-β-D-thiogalactopyranosid
ITC	Isothermal titration calorimetry
k	Velocity coefficient
K_A	Association constant
K_D	Dissociation constant
kD	Kilo-dalton
KDO	2-keto-3-deoxy-octonate
LB-Media	Luria-Bertani Media
LPS	Lipopolysaccharide
MALDI-MS	Matrix Assisted Laser Desorption Ionization Mass Spectrometry
Man	α-D-Mannose
M.O.I	Multiplicity of infection
P22	Podovirus P22

P22TSP	P22 Tailspike Protein, indexed with point mutation
P22TSPΔN	P22 Tailspike protein without N terminal head binding domain, indexed with point mutation
P22*t*	reconstituted phage P22 head with TSP, indexed with TSP point mutation
PAGE	Polyacrylamide gel elektrophoresis
Par	Paratose
PCR	Polymerase chain reaction
PFU	Plaque forming units
Rha	α-L-Rhamnose
RI	Refractive index
RT	Room temperature
RU	Repeating unit
ΔS	Entropy change
S. enterica	*Salmonella enterica*
S. Paratyphi A	*S*. Paratyphi
SDS	Sodiumdodecylsulfate
Sf6	Podovirus Sf6
SPR	Surface plasmon resonance
TEM	Transmission electron microscopy
Tris	Trishydroxyaminomethylmethane
TSP	Tailspike Protein
Tyv	Tyvelose
wt	Wildtype

Amino acids are abbreviated in single or three letter code.

The *Salmonella* nomenclature according to Le Minor and Popoff is used throughout.

4 Abstract

Carbohydrate recognition is a ubiquitous principle underlying many fundamental biological processes like fertilization, embryogenesis and viral infections. But how carbohydrate specificity and affinity induce a molecular event is not well understood. One of these examples is bacteriophage P22 that binds and infects three distinct *Salmonella enterica* (*S*.) hosts. It recognizes and depolymerizes repetitive carbohydrate structures of O antigen in its host´s outer membrane lipopolysaccharide molecule. This is mediated by tailspikes, mainly β-helical appendages on phage P22 short non-contractile tail apparatus (podovirus).

The O antigen of all three *Salmonella enterica* hosts is built from tetrasaccharide repeating units consisting of an identical main chain with a distinguished 3,6-dideoxyhexose substituent that is crucial for P22 tailspike recognition: tyvelose in *S*. Enteritidis, abequose in *S*. Typhimurium and paratose in *S*. Paratyphi. In the first study the complexes of P22 tailspike with its host's O antigen octasaccharide were characterized. *S*. Paratyphi octasaccharide binds less tightly ($\Delta\Delta G \approx 7$ kJ/mol) to the tailspike than the other two hosts. Crystal structure analysis of P22 tailspike co-crystallized with *S*. Paratyphi octasaccharides revealed different interactions than those observed before in tailspike complexes with *S*. Enteritidis and *S*. Typhimurium octasaccharides. These different interactions occur due to a structural rearrangement in the *S*. Paratyphi octasaccharide. It results in an unfavorable glycosidic bond Φ/Ψ angle combination that also had occurred when the *S*. Paratyphi octasaccharide conformation was analyzed in an aprotic environment. Contributions of individual protein surface contacts to binding affinity were analyzed showing that conserved structural waters mediate specific recognition of all three different *Salmonella* host O antigens. Although different O antigen structures possess distinct binding behavior on the tailspike surface, all are recognized and infected by phage P22. Hence, in a second study, binding measurements revealed that multivalent O antigen was able to bind with high avidity to P22 tailspike. Dissociation rates of the polymer were three times slower than for an octasaccharide fragment pointing towards high affinity for O antigen polysaccharide. Furthermore, when phage P22 was incubated with lipopolysaccharide aggregates before plating on *S.* Typhimurium cells, P22 infectivity became significantly reduced.

Therefore, in a third study, the function of carbohydrate recognition on the infection process was characterized. It was shown that large *S*. Typhimurium lipopolysaccharide aggregates triggered DNA release from the phage capsid *in vitro.* This provides evidence that phage P22 does not use a second receptor on the *Salmonella* surface for infection. P22 tailspike binding and cleavage activity modulate DNA egress from the phage capsid. DNA release occurred more slowly when the phage possessed mutant tailspikes with less hydrolytic activity and was not induced if

lipopolysaccharides contained tailspike shortened O antigen polymer. Furthermore, the onset of DNA release was delayed by tailspikes with reduced binding affinity. The results suggest a model for P22 infection induced by carbohydrate recognition: tailspikes position the phage on *Salmonella enterica* and their hydrolytic activity forces a central structural protein of the phage assembly, the plug protein, onto the host´s membrane surface. Upon membrane contact, a conformational change has to occur in the assembly to eject DNA and pilot proteins from the phage to establish infection.

Earlier studies had investigated DNA ejection *in vitro* solely for viruses with long non-contractile tails (siphovirus) recognizing protein receptors. Podovirus P22 in this work was therefore the first example for a short tailed phage with an LPS recognition organelle that can trigger DNA ejection *in vitro.* However, O antigen binding and cleaving tailspikes are widely distributed in the phage biosphere, for example in siphovirus 9NA. Crystal structure analysis of 9NA tailspike revealed a complete similar fold to P22 tailspike although they only share 36 % sequence identity. Moreover, 9NA tailspike possesses similar enzyme activity towards *S*. Typhimurium O antigen within conserved amino acids. These are responsible for a DNA ejection process from siphovirus 9NA triggered by lipopolysaccharide aggregates. 9NA expelled its DNA 30 times faster than podovirus P22 although the associated conformational change is controlled with a similar high activation barrier. The difference in DNA ejection velocity mirrors different tail morphologies and their efficiency to translate a carbohydrate recognition signal into action.

5 Introduction

5.1 Bacteriophages and their receptors

In 1989 a Norwegian group reported the high abundance of bacterial viruses, bacteriophages, to be about 2.5 x 10^8 virus particles per milliliter in aquatic environment illustrating the high concentration of phages in the biosphere [1]. Bacteriophages can be classified in a system based on their overall morphology [2]. The majority of known phages possess tail structures attached to protein capsids that contain the phage´s dsDNA. They constitute the order of caudovirales. According to their different tail morphologies they are classified into three bacteriophage families: Siphoviruses with long non-contractile tails, podoviruses with short non-contractile tails and myoviruses with long contractile tails. Bacteriophages can also be classified by genetic and structural homologies which suggest a common ancestry for all dsDNA bacteriophages [3, 4]. Moreover, crystal structures of capsids from human herpes simplex virus I and tailed phages revealed conservation of a protein fold between both, a eukaryotic and a bacterial virus [5]. It can therefore be speculated whether all dsDNA viruses share a common ancestor that diverged upon host evolution.

In absolute terms, bacteriophages would be able to interact with 1/3 of the total microbial population on earth per day leading to infection and subsequent death of the bacterial host. Therefore, phages control the microbial ecosystems and are intimately related to the spread of genetic material. Moreover they have a potential to be used in antibiotic therapy [6, 7]. All these processes rely on the infection of the bacterial host. Like any viral infection, dsDNA bacteriophage infection starts with the recognition of a specific host receptor. This is followed by irreversible attachment to the host surface and DNA release from the virus. Finally, the viral DNA has to be transported into the host cell cytoplasm.

As diverse the bacteriophage community is, as diverse are the receptors recognized on the bacterial surface [8]. The bacterial surface is a mosaic of receptors for different phages. The presence of a capsule can serve as a protective barrier against phage invasion, but, on the other hand the capsule itself can be the site for phage attachment, for example in phage K1-5 [9]. Bacteriophages can attach to pili and flagella of Gram positive and Gram negative bacteria, like *Escherichia coli* (*E. coli*) phage Chi or *Bacillus subtilis* phage PBS1 [10, 11]. Many phages utilize protein receptors that are accessible on the surface and might help to transport viral DNA into the host cell like siphovirus T5 [12]. Gram positive bacteria like *Staphylococcus aureus* or *Bacillus subtilis* are surrounded by a peptidoglycan layer employed by phages as contact site [8]. By contrast, in Gram negative bacteria the outer membrane lipopolysaccharides (LPS) can serve as

phage receptor. LPS contains a variety of different saccharide structures that vary between species.

5.2 Lipopolysaccharides

The distinct feature of Gram negative cells is their double membrane separated by a peptidoglycan layer in the periplasm (Figure 5.2.1 A) [13]. The inner membrane is built from a phospholipid bilayer, but the outermost membrane is distributed asymmetrically: The outer membrane inner leaflet is composed of phospholipids but the outer leaflet, facing the environment, consists of lipopolysaccharides (LPS). This asymmetry is maintained throughout the life cycle of bacterial cells.

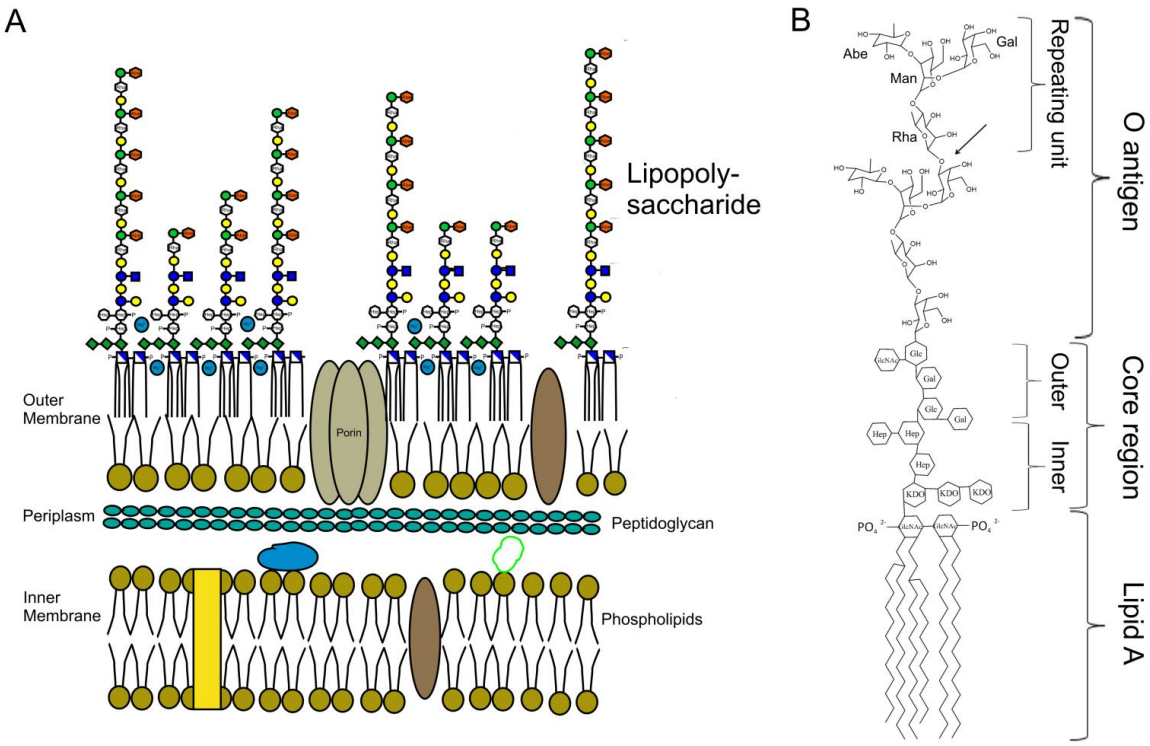

Figure 5.2.1: Lipopolysaccharides in the outer membrane of Gram negative bacteria
A: Outer membrane of Gram negative bacteria
The outer and inner membrane are separated by a peptidoglycan layer in the periplasm. The outer membrane has an asymmetric composition: the inner leaflet mainly of phospholipids, the outer of lipopolysaccharides. Lipopolysaccharides are able to interact with their negative charges via divalent ions. Saccharides in the O antigen structure are colored according to [14], an orange symbol was added for abequose.
B: *Salmonella* Typhimurium lipopolysaccharide molecule
Lipopolysaccharide consists of three distinct parts: Lipid A (schematic) which anchors the molecule in the membrane, the core region (schematic) of different saccharides links to O antigen polymer that is built from repeating units. The arrow indicates the cleavage site for P22 and 9NA tailspike.

5.2.1 Lipopolysaccharide structure and function

The major function of LPS in Gram negative bacteria is to maintain a very efficient protective membrane barrier. It is able to repel host defense factors and even antibiotics when they are either too large or too hydrophobic to pass aqueous porins [15]. LPS molecules possess three distinct domains that mediate the properties of the molecule and the membrane (Figure 5.2.1 B) [16]. The innermost moiety is lipid A which anchors the molecule in the membrane and is highly conserved within *Enterobacteriae* [17]. It is built from a β(1->6)-linked disaccharide of N-acetyl-D-glucosamine that is acylated with six or seven fatty acid chains [18]. The disaccharide is phosphorylated and negatively charged. These charges are compensated in the membrane by bivalent cations like Mg^{2+} that mediate strong intermolecular lipopolysaccharide interactions (Figure 5.2.1 A). This results in tight packaging in the outer membrane [19]. Growth conditions and stressors provoke different modifications in the lipid A region [20]. Lipid A and extracellular parts of LPS are separated by the core region. It is built from different and sometimes rare sugars often modified with phosphate or sulfate groups [21]. Particularly, the core region contains a characteristic molecule, 2-keto-3-deoxy-octonat (KDO) [22]. KDOs are characteristically found in LPS and indicative for its presence. Furthermore, this sugar activates the complement system during human infection resulting in septic shock [23]. Vital cells carry at least two KDO sugars attached to lipid A (Figure 5.2.1 B) and several core truncation mutants have been described which differ in their carbohydrate chain length [16, 17].

The core region composition differs between bacteria but is conserved within a genus, i.e. *Salmonella*. The core region links with a hexose-rich region to the outermost and third domain of the LPS molecule, the polysaccharide O antigen [16]. It is synthesized from building blocks of oligomeric saccharides, the repeating units (RU), reaching up to more than 70 in *S*. Typhimurium [24]. On the one hand, this hydrophilic carbohydrate structure is important for colonization and protects from the host´s complement system [25]. Especially the length of the carbohydrate polymer defines its protective function: Short and even no O antigen chains result in more susceptible bacterial cells [26]. On the other hand, it is specifically recognized by antibodies designating the polysaccharide moiety of LPS as O antigen [27]. O antigen differs between all bacterial species. If present it is one trait to determine different serotypes [28]. Nevertheless, the O antigen is very heterogeneous even in a single bacterial culture [29]. Intrastrain heterogeneity with non-stochiometric glycosylation, acetylation, phosphorylation and even changes in the sugar linkages occur. These modifications result from the need to adapt to different challenges in colonization, to evade host responses and to communicate within the environment.

5.2.2 Biophysical properties of lipopolysaccharides

Lipopolysaccharides are amphiphilic molecules and form complex aggregates in solution. Atomic force microscopy showed that LPS is still aggregated at concentrations of 10 pg/ml [30]. Therefore a critical micellar concentration (CMC) can only be estimated due to the resolution limits of the detection method [31, 32]. The gel to liquid crystalline (β → α) phase transition temperature for *S*. Typhimurium lipopolysaccharides depends on O antigen chain length and Mg^{2+} content [33]. Lipopolysaccharides with long hydrophilic O antigen chains have lower melting temperatures than those without but bivalent cations increase transition temperatures for all of them. The overall shape of LPS aggregates differs and influences their endotoxic activity (conformational concept) [34]. Aggregates can be lamellar, cubic or hexagonal depending on the lipid A origin, the ion and water content in the preparation as well as temperature [35]. Lamellar aggregates are likely to occur in preparation substituted with Mg^{2+} so that acyl chains are more tightly packed [19]. But the ultrastructural organization of LPS depends on many variables which are still not well understood [36]. Cryo transmission electron microscopy (cryo-TEM) of LPS carrying long O antigen chains showed vesicles up to 100 nm in diameter and planar bilayer fragments [36]. In the same study it was shown that these measured dimensions are not consistent with another applied method. Therefore, various observations in earlier studies dealing with LPS aggregation behavior have to be read carefully [37, 38]. It can be stated that the O antigen size, bivalent cation and water content, LPS composition and temperature influence characteristics of every individual LPS preparation.

5.2.3 Lysogenic conversion

Bacteriophages binding to and cleaving O antigen will not infect their hosts, if they are unable to specifically recognize the carbohydrate structures. Therefore, many of them initiate post synthetic O antigen modifications like acetylations or glucosylations when they are in the lysogenic state of their life cycle [29]. These lysogenic conversions prevent repetitive infections with the same bacteriophage. In bacteriophage P22 lysogenic conversion causes the α-1,6 glucosylation at Gal in the O antigen repeating unit [39]. Other phages, like epsilon 15, also modify specific linkages producing new types of RUs [40]. These add to the huge diversity of O antigen structures found in LPS [41].

5.3 Bacteriophage P22

Podovirus P22 was first described by Zinder and Lederberg in 1952 and belongs to the lambdoid phages [42]. It is the representative species in the P22-like phage genus. Phage P22 became a model system to study molecular biology, *Salmonella* genetics, virus morphogenesis and

evolution [43]. Furthermore, phage P22 has been characterized in many crystal and cryo EM structures as well as in functional analyses. Taken together this makes P22 an exceptionally versatile tool to understand molecular processes in more detail.

Phage P22 is a temperate phage which results in two developmental pathways during infection. In its lytic life cycle P22 particles are produced and released from its *Salmonella* host. By contrast, to enter the lysogenic cycle, its genetic material is inserted into the host's genome to be replicated during cell division. Upon induction with chemical or even mechanical stressors of the lysogenic prophage, the lytic life cycle is restored and phage particles are released from the cell [44].

5.3.1 Bacteriophage P22 assembly

The structure and assembly of phage P22 are well studied. The bacteriophage icosahedral shell is built from 415 copies of gene product (gp) 5 that form 60 hexamers and 11 pentamers leading to a 700 Å wide icosahedral capsid assembly [45-47]. The capsid protein gp5 has a conserved core structure, first found in phage HK97 and later in many *Caudoviridae* or *Herpesviridae*, although this structural homology does not imply a conserved assembly mechanism between them all [48]. In phage P22 initial assembly is guided by many scaffolding proteins that become released, when DNA is packaged (Figure 5.3.1) [49].

At one pentameric vertex of the capsid the dodecameric portal protein is deeply inserted constituting a site of entry and exit from the capsid shell [45, 50].

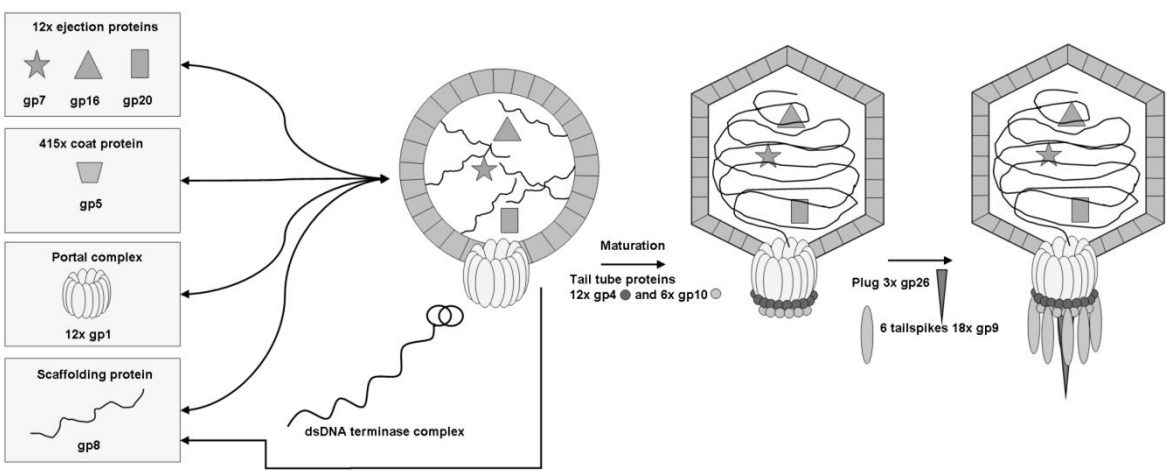

Figure 5.3.1: Schematic presentation of P22 morphogenesis pathway.
Details are described in the text. Assembly starts from six different proteins to form a prohead. After dsDNA was packaged into the capsid, tail tube proteins and plug seal the mature capsid. Six trimeric tailspikes are attached between gp4 and gp10. Figure is based on [47] and [43].

In contrast to other reported portal proteins, P22 portal has a 200 Å long α helical tube reaching into the interior of P22 capsid (Figure 5.3.2 A) [50]. Twelve copies of gp7, gp16 and gp20

contained in the phage particle are ejected from the phage upon infection. The terminase assembly (gp2 and 3) fills the procapsid with 42 kbp of viral dsDNA initiated at a specific DNA sequence, the pac site [51, 52]. ATP hydrolysis by gp2 pumps dsDNA inside the head against an increasing pressure until a head-full signal in portal and terminase proteins assign the packaging machinery to dissociate [53, 54]. In contrast to specific recognition of the pac site in concatemeric P22 DNA, the cleavage of DNA after packaging is unspecific and the fully assembled particle contains 103.8 % of terminally redundant P22 DNA [55]. During DNA packaging the procapsid expands about 15 % to constitute the mature capsid with 700 Angström (Å) diameter [56]. Finally, the tightly dsDNA packaged assembly is closed by the tail proteins (Figure 5.3.1).

5.3.2 P22 tail structure

The protruding tail complex of phage P22 on one capsid vertex is about 400 Å long and interacts with the *Salmonella* host [57]. Its exposed location supports efficient host recognition and DNA delivery. The tail tube is assembled stepwise on the portal protein in the capsid, initiated by association of twelve gp4 copies and sequentially a hexameric gp10 (Figure 5.3.1 and Figure 5.3.2 B) [58]. The resulting tube channel is wide enough to passage DNA from the capsid interior and the elongated portal structure might support efficient delivery of DNA (Figure 5.3.2 A) [50]. The portal structure containing gp4 and gp10 is able to retain packaged DNA inside the capsid, but for further crucial stabilization it is mechanically closed by one trimeric gp26, the tail plug (Figure 5.3.1 and Figure 5.3.2 C) [59]. It binds with its N terminus to gp10 to avoid uncontrolled DNA release (Figure 5.3.2 D) [60, 61]. The plug protein is protruding from the whole phage assembly and allows interaction with the membrane upon infection [59]. The plug protein gp26 is a homotrimeric 240 Å long and 20 to 35 Å wide fiber build from four distinct domains (Figure 5.3.2 C) [62]: The N terminal domains I and II form a long trimeric coiled coil but with a distinct tighter helical wind than other similar folds. At the C terminal tip of the protein, the coiled coil structure is stabilized with a triple β helix in domain III. The final amino acids in domain IV are folded into an inverted trimeric coiled coil that carries a patch of basic amino acids. In contrast to the coiled-coil structure in domains I and II, domain III and IV are highly flexible around a Gln in the hinge region suggesting a possibility for a conformational change in this region [63].

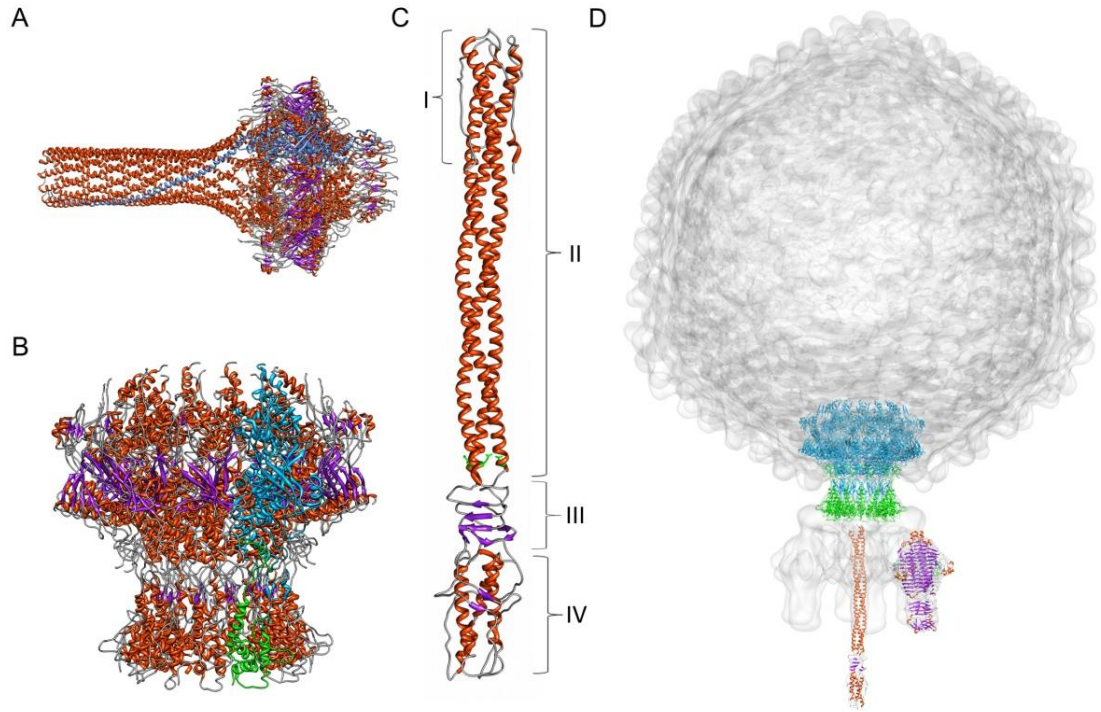

Figure 5.3.2: Phage structural proteins
A: Side view of dodecameric portal protein gp 1. The α-helical tube is inside P22 capsid and large enough to accommodate DNA. One subunit of the dodecameric assembly is colored blue. (PDB 3LJ5, [50])
B: Side view of dodecameric portal protein gp1 core (without α-helical tube domain) (one subunit colored blue) assembled to hexameric tail tube protein gp4 (one subunit green) (PDB 3LJ4, [50])
C: Trimeric plug protein gp26. The N Terminus consists of domain I, the others as indicated in the text. (PDB 2POH, [62])
D: Cryo EM structure of podovirus P22 (EMDB 1222, [45]) with density fitted portal protein gp1 core (cyan) (PDB 3LJ4), tail tube protein gp4 (green) (PDB 3LJ4), plug protein gp26 (mainly orange) (PDB 2POH) and tailspike protein gp9 (mainly violet) (see Figure 5.5.1) (PDB 1TSP, [64]).
All figures were generated with Chimera [65].

On the tail tube surface made up by gp4 and gp10, six trimeric tailspike proteins bind with their N terminal domains (Figure 5.3.1 and Figure 5.3.2 D) [57]. These head binding domains are connected via a flexible linker to the right-handed β-helical major part of the tailspikes, which are kinked about 20° with respect to the N terminus (Figure 5.5.1) [57, 64, 66]. Here, in the middle of the protein, the only known enzymatic function in the mature assembly is located: Tailspikes are able to bind and cleave the outer membrane O antigen carbohydrate of the *Salmonella* host [67-69]. In the assembly, tailspikes are bound strongly to the phage preventing lateral movements once attached to the phage [57].

Many structural and functional parts of phage P22 are found in different bacteriophages emphasizing their modularity in morphogenesis and their widespread, general function in biology [70].

5.3.3 Infection mechanism of phage P22

Phage P22 infects *S*. Typhimurium, *S*. Enteritidis, *S*. Typhi and *S*. Paratyphi [71]. During infection, phage P22 binds to its *Salmonella* host outer membrane as shown in electron microscopy [72]. Tailspikes mediate recognition of the outer membrane only if long O antigen chains are present. But irreversibility of this step is only achieved in the whole phage and not with purified tailspikes [73, 74]. For successful P22 infection at least three tailspikes are obligatory that could orient the phage towards the outer bacterial membrane [75]. Assembled to the phage tailspikes showed less enzymatic activity than purified [76]. Therefore, it was concluded that a second receptor had to be bound at the outer membrane to initiate the irreversible binding step [77]. For a successful infection DNA has to be transported over two *Salmonella* membranes. To transfer DNA to the bacterial cytoplasm ejection proteins gp7, 16 and 20 are essential [78]. Their likely function is to build up an extensible tail as proposed in podovirus T7 and observed in podovirus ε15 [79, 81].

5.4 Bacteriophage 9NA

Siphovirus 9NA is one of the virulent phages reported for *S.* Typhimurium and was first described by Wilkinson et al in 1972 [82]. It has a symmetrical head of about 600 Å width and a 1500 Å long thin non-contractile tail with a 300 Å wide baseplate as deduced from EM microscopy [83]. For successful infection, the bacterium has to express long O antigen chains, but additionally infection is dependent on membrane fatty acids [84]. The dsDNA of 9NA is about 56 kbp long and circularly permuted [85]. As P22, 9NA dsDNA is packaged into its capsid from concatemeric DNA initiated at a pack site [86]. Nevertheless, 9NA dsDNA does not hybridize with P22 dsDNA indicating little homology between those two phages and to siphovirus λ [85].

Bacteriophage 9NA possesses endorhamnosidase activity very similar to phage P22 : it cleaves the O antigen main chain of *S*. Typhimurium, *S*. Enteritidis and to lesser extent of *S*. Paratyphi resulting in the same final cleavage products [83].

5.5 Tailspikes as carbohydrate binding model system

Polysaccharides on the bacterial surface act as a physical barrier during infection but many bacteriophages use them as receptors and depolymerize these carbohydrate structures on their various bacterial hosts [87]. This activity is connected to their proteins visible in electron microscopy as spikes, protruding from the tail structure of the phage. Tailspike structures with hydrolytic activity towards O antigen have been described mainly for podoviruses like P22, Sf6, HK620, 28B, 36 and Epsilon 15 [71, 88-91].

5.5.1 P22 tailspike

P22 tailspike is a well established model system for protein folding as well as carbohydrate binding studies [92, 93]. Given its exposed position in the phage assembly the protein has to resist harsh extracellular conditions. Accordingly, it is an SDS resistant and highly thermostable trimeric protein [94]. It possesses two domains that are connected with a flexible linker (Figure 5.5.1). The 143 amino acids in the N-terminal domain fold into two β-sheets of antiparallel strands forming a dome like structure in the trimer [95]. This N terminus mediates binding to phage capsid between gp4 and gp10 as shown in (Figure 5.3.2 D) [59, 96]. The central part of the tailspike protein folds into a parallel, right-handed β-helix with thirteen coils. In the mature trimer, the subunits are interdigitated in the central part to form a triple- β-prism (Figure 5.5.1) [64].

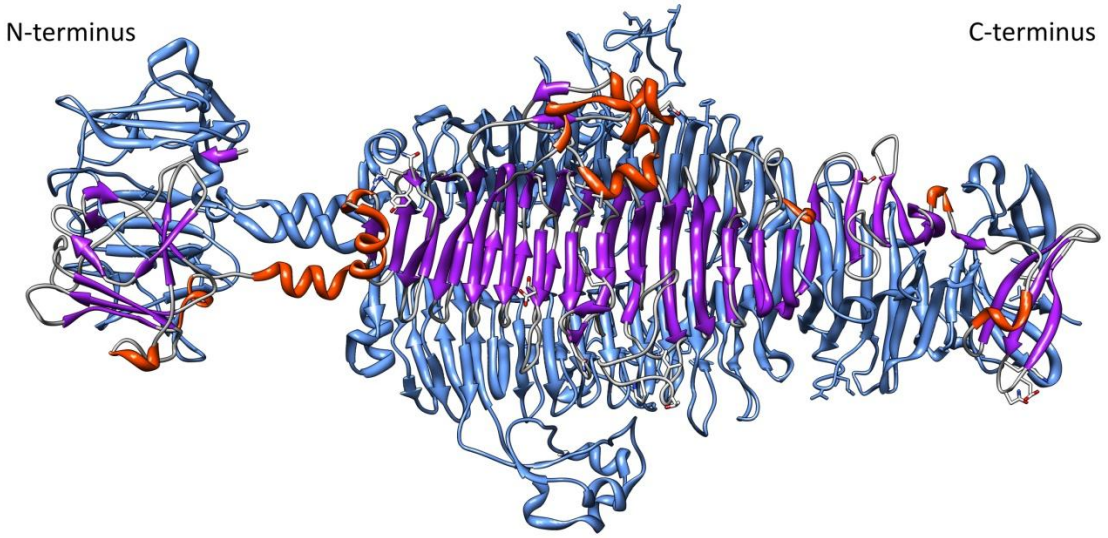

Figure 5.5.1: Structure of full length P22 tailspike
Side view of trimeric full length P22 tailspike carrying an Y108W mutation in the flexible linker (PDB 2XC1) [66]. One subunit is colored according to its secondary structure. The N-terminal dome like structure is formed by β-sheets of antiparallel strands and binds to the phage capsid. The major C-terminal domain contains a parallel β-helix and mediates host recognition.
Figure was generated with Chimera [65].

P22 tailspike is able to depolymerize the O antigen polysaccharide of all four hosts into octasaccharides [69, 71]. All hosts have an identical O antigen main chain α-D-mannose-(1→4)-α-L-rhamnose-(1→3)-α-D-galactose-(1→2) but differ in a 3,6-dideoxyhexose substitution at C-3 of mannose (Figure 7.4.1 A). It is remarkable that this specific side chain is essential for their interaction with the tailspike: tyvelose in *S*. Enteritidis and *S*. Typhi, abequose in *S*. Typhimurium, paratose in *S*. Paratyphi [68]. *S.* Typhi carries an additional glucose at C-4 of galactose [97]. In a co-crystallized P22 tailspike structure binding of the O antigen octasaccharide occurs in the

middle of the β-helix between turns 5,7 and 8 on the solvent accessible side in the three investigated hosts (Figure 7.5.1) [98]**.** Repeating unit (RU) 1 binds with the terminal rhamnose to the active site that consists of Asp392, Asp395 and Glu359 [68]. The binding of the extended host range of phage P22 is enabled by different interactions on P22 tailspike in a 3,6-dideoxyhexose binding pocket. Here, water molecules and two acidic amino acids mediate the single contact of 3,6 dideoxyhexose sugar in RU2 to the protein. The thermodynamics of this interaction will be introduced in chapter 7.

5.5.2 Other Tailspikes

Increasing knowledge of other phage gene sequences led to the discovery of other homologous tailspike structures in podovirus Sf6 and HK620 [70, 88, 89]. Both proteins are highly stable and fold into a central β-helix.

Surprisingly, a tailspike with 50 % sequence identity to P22 tailspike was found in myovirus Det7 that infects *S.* Typhimurium [99]. Without the N-terminal phage capsid binding domain, that attaches the tailspike to the baseplate of the myovirus, the central C-terminal 75 kDa protein folds into a very stable β-helical structure. Aligned residues between P22 tailspike and Det7 tailspike can be superimposed with a root mean square difference between the C-alphas of about 0.8 Å. Consequently, Det7 tailspike cleaves and binds the O antigen of its host.

In P22 tailspike, Det7 tailspike, HK620 tailspike and Sf6 tailspike water is expelled upon ligand interaction enabling direct and water-mediated hydrogen bonds. Only few aromatic side chains are present in these binding sites. These contacts are used to orient their carbohydrate ligand in their active site for glycosidic cleavage.

5.6 DNA release from bacteriophages

Commonly, phages bind irreversibly to their host cell with structures in the tail appendixes as the first step during infection [100-104]. Subsequently the phage has to start the DNA release process, most likely with a conformational change in the tail and portal components to open the closed phage capsid, thereby reversing the phage assembly step [105]. This process has been investigated *in vitro* and *in vivo*.

In vitro studies analyzing the DNA egress from the phage capsid have largely been undertaken for siphoviruses interacting with protein receptors [106-109]. The densely packaged, negatively charged DNA is confined inside the rather small protein capsid which produces a highly pressurized DNA assembly [110]. The extreme pressures inside the capsid were shown experimentally for siphovirus λ. Upon contact with its receptor LamB opposed with an external osmotic pressure of 20 atm, DNA release from the phages head was stopped [111]. This showed

that large pressures must also drive the DNA release *in vitro*. Experimental conditions especially Mg^{2+} ions influence these processes [112].

In vitro single phage analysis using phage T5 showed that DNA is ejected upon contact with its receptor *E. coli* FhuA at 75 kbp/s in a stepwise manner [113]. During ejection the DNA has to reorganize and undergoes multiple phase transitions in T5 [114]. It was speculated that these cause the stepwise DNA release [108]. In contrast, phage λ releases its DNA at 60 kbp/s after a short waiting time without any interruptions as analyzed in single particle measurements [115]. Contrary, bulk measurements *in vitro* help to understand the processes leading to the DNA egress from phage particles. These molecular machines evolved to fully shield their DNA from the surroundings but deliver their genetic material upon a specific host contact. This mechanism includes tightly controlled rearrangements to structurally open the phage. This is the rate determining step when observing bulk kinetics. Arrhenius activation enthalpies of phages SPP1, λ and T5 showed similar activation barriers of about 25-46 kcal/mol for this step [106, 109].

From *in vitro* experiments was concluded that DNA pressure in the phages capsid is not enough to transport DNA into the bacterial cytoplasm, that opposes a high osmotic pressure [116]. About 17% of the SPP1 DNA could be injected into the bacterial cell, insufficient for a successful infection [117]. It was proposed that during infection the resulting osmotic gradient over the phage into cytoplasm results in a water influx that drags the DNA inside the bacterial host [118]. Also enzymes acting in the cytoplasm could support DNA internalization by DNA binding or transcription [119, 120]. Possibly, a combined mechanism of both can be taken into account, where pressure drives the initial steps for DNA injection but enzymes in the cytoplasm exert a force on the phage DNA and pull it into the host cell against the osmotic pressure inside the cell [121].

6 Objective

Bacteriophage P22 is established as a model system for many biological problems. Although a great deal of structural and functional information is available, it remains unclear how P22 initiates infection of *Salmonella enterica*. P22 recognizes the O antigens of at least three different hosts with its tailspike proteins. This interaction has been investigated in molecular detail with *S*. Typhimurium and *S*. Enteritidis O antigen fragments. To complete the analysis, interactions between P22 tailspike and *S*. Paratyphi O antigen were to be characterized. The P22 infection mechanism is intimately connected to tailspike O antigen recognition. The characterization of tailspikes binding multivalently to lipopolysaccharide (LPS) receptors was expected to provide more biophysical details about the initiation of P22 infection. DNA ejection from bacteriophages has been shown for siphoviruses with protein receptors but neither for podoviruses nor for O antigen recognizing phages. A more holistic approach of studying the lipopolysaccharide receptor in context of the complete phage was to lead to understand of how carbohydrate binding at the molecular level is connected to a finely orchestrated infection process in the large assembly.

7 Recognition of *Salmonella* O antigens in P22 tailspike protein

Chapter 7 is a manuscript to be submitted in a modified version for publication as

Conserved structural waters mediate recognition of *Salmonella* O antigens in phage P22 tailspike protein

Dorothee Andres, Ulrich Gohlke, Nina Kristin Broeker, Wolfgang Rabsch, Udo Heinemann, Stefanie Barbirz, and Robert Seckler

Dorothee Andres performed all shown experiments with exception of the heat capacity measurements. *S*. Paratyphi mutants were constructed together with Wolfgang Rabsch at the Robert Koch Institut in Wernigerode. Crystal structure analysis of P22 tailspike complexed with O antigen octasaccharide was performed together with Ulrich Gohlke in Udo Heinemann´s group at the Max Delbrück Centrum in Berlin. Dorothee Andres evaluated all data, analyzed them in context and wrote the first manuscript. The depicted version of the manuscript has not been approved by all co-authors.

7.1 Summary

Protein interactions with complex carbohydrate structures are crucial for biological recognition processes, but the determinants of specificity and affinity of such interactions are not well understood. The tailspike protein of bacteriophage P22 (P22 TSP) recognizes the O antigen polysaccharides of several *Salmonella enterica* (*S*.) serovariants. In *S.*Typhimurium, *S*. Enteritidis, and *S*. Paratyphi A the tetrasaccharide repeat units of the respective O antigens consist of an identical main chain trisaccharide but differ in a 3,6 dideoxyhexose substituent. Here, the epimers abequose, tyvelose, and paratose determine the specific serotype.

P22 TSP recognizes O antigen octasaccharides in an extended binding site with a single 3,6-dideoxyhexose binding pocket. In this work we investigated the interaction of P22 TSP with *S.* Paratyphi A octasaccharide by X-ray crystallography, isothermal titration calorimetry and surface plasmon resonance. *S*. Paratyphi octasaccharide binds to P22 TSP less tightly ($\Delta\Delta G^0_{bind} \approx 7$ kJ/mol at 20°C) and in a different conformation compared to the other two hosts O antigens.

The contribution of individual contacts was investigated by amino-acid replacements in the dideoxyhexose binding pocket. The results suggest a crucial role of indirect interactions via two water molecules conserved in all three octasaccharide complex structures. In the X-ray structure of the *S*. Paratyphi A octasaccharide complex with P22 TSP, they are made possible by a structural change in the saccharide resulting in an energetically unfavorable glycosidic bond ϕ / ψ angle combination. This enables an intramolecular hydrogen bond not present in solution structures of *Salmonella* O antigen oligosaccharides in water but observed previously for *S*. Enteritidis tetrasaccharide in an aprotic solvent.

7.2 Introduction

Many recognition processes in biology, from oocyte fertilization(Pang, Chiu et al. 2011) to viral particle attachment (Gamblin and Skehel 2010) rely on the binding of complex oligosaccharide structures to proteins with high specificity made possible by the diversity of the sugar code (Toone 1994; Weis and Drickamer 1996; Gabius, Siebert et al. 2004). Thus it is important to understand the principles underlying the discrimination of oligosaccharides by proteins. Tailspike proteins (TSP) are homotrimeric carbohydrate binding proteins of bacteriophages, each adapted to a bacterial carbohydrate structure and mediating successful and specific host infection (Casjens 2008) (Barbirz, Müller et al. 2008). Their diversity and their high stability, together with the diversity and accessibility of their target saccharides makes them versatile tools for structural thermodynamics investigations of carbohydrate-protein interactions.

During infection, all *Salmonella* (*S*.) utilize a sophisticated array of effector proteins which are injected into the host cell cytoplasm through the bacterial injectisome (Worrall, Lameignere et al. 2011, Galan and Curtiss 1991). Despite this similarity, *Salmonellae* differ in their surface lipopolysaccharide (LPS) that generates different serotypes in this genus (Luderitz, Staub et al. 1966). This diversity results mainly from variations in the O antigen structure, the repetitive part of LPS, and is connected to different surface adhesion and host defense evasion properties (Lerouge and Vanderleyden 2002).

S. Paratyphi A (in the following: *S*. Paratyphi), *S*. Enteritidis and *S*. Typhimurium are representative examples of this diversity. They all cause enteric infections, but contrary to the other two, *S*. Paratyphi is an obligatory human pathogen and one of the major causes for enteric fever (Meltzer and Schwartz 2010). All three *Salmonella* serovars share the same O antigen main-chain trisaccharide repeating unit (RU) α-D-mannose (Man)-(1-4)- α-L-rhamnose (Rha)-(1-3)- α-D-galactose (Gal)-(1-2). But they differ in a 3,6 dideoxyhexose substituent at C-3 of mannose, being either abequose (3,6-dideoxy-D-galactose)(Abe) in *S*. Typhimurium, tyvelose (3, 6-dideoxy-D-mannose)(Tyv) in *S*. Enteritidis, or paratose (3, 6-Dideoxy-D-glucose) (Par) in *S.* Paratyphi (Figure 7.4.1 A).

These *Salmonella* strains can be infected with bacteriophage P22 that recognizes the three different O antigens with its TSP, despite the different dideoxyhexose side chains (Eriksson, Svenson et al. 1979). As the phage particle carries up to 6 homotrimeric TSP and it encounters a high density of O antigen chains, the initial attachment is multivalent and essentially irreversible (Israel 1976). Subsequent O antigen cleavage by the endorhamnosidase activity located on the TSP initiates the process leading to DNA injection and infection of the host (Andres, Baxa et al. 2010; Andres, Hanke et al. 2010 Baxa, Steinbacher et al. 1996). The main product of O antigen

cleavage by P22 TSP is an octasaccharide comprising two O antigen RU (Iwashita and Kanegasaki 1973). Crystal structures of octasaccharide hydrolysis products from *S*. Enteritidis and *S*. Typhimurium O antigens bound to P22 TSP have been determined at high resolution (Steinbacher, Baxa et al. 1996). They show that the carbohydrate interaction site in the trimeric 215 kDa protein is located centrally on the surface of the right-handed parallel β-helix comprising the main part of a P22 TSP subunit. The first RU of the octasaccharide binds to the more C-terminal subsite and carries the reducing end, which contacts the active-site carboxylate residues. Here, the stereochemically different 2'- and 4'-hydroxyls of the dideoxyhexoses are solvent-exposed. In contrast, the 3,6-dideoxyhexoses of the second RU bind into a pocket at the more N-terminal end of the octasaccharide binding site (Figure 7.5.1 A and B). Here, the 2'- and 4'-hydroxyls are involved in different, but numerically equivalent direct and indirect interactions with the protein. A thermodynamic analysis of *S*. Enteritidis octasaccharide interaction revealed that binding is driven by enthalpy and connected to a large and negative heat capacity change (Baxa, Cooper et al. 2001). Consequently, the binding affinity decreases slightly with increasing temperature, despite the increasingly negative binding enthalpy due to enthalpy-entropy compensation. The thermodynamic signature suggests a significant contribution of water release, as observed with other protein carbohydrate binding reactions (Kadirvelraj, Foley et al. 2008, Klein, Ferrand et al. 2008, Dam and Brewer 2002).

Here we report on a detailed study of *S*. Paratyphi O antigen binding to P22 TSP protein providing new insights into carbohydrate specificity. An ITC based thermodynamic analysis shows reduced affinity and enthalpic contributions, but a similar heat capacity change upon binding of *S*. Paratyphi octasaccharide compared to the saccharides from *S*. Enteritidis and *S*. Typhimurium. Whereas the latter saccharides bind in the conformation preferred in aqueous solution (Landstrom, Nordmark et al. 2008), the paratose containing octasaccharide was found to bind in a different conformation when soaked into crystals of P22 TSP. The new conformation allows the dideoxyhexose to interact with two structurally conserved water molecules, even though paratose lacks an axial hydroxyl interacting with these water molecules, when abequose or tyvelose is bound in the dideoxyhexose pocket. The new saccharide conformation is compatible with previous NMR results obtained with tyvelose containing O antigen tetrasaccharide in an aprotic environment (Bundle, Baumann et al. 1994).

7.3 Experimental Procedures

7.3.1 Materials

Sensor chip CM5 and the Amine Coupling Kit were obtained from GE Healthcare Europe GmbH, Freiburg, Germany. Standard buffer is 50 mM sodium phosphate, pH 7.0, if not otherwise stated. *S.* Typhimurium and *S*. Enteritidis octasaccharides were prepared as described and quantified by dry weights (Baxa, Steinbacher et al. 1996). All experiments were done with P22 TSP lacking the particle binding N-terminal domain. The protein was produced in *E. coli*, purified, and stored as a suspension in 40% saturated $(NH_4)_2SO_4$ as described (Steinbacher, Seckler et al. 1994). Mutants D303A, E309A, D303A/E309A and T307K were produced using the QuikChange Kit (Agilent, Santa Clara, CA). TSP molar subunit concentrations are given throughout.

7.3.2 S. Paratyphi InvA transduction

A susceptible O1 negative *S*. Paratyphi A strain was grown in LB media overnight and transduced with P22 HT int 201 propagated on *S*. Typhimurium with an InvA deletion substituted with a chloramphenicol (cm) resistance (Schmieger 1972; Galan and Curtiss 1991). Colonies that were able to grow on 20 µg/ml cm LB plates were screened for a characteristic 1277 bp PCR product and sequenced for successful transduction. The strain was named *Salmonella* Paratyphi A var. durazzo (DE(InvA):CM) WR2070 and stored in the Wernigerode *Salmonella* collection.

7.3.3 S. Paratyphi LPS and octasaccharide production

S. Paratyphi WR2070 was grown at 37°C in LB media substituted with 20 µg/ml cm overnight. *S*. Paratyphi lipopolysaccharide and O antigen polysaccharide was purified and digested with P22 TSP as described for *S*. Typhimurium (Andres, Hanke et al. 2010). P22 TSP digestion of *S*. Paratyphi O antigen polysaccharide yielded fragments that were purified by gel filtration on a Superdex 30 26/60 after polysaccharide and protein were precipitated in 90 % ethanol (Barbirz, Müller et al. 2008).

7.3.4 Binding measurements with ITC and SPR

Isothermal titration calorimetry was performed in a VP-ITC microcalorimeter (MicroCal, Inc., Northampton, MA) as described previously (Baxa, Cooper et al. 2001). Shortly, 25 µM P22 TSP was titrated with 0.5 mM octasaccharides from *S*. Typhimurium and *S*. Enteritidis in standard buffer using injections of 8 µl within 20 s, at 230 s intervals. For titrations with 0.5 mM *S*. Paratyphi octasaccharides, 50 µM P22 TSP were titrated using 12 µl injections. A first injection of 3 µl was neglected in the analysis employing the single binding site model in the Origin MicroCal analysis software (version 5.0, MicroCal, Inc.).

For SPR analysis, P22 TSP was immobilized on sensor chip CM5 in a Biacore 2000 instrument (GE Healthcare, Freiburg, Germany) with EDC/NHS coupling. Different concentrations of *S.* Typhimurium octasaccharides were injected for 2 min at a flow rate of 5 µl/min at 20 °C in standard buffer. A binding isotherm was fitted to the equilibrium signals.

7.3.5 Crystallization, data collection, and structure determination

P22 TSP crystallized in space group $P2_13$ at 4°C by hanging drop vapor-diffusion from 1.5 M $(NH_4)_2SO_4$ in 0.1 M NaP pH 10 over 1.0 M $(NH_4)_2SO_4$ in 0.1 M NaP pH 10 (Steinbacher, Seckler et al. 1994). Crystals were soaked with 2 mM *S*. Paratyphi octasaccharide in 1 M Na_2SO_4 in 0.1 M Tris-HCl pH 7.5 at room temperature for one week (Steinbacher, Baxa et al. 1996). Crystals were harvested and frozen in 1 M Na_2SO_4 in 0.1 M Tris-HCl pH 7.5 containing 20 % glycerol.

Diffraction data to 1.75 Å resolution were collected at Beamline 14.1 of the Berlin synchrotron BESSY, Helmholtz-Centrum Berlin. Data were processed with Xds (Kabsch 2006). The structure was solved by molecular replacement using MrBump (Keegan and Winn 2007) and Phaser (McCoy, Grosse-Kunstleve et al. 2007) from the Ccp4 suite (Collaborative Computational Project 1994) with P22 TSP (pdb2VFM; M. Becker, J. J. Mueller, R. Seckler, and U. Heinemann, unpublished) and without ligand coordinates as search model. In order to minimize model bias, the initial model was automatically rebuilt using ARP/wARP (Langer, Cohen et al. 2008). Subsequently, the octasaccharide ligand, three glycerol molecules, and 661 water molecules were fitted into the electron density map. Thirteen iterative cycles of interactive model building with Coot (Emsley and Cowtan 2004) and refinement with Refmac5 (Murshudov, Vagin et al. 1997) led to final R_{work} and R_{free} values of 0.136 and 0.156, respectively. Molprobity (Chen, Arendall et al. 2010) was used for validation of the model.

Statistics for data processing and model refinement are summarized in appendix Table 15.1. The initial model for the octasaccharide was generated with Sweet II (Bohne, Lang et al. 1999) and Prodrg (Schuttelkopf and van Aalten 2004). The latter program was also used for the generation of the topology file needed for refinement by Refmac5. The final model for the octasaccharide was verified with pdb-care and Carp (Lutteke and von der Lieth 2004; Lutteke, Frank et al. 2005). Amino acids interacting with the octasaccharide were analyzed with Ligand Explorer. The final model coordinates have been deposited at the Protein Data Bank with accession number 3TH0. Figures were generated with PyMOL (Schrödinger, Portland, OR).

7.4 *S.* Paratyphi A O antigen

Salmonella Paratyphi A is one of the major causes of enteric fever in humans (Meltzer and Schwartz 2010). To work with such a pathogen strain in the laboratory, we attenuated its infectivity by transducing a deletion of InvA, the *Salmonella* type III secretion system invasion protein A, from a *S*. Typhimurium strain into S. Paratyphi with the help of phage P22. This deletion prevents *S*. Typhimurium as well as other *Salmonella* serovars from entering human cells (Galan and Curtiss 1991).

A strain suitable for our analysis must not carry a lysogen P22 phage that results in an altered O antigen chain substituted with an α-1,6 glucose (Glu) at Gal in the O antigen RU (Figure 7.4.1 A) (Luderitz, Staub et al. 1966).

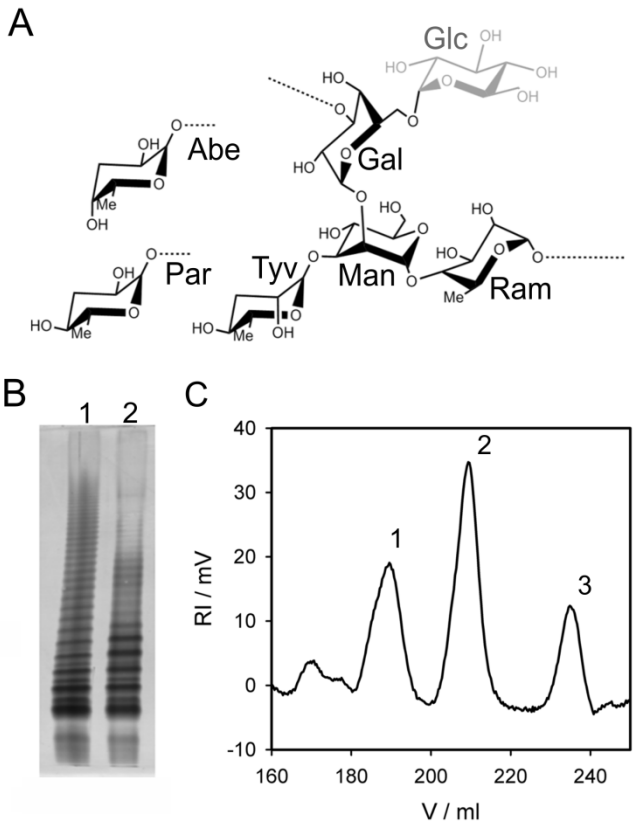

Figure 7.4.1: O antigen and preparation
A: Structure of *Salmonella* O antigen repeating units. The identical main chain consists of α-D-mannose (Man)-(1-4)-α-L-rhamnose (Rha)-(1-3)- α-D-galactose (Gal) with different dideoxyhexose substituents at C-3 of mannose, either abequose (Abe) in *S*. Typhimurium, tyvelose (Tyv) in *S*. Enteritidis, or paratose (Par) in *S.* Paratyphi.
B: Silver-stained 12.5 % SDS PAGE of 5 µg *S*. Paratyphi LPS (lane 1) and 5 µg *S*. Paratyphi LPS after incubation with 100 ng P22 TSP for 1 minute in 50 mM Tris, 4 mM $MgCl_2$ pH 7.6 (lane 2).
C: Gel filtration of *S*. Paratyphi P22 TSP digestion products on Superdex 26/30 in 50 mM NH_4CO_3 detected by refractive index change. Distinct peaks at 189 ml (1), 209 ml (2) and 234.5 ml (3) correspond to dodeca-, octa- and tetrasaccharide, respectively.

Therefore, to select a strain for P22 transduction, all *S*. Paratyphi strains in the Wernigerode collection of human pathogens were typed for their O antigen. Out of 23 *S*. Paratyphi strains, 17 (74 %) were positively tested for the P22 lysogen modification. A susceptible strain was then attenuated by P22 transduction yielding *S*. Paratyphi WR2070. From this we successfully purified lipopolysaccharide (LPS) and O antigen polysaccharide. When analyzed by SDS polyacrylamide gel electrophoresis, LPS runs as a characteristic ladder of double bands distributed from short to long

O antigen chains (Figure 7.4.1 B). Upon incubation with P22 TSP, the long chains become cleaved, yielding shorter chain-length LPS with higher electrophoretic mobility. P22 TSP is therefore active on the O antigen of *S*. Paratyphi WR2070.

7.5 P22 tailspike co crystallized with *S.* Paratyphi octasaccharide

The O antigen polysaccharide of *S*. Paratyphi WR2070 was used to purify O antigen fragments of defined length. As previously observed for *S*. Typhimurium and *S*. Enteritidis O antigens (Eriksson, Svenson et al. 1979; Baxa, Steinbacher et al. 1996), incubation of P22 TSP with *S*. Paratyphi O antigen polysaccharide yields tetra-, octa- and dodecasaccharides (Figure 7.4.1 C). Purified *S*. Paratyphi octasaccharides were soaked into pre-formed crystals of P22 TSP lacking its N-terminal, particle binding domain and the structure was solved to 1.75 Å resolution (appendix Table 15.1). The central part of the trimeric P22 TSP is folded into right-handed, parallel β-helices with 13 complete turns. Here, the 21 Å long and 8-13 Å wide site is located, where two RU of *S*. Paratyphi O antigen bind (Figure 7.5.1 A).

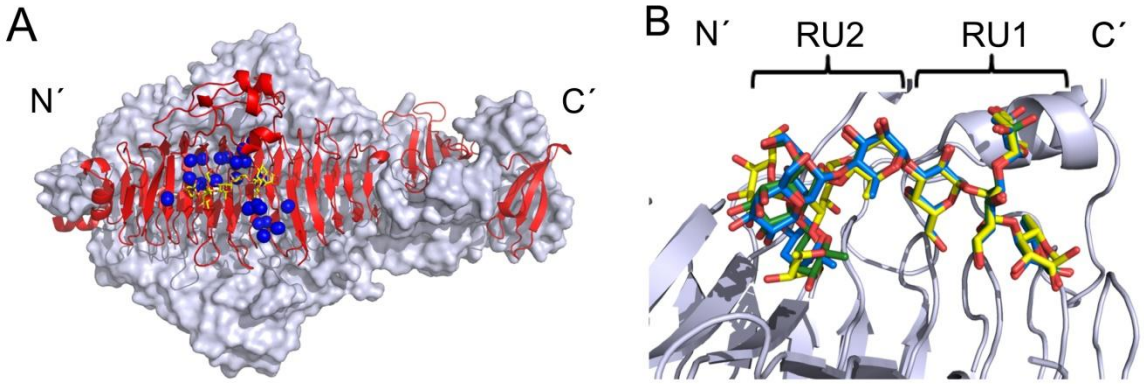

Figure 7.5.1: Crystal structures of P22 tailspike octasaccharide complexes.
A: Structure of the P22 TSP trimer illustrating the subunit architecture (red) and its binding site. An octasaccharide comprising two RU of the O antigen from *S*. Paratyphi binds to the central part of the right-handed parallel β-helix (yellow sticks). Water molecules in the binding site are conserved between all three complexes (blue spheres).
B: View of octasaccharides from *S*. Typhimurium (green carbons), *S*. Enteritidis (cyan) and *S*. Paratyphi (yellow) complexed to P22 TSP after superposition of the protein. Towards the TSP carboxy-terminus, the three RU1 at the reducing ends overlay almost perfectly. Here the O antigen specific 3,6-dideoxyhexose (top) points into the solvent. At the amino-terminal end of the binding site, the structures of RU2 deviate and the 3,6-dideoxyhexose points towards the protein.

No differences in protein conformation were observed between liganded and unliganded P22 TSP. Carbohydrate binding is mediated via hydrophobic stacking between aromatic side chains and pyranose rings as well as H bonds of the saccharide to amino acids and structural water molecules.

When the new structure is compared to the structures containing O antigen oligosaccharides from *S*. Enteritidis and *S*. Typhimurium (Steinbacher, Baxa et al. 1996), many similarities but also distinct differences become apparent. The reducing end of the first RU binds towards the C-terminus of the protein. All monosaccharide residues of the first RU have similar B-factors in all three structures and essentially identical ϕ (O_5-C_1-O_1-C'_X) and ψ (C_1-O_1-C'_X-C'_{X+1}) torsion angles, so that they superimpose very well in the structure (Table 7.1, Figure 7.5.1 B and Figure 7.5.2 A).

Table 7.1: Conformations of O antigen octasaccharides bound to P22 TSP depicted as crystallographic ϕ (O_5-C_1-O_1-C'_X) and ψ (C_1-O_1-C'_X-C'_{X+1}) torsion angles around the glycosidic bonds.

	Gal1-(1-2)-Man2		**ddHex3-(1-3)-Man2**		**Man2-(1-4)-Rha4**	
	ϕ	ψ	ϕ	ψ	ϕ	ψ
***S*. Typhimurium**	85.0	157.4	74.6	136.5	86.6	105.8
***S*. Enteritidis**	70.6	147.2	62.4	127.8	95.3	112.7
***S*. Paratyphi**	86.9	159.4	75.9	128.1	77.5	174.3
	Rha4-(1-3)-Gal5		**Gal5-(1-2)-Man6**		**ddHex7-(1-3)-Man6**	
***S*. Typhimurium**	297.6	132.3	88.2	151.0	62.4	134.4
***S*. Enteritidis**	296.0	132.9	86.3	150.4	65.2	134.0
***S*. Paratyphi**	292.0	138.3	87.9	146.7	69.0	120.0
	Man6-(1-4)-Rha8					
***S*. Typhimurium**	75.8	128.9				
***S*. Enteritidis**	80.1	128.5				
***S*. Paratyphi**	85.5	131.3				

Because the 2' and 4' hydroxyls of the different dideoxyhexoses point towards the solvent, identical interactions between O antigen and protein are possible for this RU. An 8 Å narrow elevation on the protein molds the carbohydrate backbone and enables interaction, as observed for the other two serotypes (appendix Table 15.2) (Steinbacher, Baxa et al. 1996). The terminal reducing Rha8 is bound in a flat depression in a distorted boat conformation. Thereby, its Rha8-C1 hydroxyl group is in α configuration close to the active site carboxylates of Asp392, Asp395, and Glu359 (appendix Table 15.2) (Baxa, Steinbacher et al. 1996).

The second RU binding more N-terminally is also well resolved in the structure (appendix Figure 15.1.1). Surprisingly, however, the *S*. Paratyphi RU containing paratose is shifted compared to the other oligosaccharides containing tyvelose (*S.* Enteritidis) or abequose (*S.* Typhimurium), respectively (Figure 7.5.1 B).

Especially the ψ bond angle between Man2 and Rha4 is altered by about 60° around the glycosidic bond (Table 7.1, Figure 7.5.2 A). In a CARP calculated Ramachandran Plot, this carbohydrate angle combination is shifted from the global minimum when compared to the other two serotypes, but is not forbidden (Figure 7.5.2 B to D) (Lutteke, Frank et al. 2005).

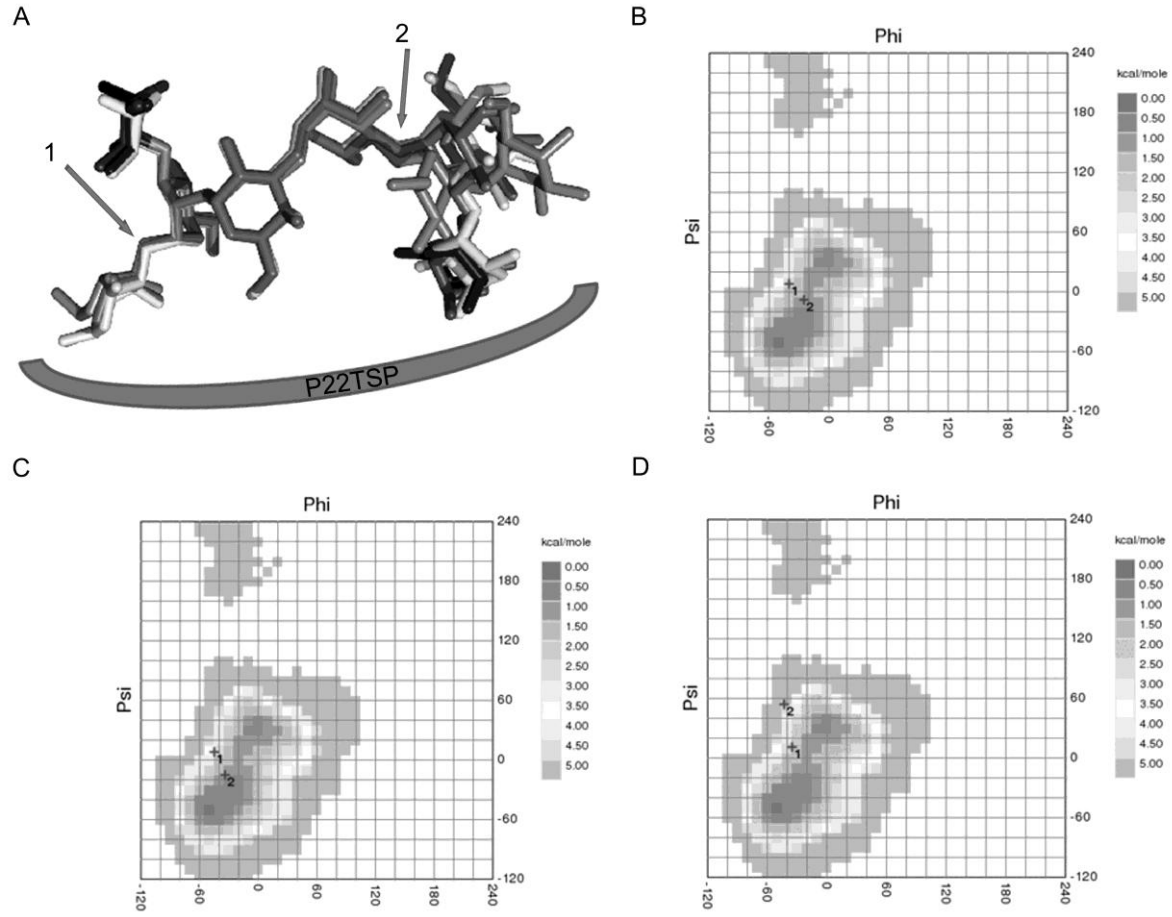

Figure 7.5.2: Ramachandran analysis of Man-Rha glycosidic torsion angles.
A: Overlay of octasaccharides illustrating the torsion angles. From light grey to black: *S*. Typhimurium (light grey), *S*. Enteritidis (dark grey) and *S*. Paratyphi (black) octasaccharides on P22 TSP surface. Number (1) indicates the location of the glycosidic oxygen of α-D-Man(6)-(1→4)-α-L-Rha(8) in RU1 at the reducing end, number (2) that of α-D-Man(2)-(1→4)-α-L-Rha(4) in RU2.
B to **D**: CARP calculated ϕ and ψ torsion angles for *S*. Typhimurium octasaccharide (B), *S*. Enteritidis octasaccharide (C), and *S*. Paratyphi octasaccharide (D) compared to the calculated Ramachandran map for α-D-Man-(1→4)-α-L-Rha as archived in GlycoMapsDB. Note that GlycoMapsDB uses NMR-like torsion angles (ϕ: H_1-C_1-O_1-C'_X, ψ: C_1-O_1-C'_X-C'_{X+1}).

As a result of this conformational difference, binding of the serotype-specific Par3 in the dideoxyhexose binding pocket is mediated differently than for the other two serotypes. Compared to Tyv and Abe in the previously determined structures, Par3 has moved towards a hydrophobic patch consisting of Leu337, Leu283 and the carbon atoms of Thr307. Here, Par3 interacts with its carbon backbone. Furthermore, two direct and two bridged hydrogen are made possible (Figure 7.5.3, appendix Table 15.2). The conformation allows direct contacts of Par3-O4 to the side chains of Glu309 and Arg285. The equatorial Par3-O2 now interacts with two structural water molecules that are hydrogen-bonded to axial hydroxyl groups when Tyv or Abe are bound in the dideoxyhexose pocket (Steinbacher, Baxa et al. 1996). When the dideoxyhexose is fixed in

this new position, the terminal Gal1 is shifted towards the protein N terminus compared to the previously determined structures of Tyv or Abe containing oligosaccharide complexes.

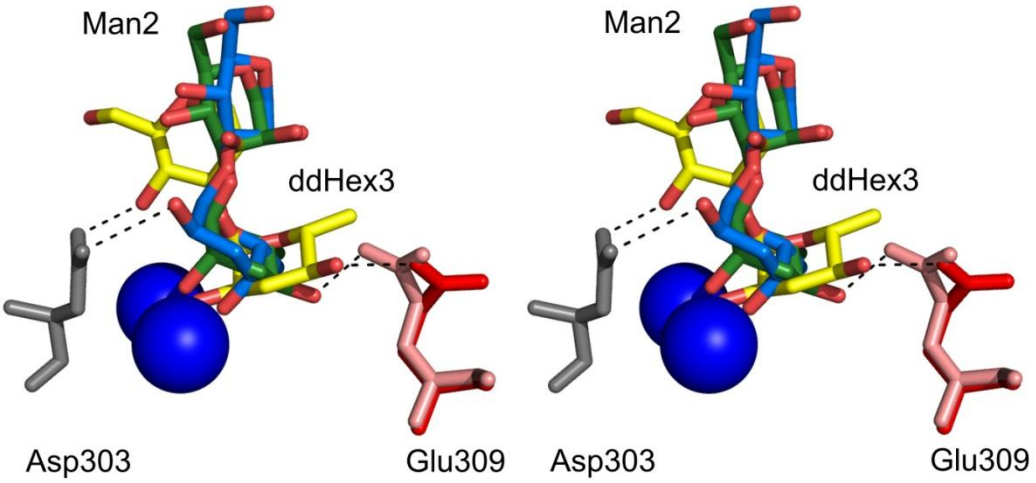

Figure 7.5.3: Interactions in the dideoxyhexose binding pocket
Hydrogen-bonding interactions of the disaccharide portion 3,6-dideoxyhexose3-(1-3)-Man2 in the binding site. *S*. Typhimurium Abe3 (cyan) binds with axial Abe3-O4 to the two conserved water molecules (blue spheres) and equatorial Abe3-O2 interacts with Asp303 (grey). *S*. Enteritidis Tyv3 (green) can bind with axial Tyv3-O2 to two conserved water molecules and via its equatorial Tyv3-O4 to Glu309 (pink). Binding of *S*. Paratyphi Par3-Man2 (yellow) occurs via equatorial Par3-O2 interacting with the conserved water molecules, its Par3-O4 interacting with Glu309 (red), and Man2-O4 with Asp303.

In all three complexes, Gal1 is not well defined by electron density resulting in very high B factors and indicating that it does not contribute significantly to the binding affinity. Further toward the reducing end, the new conformation facilitates the formation of a hydrogen bond between Man2-O4 and Asp303 (Figure 7.5.3). In the other two structures, Asp303 is involved in dideoxyhexose binding and not accessible to Man2 (Steinbacher, Baxa et al. 1996). Notably, the new conformation brings Par3-O2 to within 4 Å of Man2-O4. It is similar to a structure of an abequose containing *Salmonella* O antigen saccharide observed previously by NMR in an aprotic solvent, where Abe-O2 is hydrogen-bonded to Man2-O4. Despite the differences, the octasaccharides from all three serotypes make a similar number of contacts (appendix Table 15.2).

7.6 Octasaccharide binding measurements

The binding affinity of the *S*. Paratyphi octasaccharide to TSP (K_D= 48 ± 9 µM at 20°C), as measured by ITC, was significantly lower compared to *S*. Typhimurium octasaccharide (K_D =3.0 ± 0.13 µM) or *S*. Enteritidis octasaccharide (K_D ≈ 3 µM, (Baxa, Cooper et al. 2001)).

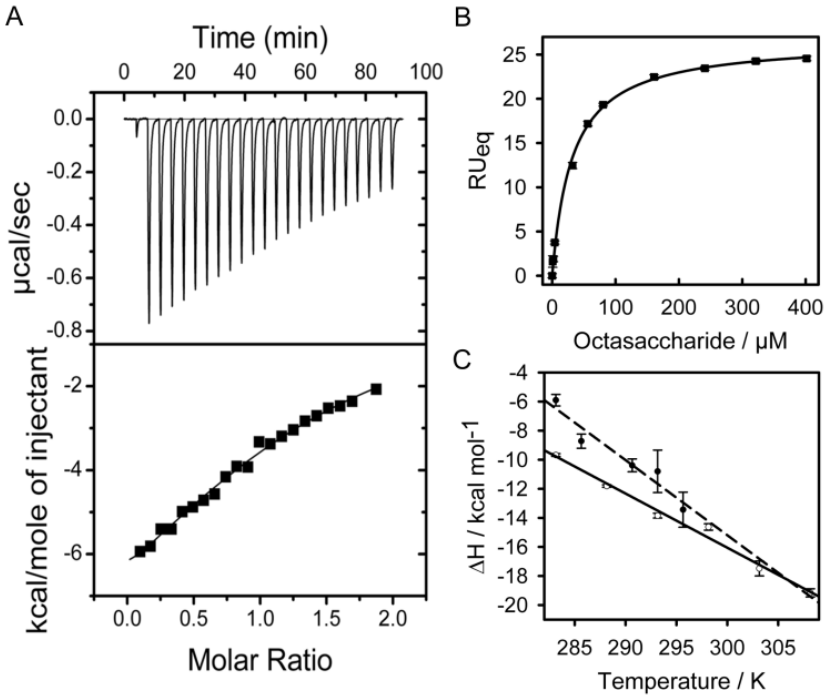

Figure 7.6.1: Thermodynamics of octasaccharide binding to P22 TSP.
A: Example ITC result for 50 µM P22 TSP ΔN subunits titrated with 12 µl 0.5 mM octasaccharides from *S*. Paratyphi per injection at 20°C in 50 mM NaP pH 7. The upper panel shows the heat release vs. time, whereas the lower panel the titration curve normalized to molar concentration. The best fit to a model with one binding site is shown in the lower panel which yields K_D=48 ± 9 µM.
B: For SPR experiments, P22 TSP was immobilized on a Biacore CM5 sensor chip. A binding isotherm fitted to plateau signals obtained with increasing concentration of *S*. Paratyphi octasaccharide in 50 mM NaP pH 7 resulted in K_D =31.9 ± 3 µM.
C: Enthalpies of three independent ITC experiments for *S*. Typhimurium (o) and *S*. Paratyphi (●) octasaccharide are plotted against temperature. Linear fits yields heat capacity changes of ΔCp = -517 ± 80 cal mol^{-1} K^{-1} for *S*. Paratyphi octasaccharide binding and ΔCp = -374± 20 cal mol^{-1} K^{-1} for *S*. Typhimurium octasaccharide.

Table 7.2: Thermodynamic parameters for octasaccharide binding to P22 TSP, as determined by ITC.

T / K	K_D / µM	N	ΔH / cal mol^{-1}	ΔS / cal mol^{-1} K^{-1}
***S*. Paratyphi**				
283.15	8.5 ± 1.26	0.97 ± 0.04	-5910 ± 396.8	2.31
285.65	36 ± 3.2	1.09 ± 0.04	-8729 ± 467.7	-10.2
290.65	47 ± 3.3	1.23 ± 0.03	-1.040E4 ± 441.8	-16.0
293.15	48 ± 9	1.29 ± 0.07	-1.081E4 ± 1160	-17.1
295.65	79.4 ± 9.6	1.27 ± 0.06	-1.345E4 ± 1208	-26.7
***S*. Typhimurium**				
283.15	1.8 ± 0.10	1.09 ± 0.01	-9688 ± 94.57	-7.9
288.3	2.1 ± 0.08	1.05 ± 0.01	-1.182E4 ± 84.37	-15.0
293.15	3.0 ± 0.13	0.83 ± 0.01	-1.386E4 ± 163.6	-22.0
298.15	3.9 ± 0.15	0.90 ± 0.01	-1.464E4 ± 221.5	-24.4
303.15	7.2 ± 0.34	0.85 ± 0.02	-1.75E4 ± 509.1	-34.0
308.15	10.1 ± 0.25	1.08 ± 0.01	-1.888E4 ±282.4	-38.2

Around 20°C, binding of all three carbohydrates to P22 TSP is driven by enthalpy ($\Delta H^0_{bind} \approx -12$ kcal/mol) and opposed by a significant unfavorable entropy change (*cf.* Figure 7.6.1 A and Table 7.2).Because of the lower affinity of the *S*. Paratyphi octasaccharide, the ITC results are somewhat less reliable compared to those for the other two sugars. Therefore, we sought to verify the ITC data using surface plasmon resonance (SPR). P22 TSP was coupled to a Biacore CM5 sensor chip and *S*. Paratyphi octasaccharide was used as the analyte. The binding isotherm measured at 20°C and depicted in Figure 7.6.1 B shows that the affinity can be determined quite reliably, despite the low molecular mass of the analyte. It results in a K_D = 39.6 ± 4 µM, which is in agreement with ITC results.

As observed previously for *S*. Enteritidis octasaccharide, both the binding enthalpy and the opposing entropy change increase in magnitude with increasing temperature. Thus, O antigen oligosaccharide binding is associated with a negative heat capacity change. The change in the constant pressure heat capacity ΔC_P determined by linear regression (Figure 7.6.1 C), i.e. assuming temperature independence of ΔC_P, amounted to -517 ± 80 cal mol^{-1} K^{-1} for *S*. Paratyphi and -373 ± 20 cal mol^{-1} K^{-1} for *S*. Typhimurium octassaccharide, respectively. Both compare well to the ΔC_P value of -430 ± 50 cal mol^{-1} K^{-1} determined earlier for *S*. Enteritidis octasaccharide (Baxa, Cooper et al. 2001). Heat capacity is a valuable measure for hydration or dehydration on solvent accessible surfaces during carbohydrate binding (Garcia-Hernandez, Zubillaga et al. 2003). Thus, the data can be taken to indicate that binding of the saccharide results in a similar change in water network or release of water from hydrophobic surfaces for all three octasaccharides.

Two acidic side chains appear to be important for ligand recognition in the dideoxyhexose binding pocket, as interpreted from the crystal structures (Figure 7.5.3): Asp303 and Glu309 form hydrogen bonds with respective equatorial OH on Tyv or Abe, respectively (Steinbacher, Baxa et al. 1996), and water mediated hydrogen bonds to the carbohydrate. We decided to probe the role of these residues by site-directed mutagenesis. As expected, mutation of the carboxylate residues to alanine reduces binding affinity and enthalpy in all three serotypes as measured by ITC (Table 7.3).

Replacement of Asp303 affects binding of *S*. Paratyphi and *S*. Typhimurium octasaccharides significantly more strongly ($K_{D,\ mutant} \approx 10\ K_{D,\ wild\ type}$) than the substitution of Glu309. *S*. Enteritidis octasaccharide binding is affected by both substitutions about equally strongly, with essentially additive effects in the double mutant Asp303Ala, Glu309Ala. In the ITC measurements, reduced binding affinities were correlated with less favorable binding enthalpies, as expected if hydrogen bonding by the carboxylate residues contributes significantly to binding (Fersht, Shi et al. 1985).

Table 7.3: Mutational effects on saccharide binding observed at 20°C

	K_D / µM	N	ΔH / cal mol^{-1}	ΔS / cal mol^{-1} K^{-1}
***S*. Paratyphi**				
D303A	560	1 (set)	-1660	13.1
E309A	90.9	2	-7107	-5.74
***S*. Typhimurium**				
D303A	32.9±5.1	1.4± 0.04	-8418.5±73.5	-8.18
E309A	2.8	1.00	-14160	-22.86
D303A/E309A	22.3±3.1	0.91±0.08	-13225±215	-23.81
***S*. Enteritidis**				
D303A	10.5±1.8	0.80±0.06	-13666±677	-23.81
E309A	8.6±0.1	0.83±0.05	-16110±728	-31.77
D303A/E309A	41.5	0.88	-17060	-38.13

Introduction of a bulky and positively charged lysine substituted for Thr307 near the bottom of the dideoxyhexose binding pocket completely abolished binding beyond the detection level of the ITC experiment. This excludes enthalpy driven binding of oligosaccharides to sites elsewhere on the TSP surface. Our data confirm that O antigen binding specificity is mediated at this site (Landstrom, Nordmark et al. 2008).

7.7 Discussion

Interactions of bacteriophage tailspike proteins (TSP) with O antigen fragments serve us as model systems to understand complex carbohydrate recognition. In this paper we report on the structure of *S*. Paratyphi O antigen octasaccharide bound to P22 TSP and on its thermodynamic binding parameters. This is the first 3D-structural information available for *S*. Paratyphi A O antigen containing the unusual dideoxyhexose monosaccharide paratose. Unexpectedly, paratose binds to the dideoxyhexose pocket of the TSP in a conformation different from that of tyvelose or abequose containing oligosaccharides from *S.* Enteritidis and *S.* Typhimurium previously investigated. This raises questions of how to predict such interactions.

In contrast to *S*. Typhimurium and *S*. Enteritidis, *S*. Paratyphi is an obligatory human pathogen. The disease spreads in Asia and has become the predominant cause of enteric fever for travelers because of unavailable vaccines and endemic antibiotic resistance (Meltzer and Schwartz 2010). According to our screen of the Wernigerode strain collection, the O antigens in the majority of *S*. Paratyphi strains should contain an α-1,6 glucosylation at Gal in the O antigen repeating unit caused by a phage P22 lysogen (Luderitz, Staub et al. 1966). Accordingly, a phage P22 lysogen is found in both *S*. Paratyphi A strains sequenced. O antigen lysogenic conversion associated with increased human pathogenicity has been reported for *Pseudomonas aeruginosa* PAO1 and bacteriophage D3 (Vaca-Pacheco, Paniagua-Contreras et al. 1999, Newton, Daniels et al. 2001).

These modifications increase the bacterial ability to adhere to human epithelial cells and bacterial resistance to human immune system. In *Salmonella* itself a stereochemically different α-glucosylation at Gal-O4 in the O antigen repeating unit of *S*. Enteritidis results in a more pathogenic strain (Rahman, Guard-Petter et al. 1997). Whether the O antigen alteration by lysogenic conversion in S. Paratyphi is a virulence factor remains to be determined (Lerouge and Vanderleyden 2002). As we wanted to compare solely the contribution of different 3,6-dideoxyhexoses in *S*. Paratyphi, *S*. Enteritidis and *S*. Typhimurium binding to P22 TSP we had to employ an unlysogenized *S*. Paratyphi strain.

Upon binding of carbohydrates to proteins, water molecules become released from the surfaces of the interaction partners. Water molecules near hydrophilic groups on the protein surface may be replaced by sugar hydroxyl groups forming hydrogen bonds to the protein (Rini, Hardman et al. 1993). Together with the water released from hydrophobic groups on the protein surface and water released from the carbohydrate, they are the main reason for a change in heat capacity upon binding. Similar heat capacity changes for all three oligosaccharides from the different *Salmonella* serotypes studied here indicate that water restructuring on and release from the surfaces should contribute equally to binding although different oligosaccharide conformers are bound (Sturtevant 1977). This may be expected as the total surface area change and the overall chemical structures of the carbohydrates are very similar (Chavelas and Garcia-Hernandez 2009).

Although 14 direct hydrogen bonds are formed between protein and carbohydrate upon binding, not all water molecules, which hydrogen-bond to hydrophilic groups on the protein or carbohydrate surfaces before complex formation, can be replaced by polar groups of the binding partners, due to the complexity of the interface between the protein and the large carbohydrate. Nevertheless, some water molecules are conserved on the protein surface between the apo and the complexed structure and involved in carbohydrate binding. Conserved structural waters are important binding factors by offering hydrogen bonding to the protein and reducing the desolvation penalty of the sugar (Ruben, Kiso et al. 2006; Nurisso, Blanchard et al. 2010). In the present case, two structurally conserved water molecules in the dideoxyhexose binding pocket (HOH1447 and HOH1468) appear to be responsible for the bound *S*. Paratyphi sugar conformer that differs from that of the other two serotypes. All three dideoxyhexoses analyzed employ hydrogen bonds between sugar hydroxyl groups to the two structural waters. The two waters are conserved in all three liganded and in the apo structure. HOH1468 is held in place by hydrogen bonding to the backbone amide of Gly304 and HOH1447 is part of a hydrogen-bonded water cluster acting as an extension of the protein surface around D303 (Toone 1994).

Mutation of this residue reduces the affinity of all three carbohydrates confirming this crucial interaction. In the structures of *S.* Enteritidis and *S.* Typhimurium O antigen complexes with P22

TSP (Steinbacher, Baxa et al. 1996), the axial hydroxyls 2 of tyvelose and 4 of abequose hydrogen-bond to the two waters. *S*. Paratyphi O antigen specific Paratose possesses two equatorial hydroxyl groups at positions C4 and C2. To achieve binding to the structural water molecules, ϕ and ψ bond angles in the bound *S*. Paratyphi octasaccharide have to change compared to the other two serotypes. Apparently, P22 TSP uses structurally conserved waters to accommodate three stereochemically different sets of hydroxyl groups of the dideoxyhexose epimers, thereby expanding the viral host range.

Carbohydrates can adopt different energy conformations in solution. NMR studies of *S*. Enteritidis octasaccharide showed that neither the protein nor the sugar structure reorganizes upon binding to P22 TSP (Landstrom, Nordmark et al. 2008). CARP results for *S*. Enteritidis octasaccharide are in very good agreement with respective NMR data (Lutteke, Frank et al. 2005, Landstrom, Nordmark et al. 2008). In all TSP oligosaccharide complex structures, the first repeating unit at the reducing end overlays perfectly and here, the hydroxyls of the dideoxyhexoses are not bound to the protein. In solution, all three O antigens should be able to adopt this low energy conformation as the most populated conformer. In contrast, the bound conformation of the second repeating unit of *S*. Paratyphi octasaccharide around the dideoxyhexose binding pocket corresponds to a rare conformation in solution, based on our CARP results.

For binding of such a rare conformation, two principle mechanisms are possible: Either the carbohydrate must adopt the bound conformation in solution before binding (conformational selection), or the carbohydrate conformation is induced after initial binding to the protein (induced fit) (Boehr, Nussinov et al. 2009). For binding by conformational selection, the conformer must be significantly populated in solution (Berger, Weber-Bornhauser et al. 1999; Gabius, Siebert et al. 2004). An induced-fit mechanism should result in a larger entropic penalty (Leder, Berger et al. 1995). Either way, the *S*. Paratyphi octasaccharide has to overcome a free energy barrier to adjust ϕ and ψ torsion angles in the observed Man(2)-Rha(4) glycosidic bond. As discussed above, CARP results predict the observed *S*. Paratyphi conformer to be rare in solution excluding a conformational selection mechanism. On the other hand, we do not measure a large difference in binding entropy compared to the other two serotypes excluding the induced fit mechanism.

Here a previous observation of Bundle and coworkers comes into account. These authors investigated binding of a synthetic abequose containing O antigen trisaccharide Gal[Abe]Man to a monoclonal antibody by NMR (Bundle, Baumann et al. 1994; Bundle, Eichler et al. 1994). In the presence of dimethylsulfoxid (DMSO), a polar aprotic solute, they observed a distinct intramolecular hydrogen bond between equatorial Abe-O2 and Man-O4 which is not present in water. This hydrogen bond is only possible with torsion angles deviating from the global minimum conformation. The conformation of the paratose containing octasaccharide bound to P22 TSP is

similar, bringing Par3-O2 and Man2-O4 into close proximity. We suggest that this conformation is favored in an environment where little water is available for hydrogen bonding and propose a mechanism for binding of *S*. Paratyphi octasaccharide to P22 TSP: The saccharide may first contact the protein surface in the conformation most probable in solution. Release of water from the carbohydrate and protein surface facilitates the conformer in which Par3-O2 and Man2-O4 of the second repeat are hydrogen bonded. Finally, upon small adjustments, paratose interacts with the two structural waters and a hydrophobic patch on the protein surface to establish binding to the protein in the dideoxyhexose pocket.

Although overall contacts are quantitatively similar they differ qualitatively in the three serotypes. Alternative hydrogen bonds to amino acids and structural waters, van-der-Waals and hydrophobic interactions are formed between *S*. Paratyphi octasaccharide and P22 TSP compared to the other two O antigens, resulting in a somewhat lower affinity. Nonetheless, bacteriophage P22 is expected to bind all three bacterial hosts with similar efficiency during infection, because multivalent interactions on the bacterial surface result in high binding avidity (Andres, Baxa et al. 2010). Our results show that P22 TSP uses indirect protein-carbohydrate interactions mediated by water molecules to accommodate different epimers and conformers and thus adjust to three different *Salmonella* hosts.

7.8 References

Andres, D., U. Baxa, et al. (2010). "Carbohydrate binding of Salmonella phage P22 tailspike protein and its role during host cell infection." Biochemical Society Transactions **038**(5): 1386-1389.

Andres, D., C. Hanke, et al. (2010). "Tailspike Interactions with Lipopolysaccharide Effect DNA Ejection from Phage P22 Particles in Vitro." Journal of Biological Chemistry **285**(47): 36768-36775.

Barbirz, S., J. J. Müller, et al. (2008). "Crystal structure of Escherichia coli phage HK620 tailspike: podoviral tailspike endoglycosidase modules are evolutionarily related." Mol Microbiol.

Baxa, U., A. Cooper, et al. (2001). "Enthalpic Barriers to the Hydrophobic Binding of Oligosaccharides to Phage P22 Tailspike Protein." Biochemistry **40**(17): 5144-5150.

Baxa, U., S. Steinbacher, et al. (1996). "Interactions of phage P22 tails with their cellular receptor, Salmonella O-antigen polysaccharide." Biophys J **71**(4): 2040-8.

Berger, C., S. Weber-Bornhauser, et al. (1999). "Antigen recognition by conformational selection." FEBS Lett **450**(1-2): 149-53.

Boehr, D. D., R. Nussinov, et al. (2009). "The role of dynamic conformational ensembles in biomolecular recognition." Nat Chem Biol **5**(11): 789-96.

Bohne, A., E. Lang, et al. (1999). "SWEET - WWW-based rapid 3D construction of oligo- and polysaccharides." Bioinformatics **15**(9): 767-8.

Bundle, D. R., H. Baumann, et al. (1994). "Solution structure of a trisaccharide-antibody complex: comparison of NMR measurements with a crystal structure." Biochemistry **33**(17): 5183-92.

Bundle, D. R., E. Eichler, et al. (1994). "Molecular recognition of a Salmonella trisaccharide epitope by monoclonal antibody Se155-4." Biochemistry **33**(17): 5172-82.

Casjens, S. R. (2008). "Diversity among the tailed-bacteriophages that infect the Enterobacteriaceae." Res Microbiol **159**(5): 340-8.

Chavelas, E. A. and E. Garcia-Hernandez (2009). "Heat capacity changes in carbohydrates and protein-carbohydrate complexes." Biochem J **420**(2): 239-47.

Chen, V. B., W. B. Arendall, 3rd, et al. (2010). "MolProbity: all-atom structure validation for macromolecular crystallography." Acta Crystallogr D Biol Crystallogr **66**(Pt 1): 12-21.

Collaborative Computational Project, N. (1994). "The CCP4 suite: programs for protein crystallography." Acta Crystallogr D Biol Crystallogr **50**(Pt 5): 760-3.

Dam, T. K. and C. F. Brewer (2002). "Thermodynamic studies of lectin-carbohydrate interactions by isothermal titration calorimetry." Chem Rev **102**(2): 387-429.

Emsley, P. and K. Cowtan (2004). "Coot: model-building tools for molecular graphics." Acta Crystallogr D Biol Crystallogr **60**(Pt 12 Pt 1): 2126-32.

Eriksson, U., S. B. Svenson, et al. (1979). "Salmonella phage glycanases: substrate specificity of the phage P22 endo-rhamnosidase." J Gen Virol **43**(3): 503-11.

Fersht, A. R., J.-P. Shi, et al. (1985). "Hydrogen bonding and biological specificity analysed by protein engineering." Nature **314**(6008): 235-238.

Gabius, H. J., H. C. Siebert, et al. (2004). "Chemical biology of the sugar code." Chembiochem **5**(6): 740-64.

Galan, J. E. and R. Curtiss, 3rd (1991). "Distribution of the invA, -B, -C, and -D genes of Salmonella typhimurium among other Salmonella serovars: invA mutants of Salmonella typhi are deficient for entry into mammalian cells." Infect. Immun. **59**(9): 2901-2908.

Gamblin, S. J. and J. J. Skehel (2010). "Influenza hemagglutinin and neuraminidase membrane glycoproteins." J Biol Chem **285**(37): 28403-9.

Garcia-Hernandez, E., R. A. Zubillaga, et al. (2003). "Structural energetics of protein-carbohydrate interactions: Insights derived from the study of lysozyme binding to its natural saccharide inhibitors." Protein Sci **12**(1): 135-42.

Israel, V. (1976). "Role of the bacteriophage P22 tail in the early stages of infection." J Virol **18**(1): 361-4.

Iwashita, S. and S. Kanegasaki (1973). "Smooth specific phage adsorption: endorhamnosidase activity of tail parts of P22." Biochem Biophys Res Commun **55**(2): 403-9.

Kabsch, W. (2006). XDS. International Tables for Crystallography. M. G. Rossmann and E. Arnold. **F:** 730-734.

Kadirvelraj, R., B. L. Foley, et al. (2008). "Involvement of water in carbohydrate-protein binding: concanavalin A revisited." J Am Chem Soc **130**(50): 16933-42.

Keegan, R. M. and M. D. Winn (2007). "Automated search-model discovery and preparation for structure solution by molecular replacement." Acta Crystallogr D Biol Crystallogr **63**(Pt 4): 447-57.

Klein, E., Y. Ferrand, et al. (2008). "Solvent effects in carbohydrate binding by synthetic receptors: implications for the role of water in natural carbohydrate recognition." Angew Chem Int Ed Engl **47**(14): 2693-6.

Landstrom, J., E. L. Nordmark, et al. (2008). "Interaction of a Salmonella enteritidis O-antigen octasaccharide with the phage P22 tailspike protein by NMR spectroscopy and docking studies." Glycoconj J **25**(2): 137-43.

Langer, G., S. X. Cohen, et al. (2008). "Automated macromolecular model building for X-ray crystallography using ARP/wARP version 7." Nat Protoc **3**(7): 1171-9.

Leder, L., C. Berger, et al. (1995). "Spectroscopic, calorimetric, and kinetic demonstration of conformational adaptation in peptide-antibody recognition." Biochemistry **34**(50): 16509-18.

Lerouge, I. and J. Vanderleyden (2002). "O-antigen structural variation: mechanisms and possible roles in animal/plant–microbe interactions." FEMS Microbiology Reviews **26**(1): 17-47.

Luderitz, O., A. M. Staub, et al. (1966). "Immunochemistry of O and R antigens of Salmonella and related Enterobacteriaceae." Microbiol. Mol. Biol. Rev. **30**(1): 192-255.

Lutteke, T., M. Frank, et al. (2005). "Carbohydrate Structure Suite (CSS): analysis of carbohydrate 3D structures derived from the PDB." Nucleic Acids Res **33**(Database issue): D242-6.

Lutteke, T. and C. W. von der Lieth (2004). "pdb-care (PDB carbohydrate residue check): a program to support annotation of complex carbohydrate structures in PDB files." BMC Bioinformatics **5**: 69.

McCoy, A. J., R. W. Grosse-Kunstleve, et al. (2007). "Phaser crystallographic software." J Appl Crystallogr **40**(Pt 4): 658-674.

Meltzer, E. and E. Schwartz (2010). "Enteric fever: a travel medicine oriented view." Current Opinion in Infectious Diseases **23**(5): 432-437.

Murshudov, G. N., A. A. Vagin, et al. (1997). "Refinement of macromolecular structures by the maximum-likelihood method." Acta Crystallogr D Biol Crystallogr **53**(Pt 3): 240-55.

Newton, G. J., C. Daniels, et al. (2001). "Three-component-mediated serotype conversion in Pseudomonas aeruginosa by bacteriophage D3." Molecular Microbiology **39**(5): 1237-1247.

Nurisso, A., B. Blanchard, et al. (2010). "Role of water molecules in structure and energetics of Pseudomonas aeruginosa lectin I interacting with disaccharides." J Biol Chem **285**(26): 20316-27.

Pang, P. C., P. C. Chiu, et al. (2011). "Human sperm binding is mediated by the sialyl-Lewis(x) oligosaccharide on the zona pellucida." Science **333**(6050): 1761-4.

Rahman, M. M., J. Guard-Petter, et al. (1997). "A virulent isolate of Salmonella enteritidis produces a Salmonella typhi-like lipopolysaccharide." J Bacteriol **179**(7): 2126-31.

Rini, J. M., K. D. Hardman, et al. (1993). "X-ray crystal structure of a pea lectin-trimannoside complex at 2.6 A resolution." J Biol Chem **268**(14): 10126-32.

Ruben, A. J., Y. Kiso, et al. (2006). "Overcoming roadblocks in lead optimization: a thermodynamic perspective." Chem Biol Drug Des **67**(1): 2-4.

Schmieger, H. (1972). "Phage P22-mutants with increased or decreased transduction abilities " Molecular and General Genetics MGG **119**(1): 75-88.

Schuttelkopf, A. W. and D. M. van Aalten (2004). "PRODRG: a tool for high-throughput crystallography of protein-ligand complexes." Acta Crystallogr D Biol Crystallogr **60**(Pt 8): 1355-63.

Steinbacher, S., U. Baxa, et al. (1996). "Crystal structure of phage P22 tailspike protein complexed with Salmonella sp. O-antigen receptors." Proc Natl Acad Sci U S A **93**(20): 10584-8.

Steinbacher, S., R. Seckler, et al. (1994). "Crystal structure of P22 tailspike protein: interdigitated subunits in a thermostable trimer." Science **265**(5170): 383-6.

Sturtevant, J. M. (1977). "Heat capacity and entropy changes in processes involving proteins." Proc Natl Acad Sci U S A **74**(6): 2236-40.

Toone, E. J. (1994). "Structure and energetics of protein-carbohydrate complexes." Current Opinion in Structural Biology **4**(5): 719-728.

Vaca-Pacheco, S., G. L. Paniagua-Contreras, et al. (1999). "The Clinically Isolated FIZ15 Bacteriophage Causes Lysogenic Conversion in Pseudomonas aeruginosa PAO1." Current Microbiology **38**(4): 239-243.

Weis, W. I. and K. Drickamer (1996). "Structural basis of lectin-carbohydrate recognition." Annu Rev Biochem **65**: 441-73.

Worrall, L. J., E. Lameignere, et al. (2011). "Structural overview of the bacterial injectisome." Current Opinion in Microbiology **14**(1): 3-8.

8 Carbohydrate binding of *Salmonella* phage P22 tailspike protein and its role for infection

Chapter 8 has been published as

Carbohydrate binding of *Salmonella* phage P22 tailspike protein and its role during host cell infection

Reproduced with permission from

Dorothee Andres, Ulrich Baxa, Christin Hanke, Robert Seckler and Stefanie Barbirz, 2010

Biochemical Society Transactions **038**(5): 1386-1389.

The final version of record is available at

http://www.biochemsoctrans.org/bst/038/bst0381386.htm

Dorothee Andres designed plaque forming assay and performed all shown experiments. She evaluated biophysical and *in vivo* data in context and wrote the manuscript together with Stefanie Barbirz (Physikalische Biochemie, Universität Potsdam).

8.1 Summary

Tailpike proteins (TSP) are essential infection organelles of bacteriophage P22. Upon infection, P22TSP binds to and cleaves the O antigen moiety of the lipopolysaccharide (LPS) of its *Salmonella* host. To elucidate the role of TSP during infection we have studied binding to oligosaccharides and polysaccharides of *Salmonella* Typhimurium and Enteritidis *in vitro*. P22TSP is a trimeric β-helical protein with a carbohydrate binding site on each subunit. Octasaccharide O antigen fragments bind to P22TSP with micromolar dissociation constants. Moreover, P22TSP is an endorhamnosidase and cleaves the host O antigen. Catalytic residues lie at the periphery of the high affinity binding site which enables unproductive binding modes resulting in slow hydrolysis. However, the role of hydrolysis function during infection remains unclear. Binding of polysaccharide to P22TSP is of high avidity with slow dissociation rates when compared to oligosaccharides. *In vivo*, the infection of *Salmonella* with phage P22 can be completely inhibited by the addition of LPS, indicating that binding of phage to its host via TSP is an essential step for infection.

8.2 Introduction

The outer membrane of Gram-negative bacteria builds an effective barrier against host immune systems and macromolecules like antibiotics (Nikaido 2003). Protection mainly comes from lipopolysaccharide (LPS) located at the outermost membrane leaflet. Bacteriophages, however, can overcome this obstacle without destroying the cell. Upon infection these fascinating molecular machines recognize specific receptors on bacterial surfaces that subsequently trigger DNA ejection from the phage. Whereas some tailed phages like T4 or T7 bind to core saccharides of LPS before contacting a protein receptor for DNA release (Leiman, Kanamaru et al. 2003) others are restricted to hosts of which they specifically recognize the O antigen, i.e. the *Salmonella* phages P22, ε15 or ε34 (Lindberg 1977). These phages also have glycanase activity and shorten the length of the O antigen during infection. The purpose of O antigen hydrolysis during the infection process so far remains obscure and different functions have been discussed. Enzymatic cleavage of polysaccharide might facilitate access to the membrane and to a secondary receptor (Lindberg 1977; Israel 1978). Also, phages hydrolysing their receptor would be able to dissociate and rebind and could thus move on the cell surface to find a good position for infection (Bayer, Takeda et al. 1980). Additionally, it was proposed that the hydrolysis function could be important for release of newly synthesized phages upon cell lysis from cell debris like in influenza virus (Liu, Eichelberger et al. 1995). We have intensively studied the tailspike protein (TSP) of *Salmonella* phage P22, a double stranded DNA phage with short, non-contractile tail and its role in the infection process. Up to six TSP are attached to the phage tail and recognize the host cell O antigen (Israel, Anderson et al. 1967). However it so far remains unknown how the carbohydrate binding event leads to DNA ejection into the host. Our results indicate that a multivalent lectin like fixation of phage on the cell surface via TSP is an essential step during the infection process.

8.3 *In vitro* oligosaccharide binding studies with P22 tailspike protein

The tailspike proteins (TSP) of bacteriophage P22 recognizes and cleaves the O antigen moiety of the LPS of *Salmonella enteric*a spp. (Baxa, Steinbacher et al. 1996). One O antigen repeat unit has the composition α-D-Gal*p*-(1-4)-α-D-Man*p*-(1-4)-α-L-Rha*p*-(1-3) and varies in the substitution of the mannose with a dideoxyhexose substituent in different serotypes (Luderitz, Staub et al. 1966). P22TSP is a trimer composed of three right-handed β-helices oligomerized via a C-terminal trimerisation domain (Figure 8.3.1 A). It has endorhamnosidase activity and cleaves the glycosidic linkage of the rhamnopyranoside producing octasaccharides of two repeat units (Eriksson, Svenson et al. 1979; Steinbacher, Seckler et al. 1994). Two aspartic and one glutamic acid make up

the active site and mutants have a strongly reduced enzymatic activity (Baxa, Steinbacher et al. 1996). The octasaccharide binding site is located on the solvent exposed groove formed by the β-helix (Steinbacher, Baxa et al. 1996) (Figure 8.3.1 B).

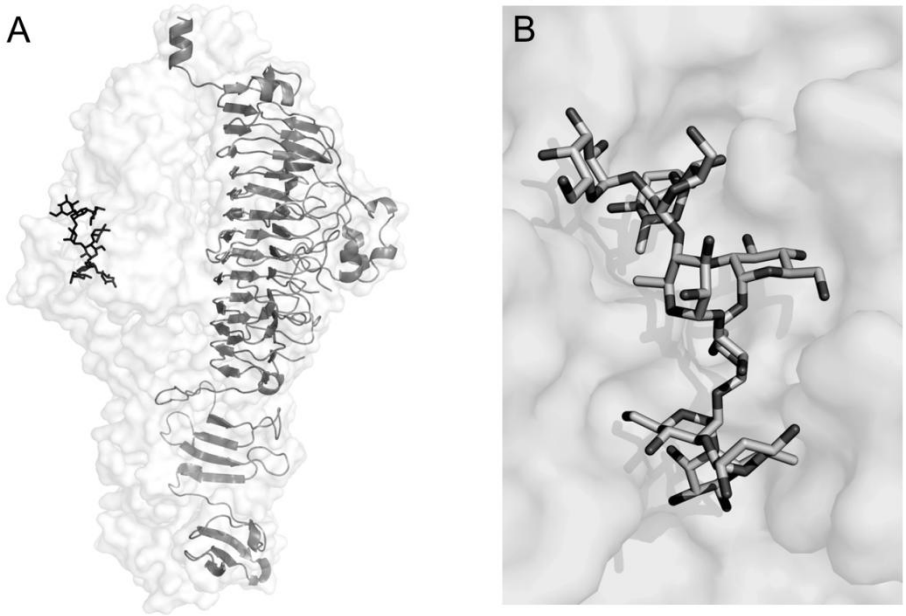

Figure 8.3.1: P22 Tailspike in complex with O antigen
A: Structure of phage P22 tailspike trimer lacking the N-terminal capsid binding domain. Side view of a surface representation with one subunit as ribbon drawing. N-terminus points up. Each subunit has an O antigen binding site, as an example, an O antigen octasaccharide of *S*. enteritidis binding to P22TSP is shown in stick representation (Steinbacher, Baxa et al. 1996).
B: Binding surface for the octasaccharide on P22TSP (same orientation as in A). Nearly all surface exposed amino acids contact the saccharide directly via H-bonds (Baxa, Cooper et al. 2001). The reducing end of the octasaccharide points towards the active site residues that terminate the groove at the lower end. Figure generated with PyMOL (DeLano 2002).

Dideoxyhexose substituents of three different serotypes are recognized and enable phage activity on an extended host range. Interaction of P22TSP with oligosaccharides of defined composition was intensively studied using a protein fluorescence quench upon binding or isothermal titration calorimetry (Baxa, Steinbacher et al. 1996; Baxa, Cooper et al. 2001). It was shown that a minimum of two repeat units, corresponding to an octasaccharide, are required for high affinity binding and a free enthalpy yield of about 30 kJ/mol per binding site. Oligosaccharides of three repeat units bind with similar affinities indicating that no additional high affinity binding sites were present. A large negative binding enthalpy upon binding was observed which strongly depended on temperature, together with a large heat-capacity change. Given good enthalpy-entropy compensation it was concluded that binding to P22TSP is enthalpically driven due to

hydrophobic interactions between sugar and protein. Stopped-flow measurements showed the binding equilibrium to be highly dynamic. By contrast, hydrolysis rates of fluorescently labelled dodecasaccharides were also measured and were small compared to the dissociation rates (Baxa, Steinbacher et al. 1996). For cleavage of a dodecasaccharide at 10° C k_{cat} is 0.01 s^{-1} indicating that even at physiological temperature hydrolysis is slow compared to oligosaccharide binding. This is substantiated by the special architecture of the active site where the catalytic residues lie at the end of a high affinity binding groove (Figure 8.3.1 B). Therefore, the smallest hydrolysis products obtained of polysaccharide digests with P22TSP are octasaccharides corresponding to two repeat units. They cannot be cleaved further due to lacking high affinity binding sites beneath the active site residues. Moreover, from this architecture an unproductive binding mode for hydrolysis products results that can slow down polysaccharide hydrolysis. Hydrolysis products that are multiples of O antigen repeats have also been found for other phages, i.e. coliphage Ω8 (Reske, Wallenfels et al. 1973) or *Shigella* phage Sf6 (Lindberg, Wollin et al. 1978) indicating that this is particular feature of phage glycanases active on O antigen. These findings illustrate that P22TSP counterbalances two features in its O antigen binding site, a lectin-like carbohydrate binding function and a glycosidase activity. As discussed below, both are essential for the phage infection process.

8.4 *In vitro* polysaccharide binding studies with P22 TSP

Natural receptor of bacteriophage P22 is the polysaccharide moiety of the LPS of the *Salmonella* host (Lindberg 1977). However, polysaccharide is a polydisperse mixture of different chain lengths which prevents quantification of molar binding affinities. When polysaccharide purified from *S*. Typhimurium was added to P22TSP tryptophane fluorescence was quenched, analog to oligosaccharide binding [8] (Figure 8.4.1 A). To avoid polysaccharide cleavage the active site mutant P22TSP D392N was used, which binds octasaccharides with similar affinities as the wild type but has 1/30,000 reduced turnover rate constant for cleavage (Baxa, Steinbacher et al. 1996). We measured fluorescence kinetics of polysaccharide binding to P22TSP at different concentrations with manual mixing to quantify polysaccharide affinity of P22TSP (Figure 8.4.1 B). Relaxation to binding equilibrium takes place in a time scale of about 2 min. The data was fitted to a biexponential model. The fast phase yielded apparent rate constants k_{app} for the initial binding event whereas the much slower phase was independent of polysaccharide concentration. Apparent rate constants k_{app} were determined at different concentrations of polysaccharide.

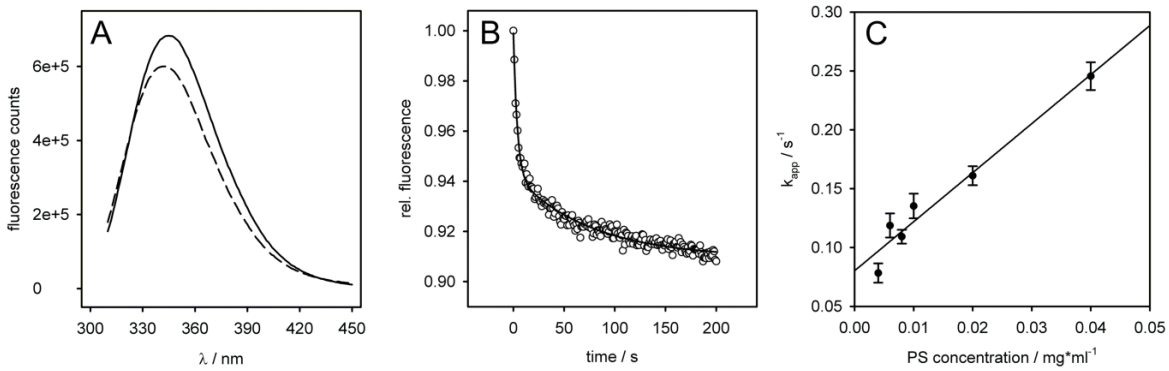

Figure 8.4.1: Binding of P22TSP to polysaccharide.
The preparation of O antigen polysaccharide has been described (Luderitz, Staub et al. 1966). Enzymatically inactive mutant P22TSP D392N (Baxa, Steinbacher et al. 1996) was incubated with polysaccharide of *S*. Typhimurium.
A: Protein fluorescence spectra (λ_{ex}= 295 nm) of 0.17 µM P22TSP D392N with 0.06 mg/ml polysaccharide (dashed line) or without polysaccharide (solid line).
B: Kinetic trace of change in intrinsic tryptophan fluorescence of P22TSP D392N (λ_{em}= 350 nm) at 10 °C (open circles). Relaxation to binding equilibrium could best be described with a biexponential model with k_1= 0.262 ± 0.017 s^{-1} and k_2= 0.013 ± 0.001 s^{-1} (solid line).
C: Apparent rate constants k_{app} were determined at different polysaccharide concentrations as illustrated in B. The determination of the dissociation rate constant from a linear plot of k_{app} against polysaccharide concentration has been described (Baxa, Cooper et al. 2001). Accordingly, the ordinate intercept of the linear regression yields a k_{diss} of 0.081 ± 0.006 s^{-1}. Error bars show the standard deviation of three independent experiments for each k_{app}.

From this a dissociation rate constant k_{diss} for polysaccharide of 0.08 s^{-1} was calculated (Figure 8.4.1 C), which indicates strong binding. The dissociation rate constant for an octasaccharide of *S*. Enteritidis was determined previously in stopped flow experiments to be 0.25 s^{-1} (Baxa, Cooper et al. 2001). This means that the oligosaccharide dissociates about 3 times faster than the polysaccharide. The P22TSP trimer has three identical, independent binding sites with affinity for octasaccharide O antigen repeats. Polysaccharide can hence be regarded as a multivalent ligand which binds to P22TSP with high avidity. Moreover, only the high affinity binding sites add to P22TSP avidity. If further low affinity carbohydrate binding sites were present in P22TSP the difference of dissociation rates between polysaccharide and octasaccharide would be more pronounced.

8.5 Role of polysaccharide during P22 phage infection *in vivo*

Different roles of P22TSP during the infection could be imagined from our binding experiments. Unambiguously, phages need P22TSP to recognize their hosts by detecting the correct serotype. Moreover, via the O antigen phage P22TSP might sense the presence of prophages. These cause serotype conversions, i.e. glucosylations or acetylations of O antigens , that TSP no longer can bind to or cleave and that result in an effective infection barrier (Iwashita and Kanegasaki 1973; Brussow, Canchaya et al. 2004). Moreover, it is reasonable that phages have to be fixed and

positioned on the cell surface in order to inject their DNA properly. To show that strong binding is a prerequisite for infection we incubated P22 phages with LPS for different times prior to infection of *S.* Typhimurium (Figure 8.5.1).

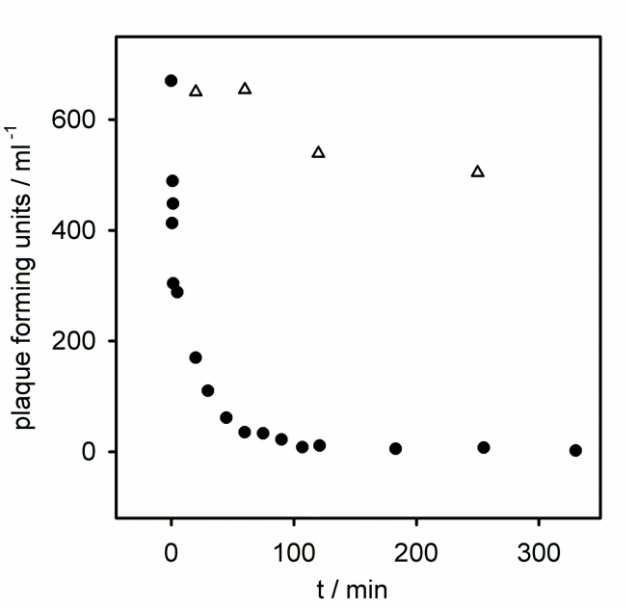

Figure 8.5.1: Inhibition of phage P22 *in vivo* plaque forming by lipopolysaccharide.
The plaque forming assay and the preparation of LPS have been described elsewhere (Luderitz, Staub et al. 1966; Eriksson and Lindberg 1977). $8*10^4$ P22 phages were incubated with 2.5 µg/ml of purified *S.* Typhimurium LPS (filled circles) or buffer (open triangles) for different time periods prior to plating on *S.* Typhimurium. Plaques were counted after overnight incubation at 37 °C.

After 90 s of LPS incubation infectivity already decreased and was only half of the initial value. This time scale is in good agreement with the kinetics of polysaccharide binding to P22TSP as described above. After 100 minutes no more infective phage could be detected. Hence the polysaccharide moieties of LPS have bound to the phages and blocked the binding sites on the TSP so that it cannot position on the host cell membrane for infection. However, we cannot exclude additional interactions of LPS core sugars or lipid A moiety with the phages. Our results clearly indicate that for proper infection phage P22 has to bind the *Salmonella* host O antigen with its TSP. For this they recognize stretches of two repeating units on the polysaccharide. Each phage has up to six TSP [7] and hence can bind to the host cell membrane with high avidity. Still, more information is needed to draw a complete picture of the infection process, especially about the role of the endorhamnosidase activity. It might on the one hand help the phage to get closer to the membrane to sense a secondary receptor. On the other hand enzymatic cleavage of LPS would be advantageous when newly synthesized phages have to dissociate from LPS on cell debris after lysis of the host bacterium (Bayer, Takeda et al. 1980). TSP is able to cleave O antigen on LPS, so why would phages not simply release themselves from LPS and subsequently infect *Salmonella*, in contrast to our observations in the plaque forming assay where phages get inactivated? Experiments with oligosaccharides as described above showed that binding equilibriums are fast compared to hydrolysis. Hence, one might speculate that after fixation of phage on the LPS

membrane via O antigen binding an additional event takes place that would be able to start DNA release. However, new experimental setups are needed to detect this. In future these might help to explain how carbohydrate recognition events direct the following steps of the infection mechanism.

8.6 Acknowledgements

We thank Carolin Doering for excellent technical assistance.

8.7 References

1 Nikaido, H. (2003) Molecular basis of bacterial outer membrane permeability revisited. Microbiol. Mol. Biol. Rev. 67, 593-656

2 Leiman, P. G., Kanamaru, S., Mesyanzhinov, V. V., Arisaka, F. and Rossmann, M. G. (2003) Structure and morphogenesis of bacteriophage T4. Cell Mol Life Sci. 60, 2356-2370

3 Lindberg, A. A. (1977) Bacterial Surface Carbohydrates and Bacteriophage Adsorption, In Surface carbohydrates of the procaryotic cell (Sutherland, I., ed), pp 289 - 356, Academic Press, London.

4 Israel, V. (1978) A model for the adsorption of phage P22 to Salmonella typhimurium. J. Gen. Virol. 40, 669 - 673

5 Bayer, M. E., Takeda, K. and Uetake, H. (1980) Effects of receptor destruction by Salmonella bacteriophages epsilon 15 and c341. Virology 105, 328-337

6 Liu, C., Eichelberger, M. C., Compans, R. W. and Air, G. M. (1995) Influenza type A virus neuraminidase does not play a role in viral entry, replication, assembly, or budding. J. Virol. 69, 1099-1106

7 Israel, J. V., Anderson, T. F. and Levine, M. (1967) In vitro morphogenesis of phage P22 from heads and base-plate parts. Proc. Natl. Acad. Sci. 57, 284-291

8 Baxa, U., Steinbacher, S., Miller, S., Weintraub, A., Huber, R. and Seckler, R. (1996) Interactions of Phage P22 Tails with Their Cellular Receptor, *Salmonella* O-Antigen Polysaccharide. Biophys. J. 71, 2040-2048

9 Luderitz, O., Staub, A. M. and Westphal, O. (1966) Immunochemistry of O and R antigens of Salmonella and related Enterobacteriaceae. Bacteriol Rev. 30, 192-255

10 Steinbacher, S., Seckler, R., Miller, S., Steipe, B., Huber, R. and Reinemer, P. (1994) Crystal structure of P22 tailspike protein: interdigitated subunits in a thermostable trimer. Science. 265, 383-386

11 Eriksson, U., Svenson, S. B., Lonngren, J. and Lindberg, A. A. (1979) Salmonella phage glycanases: substrate specificity of the phage P22 endo-rhamnosidase. J. Gen. Virol. 43, 503-511

12 Steinbacher, S., Baxa, U., Miller, S., Weintraub, A., Seckler, R. and Huber, R. (1996) Crystal structure of phage P22 tailspike protein complexed with *Salmonella* sp. O-antigen receptors. Proc. Natl. Acad. Sci. USA. 93, 10584-10588

13 Baxa, U., Cooper, A., Weintraub, A., Pfeil, W. and Seckler, R. (2001) Enthalpic barriers to the hydrophobic binding of oligosaccharides to phage P22 tailspike protein. Biochemistry 40, 5144-5150

14 Reske, K., Wallenfels, B. and Jann, K. (1973) Enzymatic degradation of O-antigenic lipopolysaccharides by coliphage omega 8. Eur. J. Biochem. 36, 167-171

15 Lindberg, A. A., Wollin, R., Gemski, P. and Wohlhieter, J. A. (1978) Interaction between bacteriophage Sf6 and Shigella flexneri. J. Virol. 27, 38-44

16 Iwashita, S. and Kanegasaki, S. (1973) Smooth specific phage adsorption: endorhamnosidase activity of tail parts of P22. Biochem. Biophys. Res. Commun. 55, 403-409

17 Brussow, H., Canchaya, C. and Hardt, W. D. (2004) Phages and the evolution of bacterial pathogens: from genomic rearrangements to lysogenic conversion. Microbiol. Mol. Biol. Rev. 68, 560-602

18 DeLano, W. L. (2002) The PyMOL Molecular Graphics System, DeLano Scientific, San Carlos, CA, USA.

19 Eriksson, U. and Lindberg, A. A. (1977) Adsorption of phage P22 to *Salmonella typhimurium*. J. Gen. Virol. 34, 207-221

9 Tailspike interactions with lipopolysaccharide effect DNA ejection from phage P22 *in vitro*

Chapter 9 was originally published as

Tailspike interactions with lipopolysaccharide effect DNA ejection from phage P22 particles *in vitro*

Dorothee Andres, Christin Hanke, Ulrich Baxa, Anaït Seul, Stefanie Barbirz, and Robert Seckler.

Journal of Biological Chemistry. 2010. **285**(47): 36768-36775.

Dorothee Andres designed and performed all shown experiments with exception of the gel filtration analysis. DNA ejection studies were performed together with a supervised undergraduate student, Christin Hanke. Dorothee Andres evaluated all data, analyzed them in context and wrote the first manuscript.

9.1 Summary

Initial attachment of bacteriophage P22 to the *Salmonella* host cell is known to be mediated by interactions between lipopolysaccharide (LPS) and the phage tailspike proteins (TSP), but the events that subsequently lead to DNA injection into the bacterium are unknown. We used the binding of a fluorescent dye and DNA accessibility to DNase and restriction enzymes to analyze DNA ejection from phage particles *in vitro*. Ejection was specifically triggered by aggregates of purified *Salmonella* LPS but not by LPS with different O antigen structure, by lipid A, phospholipids, or soluble O antigen polysaccharide. This suggests that P22 does not use a secondary receptor at the bacterial outer membrane surface. Using phage particles reconstituted with purified mutant TSP *in vitro*, we found that the endorhamnosidase activity of TSP degrading the O antigen polysaccharide was required prior to DNA ejection *in vitro* and DNA replication *in vivo*. If, however, LPS was pre-digested with soluble TSP, it was no longer able to trigger DNA ejection, even though it still contained 5 O antigen oligosaccharide repeats. Together with known data on the structure of LPS and phage P22, our results suggest a molecular model, according to which TSP position the phage particle on the outer membrane surface for DNA ejection. They force gp26, the central needle and plug protein of the phage tail machine, through the core oligosaccharide layer and into the hydrophobic portion of the outer membrane, leading to refolding of the gp26 *lazo*-domain, release of the plug, and ejection of DNA and pilot proteins.

9.2 Introduction

Over nearly six decades *Salmonella enterica* bacteriophage P22 has been used as model system in molecular biology (Prevelige 2006). It belongs to the morphological class of *Podoviridae*, bacteriophages with short, non-contractile tails and icosahedral heads filled with dsDNA (Israel, Anderson et al. 1967). The assembly and maturation pathway of phage P22 has been studied thoroughly (Teschke and Parent 2010). After assembly of empty procapsids, the 42 kbp genome is packaged. This process terminates via a pressure dependent head-full sensing mechanism. In the following the head is sealed by gene products gp4, gp10 and gp26 to prevent DNA leakage. Finally, up to six trimers of gp9 bind to complete and stabilize the assembly (Israel, Anderson et al. 1967). Gp9 is the tailspike protein (TSP) required for host cell attachment. TSP has been studied as a model system for protein folding and protein carbohydrate interactions (Seckler 1998; Baxa, Cooper et al. 2001). Three subunits with parallel right-handed β-helix fold make up the native trimer of 215 kDa (Steinbacher, Seckler et al. 1994; Steinbacher, Miller et al. 1997). A long, surface exposed groove on each subunit specifically recognizes the O antigen portion of the *Salmonella* host LPS and harbors an endorhamnosidase activity, cleaving the α-(1→3) glycosidic linkages between rhamnose and galactose and producing dimers of 2 O antigen repeat units (RU) as the main product (Baxa, Steinbacher et al. 1996; Steinbacher, Baxa et al. 1996).

The phage genome and accompanying pilot proteins must cross the outer and inner membranes without affecting the vitality of the cell. This is a crucial event in phage infection. In the outer membrane of Gram negative bacteria, proteins are embedded in an asymmetric bilayer with phospholipids on the periplasmic side and tightly packed lipid A molecules on the extracellular side (Snyder, Kim et al. 1999). On the extracellular side lipid A is decorated with a hydrophilic sugar core. This special architecture creates an effective LPS outer barrier repulsing large hydrophilic as well as small hydrophobic molecules (Nikaido 2003). In *Salmonella* cells, about 50 % of the LPS molecules may carry polysaccharide chains of varying length and composition, the O antigen, which accounts for the high serological diversity of strains (Raetz and Whitfield 2002; Nikaido 2003). In many cases phages use LPS as first receptor initiating a series of molecular events that result in transmission of genetic material into the host cytosol. These infection mechanisms have been studied for different phage morphologies (Leiman, Chipman et al. 2004; Grayson, Han et al. 2007; Roucourt and Lavigne 2009; Chang, Kemp et al. 2010), but a general picture does not emerge. Apparently, phages developed individual strategies to surmount the two membranes and periplasmic space of Gram negative hosts. Several phage receptors in the LPS containing outer membrane have been studied in some detail. *E. coli* phage T4, which undergoes tail sheath contraction during infection, uses its long tail fibers to recognize the host cell. This

leads to the release of short tail fibers that fix the phage to the LPS core structure. *In vitro*, high LPS concentrations can promote T4 tail sheath contraction but not DNA ejection (Leiman, Chipman et al. 2004). Podovirus T7 tail fibers interact with LPS structures on different host strains and thus mediate early steps of infection (Molineux 2006). By contrast λ or T5, phages with long, non-contractile tails, do not use LPS but membrane protein receptors. *In vitro* the purified receptor proteins are sufficient to trigger DNA release (Mangenot, Hochrein et al. 2005; Grayson, Han et al. 2007). In the case of phage P22, LPS recognition and cleavage is thought to be necessary for recognition of a putative secondary receptor (Prevelige 2006). Interaction with this secondary receptor would then initiate a couple of events that enable the short-tailed P22 phage to translocate material over two membranes and the periplasmic space. *In vivo* experiments with phage T7 showed that proteins gp15 and gp16 translocate DNA to the cytoplasm (Chang, Kemp et al. 2010). However, neither the role of initial LPS binding and O antigen hydrolysis for infection nor the dependence of subsequent infection steps on these initial events have been investigated in molecular detail in podoviruses.

In the present work we have developed an *in vitro* DNA ejection assay for phage P22. We find that incubation of P22 phage particles with purified *Salmonella* LPS is sufficient to trigger complete DNA ejection of phage P22. Thus, no secondary receptor is required. Using phage particles reconstituted with mutant TSP, we find that both TSP functions, LPS binding and hydrolysis are required to trigger ejection. Based on our results we propose a molecular model of the initial steps of the phage P22 infection mechanism.

9.3 Experimental Procedures

9.3.1 Materials

Fluorescence dye YO-PRO-1 iodide (491/509) was obtained from Invitrogen GmbH (Darmstadt, Germany); 3,5-dinitrosalicylic acid (DNSA) was obtained from Sigma (St. Louis, USA). All other chemicals used during this study were of highest purity. Standard buffer in all experiments is 50 mM Tris/HCl pH7.6, 4 mM $MgCl_2$. For fluorescence measurements we used plastic cuvettes from Roth (Karlsruhe, Germany). LPS from *E. coli* IHE was received from Nina Lorenzen, Universität Potsdam, Germany.

The clear plaque mutant H5 of P22 contains a wild-type gene 9 coding for the TSP and was used in all experiments with P22 phages unless indicated otherwise. It was kindly provided by Dr. Wolfgang Rabsch, Robert Koch Institut Wernigerode, Germany. The following strains of *Salmonella enterica enterica,* serovar Typhimurium (*S*. Typhimurium) were employed: DB7155 LT2 (Winston, Botstein et al. 1979), SupE, amber suppressor strain; DB7136 LT2 (Winston, Botstein et

al. 1979); DB7136 $c_2$ts30 containing the temperature sensitive P22 prophage $c_2$ts30 (13- *am* / 9- *am*), a kind gift from Cameron Haase-Pettingell, MIT (Daniel, Chia-li et al. 2002).

9.3.2 Preparation of P22 tailspike proteins, P22 phage and P22 heads.

Purification of full length and amino-terminally shortened P22TSP has been described elsewhere (Miller, Schuler et al. 1998). TSP mutant T307K was obtained using the QuickChange Kit (Stratagene) for site-directed mutagenesis according to the manufacturer's instructions. TSP concentrations are given as molar concentrations of trimers.

P22 phages were purified from *Salmonella* Typhimurium DB 7136 LT2 cell lysates. Cells debris was centrifuged at 5000 × g for 15 min, before phages were collected at 35000 × g. Phages were resuspended in standard buffer and centrifuged in a CsCl gradient (1.3 g ml^{-1} –1.7 g ml^{-1}) for 2.5 hours at 98300 × g. Phage suspensions were harvested and dialyzed against standard buffer. Infectious particle concentrations as plaque forming units (PFU) were quantified by plating on *S*. Typhimurium DB 7136.

Phage heads for *in vitro* assembly assays were obtained from *S.* Typhimurium DB7136 $c_2$ts30. This strain contains a P22 mutant lysogen deficient in lysis (13- *am*) as well as in tailspike formation (9- *am*) and will accumulate TSP-less heads intracellularly upon induction (Daniel, Chia-li et al. 2002). To reconstitute tailed phages, phage heads were incubated with excess TSP for one hour at 37°C (Israel, Anderson et al. 1967), centrifuged in a CsCl gradient from 1.3 g·ml^{-1} to 1.7 g·ml^{-1} for 2.5 hours at 98300 × g and dialyzed against standard buffer. Infectious reconstituted phages were quantified by plating on *amber* suppressor strain *S*. Typhimurium DB 7155.

9.3.3 Determination of phage particle concentration.

Biochemical concentrations of particles were determined by 10 % SDS polyacrylamide gel electrophoresis (SDS PAGE). Phages were heated to 100 °C for 5 min in 1.5 % SDS and subjected to SDS PAGE. After silver-staining (Heukeshoven and Dernick 1988), the TSP bands were quantified densitometrically with the program Gelscan 5.1 (BioSciTec GmbH; Frankfurt, Germany) and phage concentration was calculated from a TSP standard curve under the assumption that every phage bound 6 TSP. Particle concentrations for every phage preparation were calculated from three independent experiments.

9.3.4 Lipopolysaccharide samples from S. Typhimurium.

The preparation of LPS has been described (Darveau and Hancock 1983) (Westphal 1965). After re-suspension in standard buffer, purified LPS was present in small aggregates with an average Stokes radius of 90 nm, as determined by dynamic light scattering. It was free of nucleic acids and proteins, as shown by the absence of near-ultraviolet absorbance and by SDS PAGE. Aliquots of 1

mg/ml LPS suspension were stored in standard buffer at -40°C. Lipid A and O antigen polysaccharide were obtained by the acid hydrolysis method of Freeman (Freeman and Philpot 1942), but using purified LPS as the starting material.

O antigen digestion of 1 mg/ml purified LPS with 200 µg/ml TSP was performed in standard buffer at 37°C overnight. TSP was removed by phenol:water extraction, and after excessive dialysis of the watery phase against distilled water, digested LPS was pelleted by ultracentrifugation (Westphal 1965). The product was lyophilized and stored at -20°C in standard buffer.

15% SDS PAGE of 750 ng LPS and its TSP digestion products were performed after a published protocol and gels were silver-stained (Heukeshoven and Dernick 1988).

9.3.5 Fluorescence DNA ejection assay.

5 or 10 µg/ml LPS from *S*. Typhimurium DB7155 and 1.1 µM Yo-Pro were equilibrated to 37°C in standard buffer. Dye fluorescence was excited at 491 nm and detected at 509 nm. After addition of phages to the final concentration of 3.7×10^9 particle/ml (P22) or 7×10^9 particles/ml (reconstituted phages) ejection was followed for a total of 18000 s. At the end of each ejection time course, DNAse I (10 µg/ml) was added as a control for DNA accessibility. With the concentrations used, dye and LPS were not limiting signal changes.

9.3.6 Agarose gel electrophoresis of phages.

1.8×10^{11} particles/ml of phages P22 and P22t_{mutant} were incubated with 0.24 mg/ml LPS from *S*. Typhimurium at 37°C in standard buffer over night. For a control, same amount of phages was incubated at 40°C for 2 hours in 6 M guanidinium chloride, and chemically released DNA purified with QIAprep Spin Miniprep Kit (Qiagen GmbH, Hilden). Released DNA was either cleaved with 5 to 10 U of indicated restriction enzyme (RE) or digested with 100 µg/ml DNAse I. Digestion products and assembled phages were analyzed on a 1% agarose gel and stained with ethidium bromide.

9.3.7 Saccharide binding and hydrolysis by TSP

Fluorescence titrations were performed and data fitted to an independent binding site model as described (Baxa, Steinbacher et al. 1996; Andres, Baxa et al. 2010). Hydrolytic activity of 0.09 µM TSP with 12 mg/ml O antigen polysaccharide from *S*. Typhimurium was measured at 37°C in 50 mM phosphate buffer pH 7. Initial rates of hydrolysis were determined by colorimetry with 3,5-dinitrosalicyclic acid (DNSA) (Seckler, Fuchs et al. 1989), where reducing ends are quantified using a glucose calibration curve. In this assay, the wild-type protein produced 207±17 µM

reducing ends per min, whereas the activities of the mutant TSP were reduced to 0.33±0.02 µM/min for D392N, 0.19±0.05 µM/min for D395N, and 27.5±1.7 µM/min for T307K, respectively. To determine the size of hydrolysis products, the enzymatic reaction at 10 °C was stopped with 0.125 M HCl and the product oligosaccharides were analyzed on a Superdex Peptide HR 10/30 with refractive-index detection.

9.4 P22 DNA is released specifically upon contact with LPS from S. Typhimurium.

To study elementary steps of the infection of *Salmonella enterica* by bacteriophage P22, we designed a fluorescence assay monitoring phage DNA ejection *in vitro*. We chose the fluorescent dye Yo-Pro which had been shown not to affect stability of T5 phages but to bind DNA in solution rapidly (Eriksson, Hardelin et al. 2007). When purified phage P22 was incubated with purified LPS from *S*. Typhimurium, we observed an increasing dye fluorescence signal that reached a plateau value after about 300 minutes at 37°C (Figure 9.4.1).

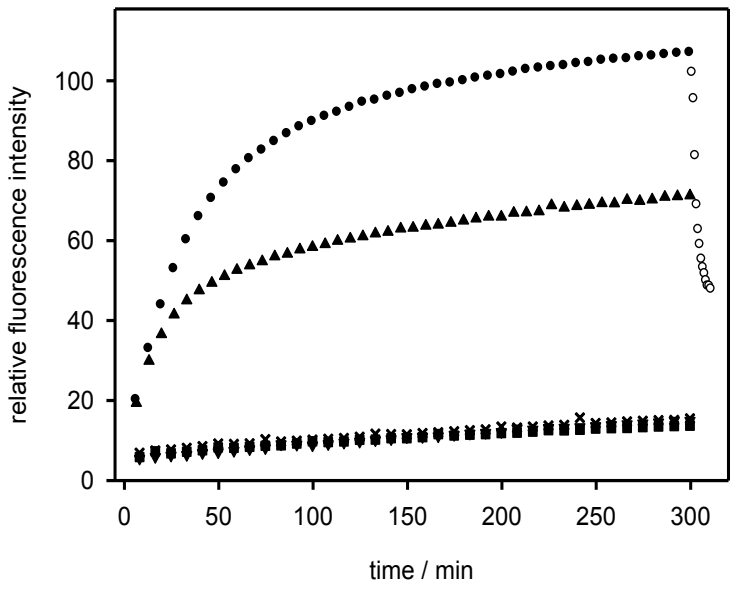

Figure 9.4.1 : *In-vitro* DNA ejection from phage P22 particles.
To follow DNA ejection at 37°C, we added 3.7×10^9 phage P22 particles to 5 µg/ml *S*. Typhimurium LPS and a fluorescent DNA-binding dye (●). Addition of DNase reversed the fluorescence increase, indicating DNA became released from the phage (○). When 11 nM free TSP were added 10 min after the phage particles, less DNA became ejected (▲). Neither LPS from *E. coli* (▼), digested *S*. Typhimurium LPS (■), nor its lipid A mixed with O antigen polysaccharide (✖) were able to trigger DNA release from phage P22. Standard deviations from three independent experiments are not more than 4% of total fluorescence for every experiment.

We concluded that DNA became accessible to Yo-Pro staining upon ejection from the phage. The time course and the extent of the rise in fluorescence intensity did not change, when the LPS concentration was increased tenfold (data not shown). By contrast, the maximum signal scaled with the number of phage particles used in the assay. The gain in fluorescence was negligible, when either phages or LPS were incubated alone. DNA was specifically released of phage P22 only with its natural receptor *S*. Typhimurium LPS. If phage P22 was incubated with LPS from *E. coli* or phospholipids extracted from *S*. Typhimurium, no fluorescence increase was observed.

To confirm that the fluorescence signal originated from DNA in solution we added DNase I after the maximum signal was reached. As a result, the fluorescence increase was rapidly reversed (Figure 9.4.1), consistent with the fact that the intercalating dye binds to double-stranded DNA with high affinity, but does not stain nucleotide fragments produced by the enzyme. The rise in dye fluorescence indicating DNA ejection occurred with a half-time of about 30 min at 37°C and without a resolvable lag phase. We refrained from using a mathematical model to describe the data, because multiple events, such as signal transduction in the ejection machinery and conformational changes during the ejection process might contribute to the observed ejection kinetics.

When we added a large excess of purified TSP simultaneously with the phage P22 to the LPS in the assay, no fluorescence intensity increase was observed. TSP is an endorhamnosidase hydrolyzing the O antigen part of LPS. Thus, in our assay, TSP either had destroyed all LPS receptors, before phage P22 was able to start DNA ejection, or excess TSP had rapidly blocked all binding sites for phage particles on the LPS aggregates. When TSP was added 10 min after phage P22, only about 60 % of the maximum fluorescence signal was reached (Figure 9.4.1). In this experiment, the signal increase observed after addition of TSP must be due to those phage particles already poised to eject their DNA at the time point of TSP addition, because free TSP completely blocked DNA ejection when added simultaneously with phage particles. The observations shed light on the origin of the time course of the fluorescence increase. If DNA ejection was triggered at the very beginning of the experiment in a large number of phages, but DNA release from a single particle was a slow process, the signal increase would persist even upon the sudden destruction or blockage of the LPS receptor by added TSP. The measured signal must therefore represent multiple fast events that add up to the final curve.

9.5 P22 releases its DNA completely upon contact with LPS.

Quantifying released DNA from the fluorescence signal is not straightforward. For that reason we analyzed phage preparations before and after incubation with LPS on ethidium bromide stained

agarose gels (Figure 9.5.1). The phage preparation itself has a net negative charge and therefore can migrate into the gel. DNA inside the capsids can be stained with ethidium bromide resulting in a fuzzy doublet band at a position between the 4 and 5 kbp markers.

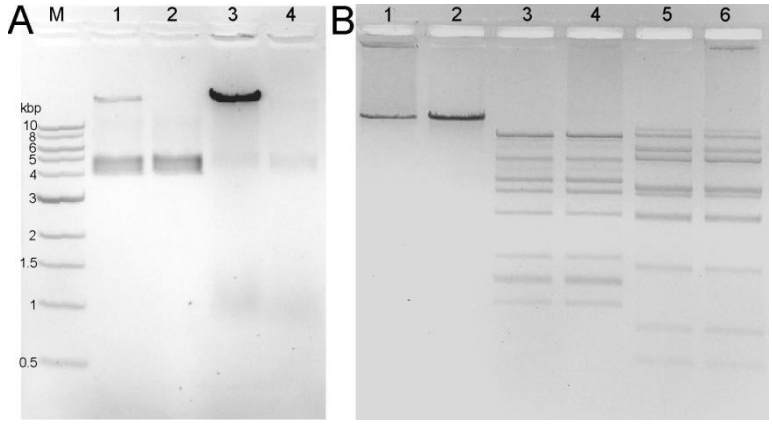

Figure 9.5.1: Agarose gel electrophoresis of phage P22 and its ejection products.
A: EtBr stained 1% agarose gel electrophoresis, with 1.75×10^9 complete P22 phages (1) or complete phage particles with 10 µg/ml DNase (2), 1.75×10^9 phage particles incubated with LPS over night (3), thereafter with 10 µg/ml DNAse (4).
B: Electrophoretic analysis of DNA released from intact phage particles upon incubation with LPS (1, 3, 5) and of phage DNA purified from denatured particles (2, 4, 6), either untreated (1, 2) or digested with AvaI (3, 4) or ClaI (5, 6).

The doublet character of this band disappears at lower agarose concentrations (not shown) and appears to be an electrophoresis artifact rather than reflect heterogeneity of the phage particles. When complete P22 DNA was liberated from phage capsids with guanidinium chloride, it only migrated very slowly in the gel, in agreement with its large size of 43 kbp. After incubation of phage P22 with LPS the band corresponding to intact phages disappeared and the amount of free phage DNA increased. DNA that was liberated by LPS could be fully digested with DNase I. Accordingly, phage particles incubated with LPS appeared intact but empty in negative-stained electron micrographs (data not shown). To further probe whether the LPS trigger provokes full or only partial ejection of phage DNA, we digested LPS-treated phage preparations with restriction endonucleases ClaI and AvaI (Figure 9.5.1 B). DNA was fully accessible to both enzymes and showed the same cleavage pattern when either released from phage particles upon incubation with LPS or purified after disruption of phage particles in 6 M guanidinium chloride. Fully assembled phages were not accessible to DNase I or restriction enzymes. From this we conclude that every P22 phage that has been triggered to eject by contact with LPS releases its DNA completely.

9.6 The endoglycosidase activity of TSP is essential for infection of *Salmonella* by phage P22.

Functional TSP are essential for phage P22, but it is not known, at which steps of the infection cycle the binding and enzymatic functions of TSP are required. TSP-less heads can be accumulated in *Salmonella* cells infected with P22 carrying amber mutations TSP gene 9 and in gene 13 required for cell lysis. When purified TSP-less heads are incubated with purified TSP, they bind irreversibly and functional phages result (Israel, Anderson et al. 1967). Due to the amber mutations in their genome, infectivity of the reconstituted phages has to be probed on a *Salmonella* strain producing an amber suppressor tRNA. Once the reconstituted phage has infected a cell, progeny with fully functional TSP is produced resulting in formation of clear plaques on the glutamine inserting amber suppressor strain *S*. Typhimurium DB7155 (Daniel, Chia-li et al. 2002). This provides us with a tailing assay to probe the role of TSP for infection.

In order to understand the role of LPS binding and hydrolysis by TSP in the infection process we reconstituted phage head preparations with different mutant tailspikes (P22t_{mutant}). Reconstituted particles were re-purified by density gradient ultracentrifugation to remove excess TSP. The mutant TSPs employed have reduced hydrolytic activity towards O antigen polysaccharide as quantified from the amount of reducing ends released. In comparison to the wild-type protein, the activity towards O antigen polysaccharide at 37 °C was reduced for TSP mutant D392N to 0.2 % and for D395N to 0.1 %, respectively (see Experimental Procedures). Interestingly, these two mutants also showed reduced infectivity in the tailing assay, where we observed $5.1\pm0.7\times10^7$ plaques for P22t_{D392N} and $2.4\pm0.7\times10^7$ plaques for P22t_{D395N}. As the same number of reconstituted particles containing wild-type TSP (P22t_{wt}) formed $4.8\pm1.0\times10^{11}$ plaques, both mutants are about a thousand times less infective than P22t_{wt}, in agreement with their reduced activity towards O antigen.

Additionally, we probed a binding deficient mutant in the tailing assay. Whereas oligosaccharide binding is unaffected by the mutations at Asp392 or Asp395 (Baxa, Steinbacher et al. 1996; Baxa, Cooper et al. 2001), no binding of O antigen octasaccharide to TSP_{T307K} was detected by isothermal titration calorimetry at saccharide concentrations up to 0.5 mM. Despite the strongly reduced binding affinity to the short oligosaccharide, TSP_{T307K} displayed high endorhamnosidase activity towards soluble polysaccharide substrate. The initial rate of reducing end formation measured for the mutant was 27.5±1.7 µM/min, about 14 % of the rate measured for the wild type under the same conditions. Although the polysaccharide binds to TSP much more tightly than short oligosaccharides (see below), the substrate concentration in the assay may not have been saturating for the mutant. Hence, the residual activity observed provides a lower estimate

and catalytic turnover appear largely unaffected by the T307K substitution. Accordingly, reconstituted P22t_{T307K} particles formed the same number of plaques in the tailing assay ($5.0\pm1.7\times10^{11}$) as particles reconstituted with wild-type TSP ($4.8\pm1.0\times10^{11}$)). We conclude that significant catalytic activity towards O antigen is required for P22 infection of *Salmonella* cells prior to phage DNA replication.

9.7 DNA ejection requires the endorhamnosidase activity of TSP.

We wanted to elucidate whether the *in vivo* infection behavior directly and solely reflected interactions of TSP with LPS. For that reason we measured *in vitro* DNA ejection kinetics of mutant reconstituted phages (Figure 9.7.1). Because of the reduced plaque forming activity of particles containing mutant TSP, we calculated P22t_{wt}, P22t_{T307K}, P22t_{D392N} and P22t_{D395N} particle concentration from a silver stained 10 % SDS PAGE to ensure identical particle concentrations. When we compared PFU to biochemically determined concentrations of phage particles, we found that around 7 % of the reconstituted P22t_{wt} particles were able to form a plaque on *Salmonella enterica*, in agreement with previous observations on the amount of TSP necessary to titrate P22 heads (Mitraki, Danner et al. 1993). The efficiency of plating determined in the same way for complete P22 particles isolated from cell lysates was 17 %.

Therefore, we doubled the amount of reconstituted phages and LPS in the ejection assay to gain enough signal for our experimental set-up. Upon incubation with LPS, phage particles reconstituted *in vitro* with wild-type TSP showed DNA ejection kinetics similar to those of particles assembled *in vivo* and the fluorescence was equally sensitive to DNase digestion. For both, P22t_{D392N} and P22t_{D395N}, the initial rate of the fluorescence increase was dramatically reduced (Figure 9.7.1).

If the final fluorescence signal observed after 300 min is set to 100 % for P22t_{wt}, the signal observed at this time for reconstituted phages P22t_{D392N} and P22t_{D395N} amounts to 44 % and 34 %, respectively. The smaller amount of DNA released with both endorhamnosidase-defective mutants is in agreement with their low infectivity. DNA ejection of phages carrying the low affinity TSP mutant T307K was somewhat decelerated compared to P22t_{wt}, although their infectivity had been indistinguishable. For P22t_{T307K} ejection was delayed about 5 min and the ejection half-time shifted to 87 min compared to 60 min for P22t_{wt}. The *lag* observed with P22t_{T307K} may be due to delayed initial adsorption or to the slightly reduced enzymatic activity of the mutant. From our observations on DNA ejection from phage particles carrying mutant TSP we conclude that the hydrolytic activity of TSP is required for efficient DNA ejection in the infection cycle of phage P22.

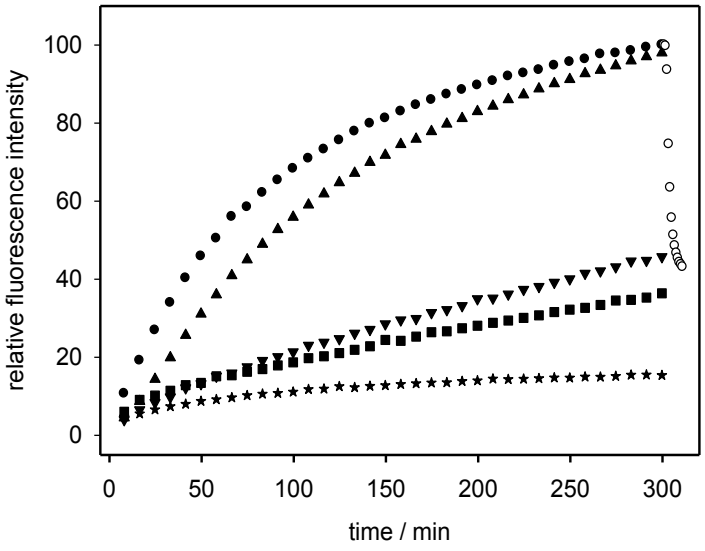

Figure 9.7.1: TSP endorhamnosidase mutations delay DNA ejection from phage P22.
The fluorescence ejection assay was used to follow DNA release from reconstituted phage particles carrying different TSP variants. To 10 µg/ml *S.* Typhimurium LPS and the fluorescent dye, 7.2×10^9 reconstituted phage particles (P22t_{mutant}) were added at 37°C: ●, P22t_{wt}; ▲, P22t_{T307K}; ▼, P22t_{D392N}; ■, P22t_{D395N}. ○, fluorescence decrease after addition of DNase I; ★, P22t_{wt} control without LPS. The standard deviation of fluorescence signals between repeated experiments was below 0.5%.

9.8 Tailspike proteins are necessary for attachment and direction of phage towards the membrane.

Affinity and activity of TSP had been extensively studied before with oligosaccharides (Baxa, Steinbacher et al. 1996), but less extensively with its natural substrate, which is O antigen polysaccharide. P22TSP has three binding sites with micromolar affinity for O antigen octasaccharide fragments. The binding affinity increases only slightly with increasing length of oligosaccharides (Baxa, Cooper et al. 2001). Unfortunately, the polydisperse character of O antigen polysaccharide hampers the quantification of TSP affinity towards O antigen. Nevertheless, we titrated a TSP mutant defective in polysaccharide cleavage (TSP_{D392N}) with polysaccharide and measured protein fluorescence quenching. We obtained a kinked binding curve, characteristic for high affinity binding (Figure 9.8.1 A). Binding equilibrium was thus largely driven towards the TSP polysaccharide complex due to the multivalent nature of the polysaccharide ligand. For a phage with six TSP and 18 binding sites this means strong fixation on the O antigen receptor.

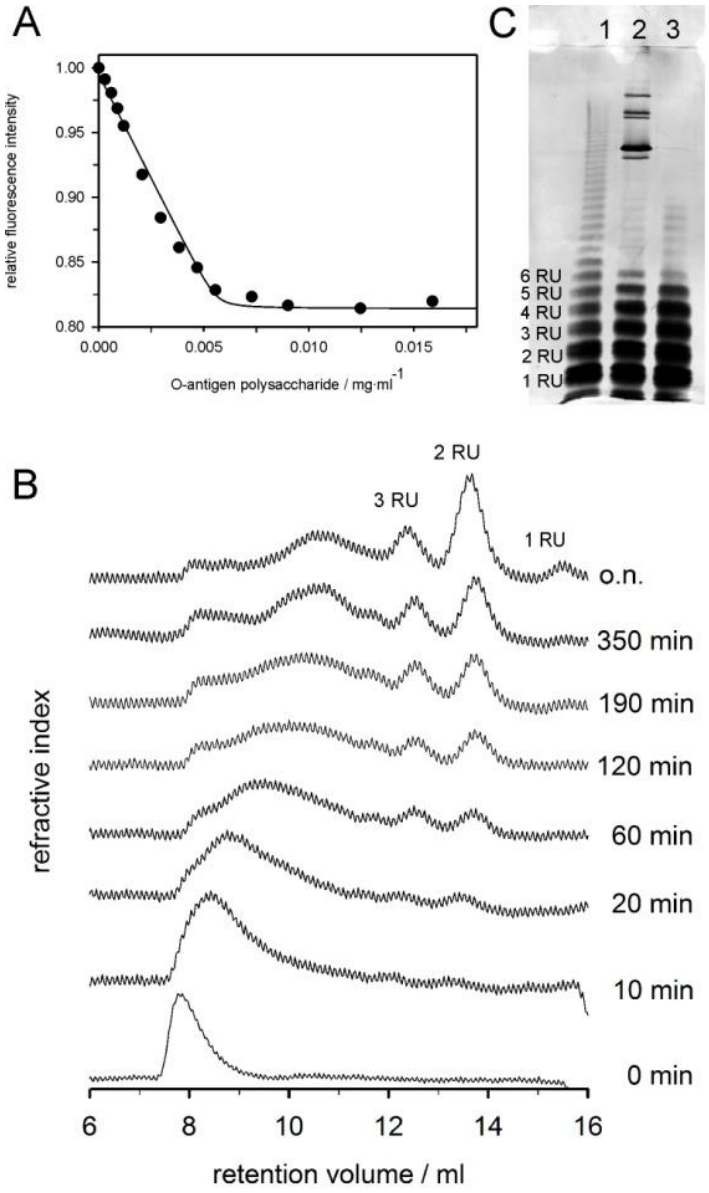

Figure 9.8.1: Binding and hydrolysis activity of TSP.
A: Fluorescence binding titration of *S*. Typhimurium O antigen polysaccharide at 10 °C. Tryptophane fluorescence of 0.11 µM TSP_{D392N} was excited at 295 nm and quenching upon binding followed at 350 nm.
B: Kinetics TSP O antigen polysaccharide cleavage. Samples were analyzed after the indicated times on a Superdex Peptide HR 10/30.
C: 15 % SDS PAGE of LPS cleavage products. 15% silverstained SDS PAGE of (1) purified LPS fraction, (2) LPS incubated with phage P22 and (3) LPS digested with TSP and purified.

Hydrolysis of *Salmonella* O antigen by P22 TSP produces oligosaccharide fragments comprising at least two RU (Iwashita and Kanegasaki 1976). We incubated polysaccharide with TSP and analyzed the kinetics of product formation using gel filtration (Figure 9.8.1 B). Elution profiles of hydrolysis products showed large cleavage products after short incubation times and illustrated that TSP is an endoenzyme that is able to bind with high affinity on any site on its substrate. With incubation time, the exclusion peak broadens and is shifted towards smaller sizes before cleavage end products octa- and tetrasaccharides appear. These end products had also been observed earlier in preparations with the phage (Iwashita and Kanegasaki 1976).They are a consequence of the special arrangement of catalytic residues which lie at the end of a high affinity binding pocket (Figure 9.10.1 A).

9.9 O antigen hydrolysis and DNA ejection are not separable processes.

We wanted to analyze whether phage P22 can destroy its LPS receptor completely. Therefore, we incubated it with purified LPS and analyzed chain distributions using SDS-PAGE (Figure 9.8.1 C). Undigested LPS showed a typical ladder pattern representing the distribution of different O antigen chain lengths with different numbers of repeat units (RUs). Upon incubation of LPS with phage P22 at 37°C, LPS molecules with long O antigen chains disappeared and short chains accumulated. Interestingly, only bands up to five RUs enriched upon incubation with phage and molecules carrying six repeat units appeared to be cleaved poorly. Moreover, we obtained the same cleavage pattern when we incubated LPS with purified TSP instead of whole phages. Prolonged incubation times and high TSP concentrations could not shift the observed pattern towards shorter chain lengths. Probably TSP access to the LPS core is sterically hindered. This is in agreement with our gel filtration experiment where we did not observe any short chained core saccharides.

We purified LPS after digesting long chains with TSP and used this short chain LPS in our *in vitro* ejection assay. Digested LPS is not longer able to trigger phage DNA ejection (Figure 8.3.1). Moreover, we tested whether simultaneous enzymatic cleavage of soluble O antigen polysaccharide in the presence of lipid A molecules was sufficient to promote DNA expulsion. No signal was obtained, independent of the order of addition of lipid A and polysaccharide (Figure 8.3.1). This clearly showed that ejection of DNA does not occur solely upon hydrolysis of O antigen polysaccharide. Apparently, O antigen receptor and lipid A have to be assembled in one molecule and built up one LPS leaflet to promote DNA release. Cleavage of O polysaccharide by TSP and DNA ejection appear to be intimately linked processes and ejection is not triggered by a structure on LPS that merely became accessible upon digestion of O antigen chains.

9.10 Discussion

Although it has long been established that the interaction of tailspikes with LPS is responsible for initial adsorption of phage P22 and thus determines its host range (Lindberg 1977), a putative secondary receptor that may trigger DNA ejection has remained elusive (Chang, Weigele et al. 2006). Prompted by our observation that purified LPS inactivates phage P22 particles *in vitro* (Andres, Baxa et al. 2010), we set up a DNA ejection assay using a fluorescent DNA binding dye. We found that DNA ejection from the phage particles was efficiently triggered when P22 virions were incubated with full length LPS from *S.* Typhimurium. The interactions resulting in DNA release are highly specific. No ejection was observed when P22 virions were exposed to LPS from

a different enterobacterium, to *Salmonella* phospholipids or to soluble *S*. Typhimurium O antigen polysaccharide. Under our *in vitro* conditions, LPS forms multilamellar and rigid structures the outer surfaces of which resemble the outer membrane of Gram negative bacteria (Snyder, Kim et al. 1999; Nikaido 2003). Neither upon incubation with EDTA-treated LPS that has lost its multilamellar character, nor with LPS pre-digested with TSP or with lipid A aggregates do we observe any DNA release. Our results suggest that LPS is the only receptor for phage P22 at the *Salmonella* outer membrane.

Six TSP together form the cell attachment apparatus of phage P22. Its interaction with the outer membrane LPS is multivalent and thus essentially irreversible. Although TSP display endorhamnosidase activity and hydrolyze the LPS O antigen chains, phages will not dissociate from LPS upon a single hydrolysis event. This confers processivity to O antigen hydrolysis. Processive TSP have also been found in phages infecting encapsulated bacteria (Schwarzer, Stummeyer et al. 2009). Here, processivity appears to result from secondary polysaccharide binding sites on the same protein, whereas there is no evidence for secondary LPS binding sites on P22 TSP. Our *in-vitro* tailing experiments shed light on the role of this hydrolytic activity in early steps of the infection cycle but does not allow us to access functions in later stages. This is because the mutant TSPs used to complement the heads *in vitro* are not encoded in the phage genome and hence, the phage progeny does not carry mutant TSP. We found that reconstituted phage particles are unable to initiate plaque formation, when they carry mutant TSP lacking endorhamnosidase activity. This proves that O antigen hydrolysis function is required prior to phage DNA replication. Moreover, DNA ejection from reconstituted particles *in vitro* was dramatically slowed down when the particles carried mutant TSP and was correlated to the residual endorhamnosidase activity of the TSP mutants attached to the phage heads. Hence, O antigen hydrolysis is prerequisite to DNA ejection. In addition to its role in the early phase of the infection cycle, the receptor destroying activity of TSP might also be important to prevent newly assembled P22 particles from sticking to cell wall debris upon lysis. This would be analogous to the role of influenza virus neuraminidase (Liu, Eichelberger et al. 1995). We observed that free TSP can prevent LPS-triggered DNA ejection. Accordingly, the receptor-inactivating activity of free TSP released upon cell lysis would avoid the loss of infectious phages due to interaction with membrane fragments. Indeed, TSP is encoded in a late structural gene and abundantly synthesized so that excess TSP not bound to phage particles accumulates in the cell (Berget and Poteete 1980) and is released upon cell lysis. Consequently, in our *in vitro* experiments we observed that LPS pretreated with soluble TSP endorhamnosidase cannot trigger DNA ejection. Therefore, O antigen hydrolysis appears important both in early and late phases of the infection cycle. Its function in the early phase by far surpasses the simple clearing the

polysaccharide layer to render the cell surface accessible for P22 particles. Rather, hydrolysis by TSP must be intimately connected to the whole triggering process.

From our experiments we propose a molecular model of how infection of phage P22 might be started. As a first step, phage binding to LPS O-polysaccharide occurs via 6 trimeric TSP. Then, concomitantly with O antigen cleavage by TSP, the phage particle decends towards the outer membrane surface. We observed that O antigen cleavage reproducibly stops at a level of 5 RU attached to the lipid A portion and the LPS core saccharides, when LPS particles are treated with TSP or P22 phage. A similar number of remaining O antigen repeats has been observed upon treatment of aldehyde-fixed *Shigella* cell with phage Sf6 TSP, a close functional and structural relative of P22 TSP (Chua, Manning et al. 1999; Muller, Barbirz et al. 2008). To us this suggests that the length of the remaining O antigen is specific and functional and may be intimately linked to the signal transmitted to open the portal. According to molecular modeling studies combined with X-ray powder diffraction experiments, 5 O antigen repeats on *S*. Typhimurium LPS can be estimated to extend on average 7 nm from the lipid A-core portion (Kastowsky, Gutberlet et al. 1992).

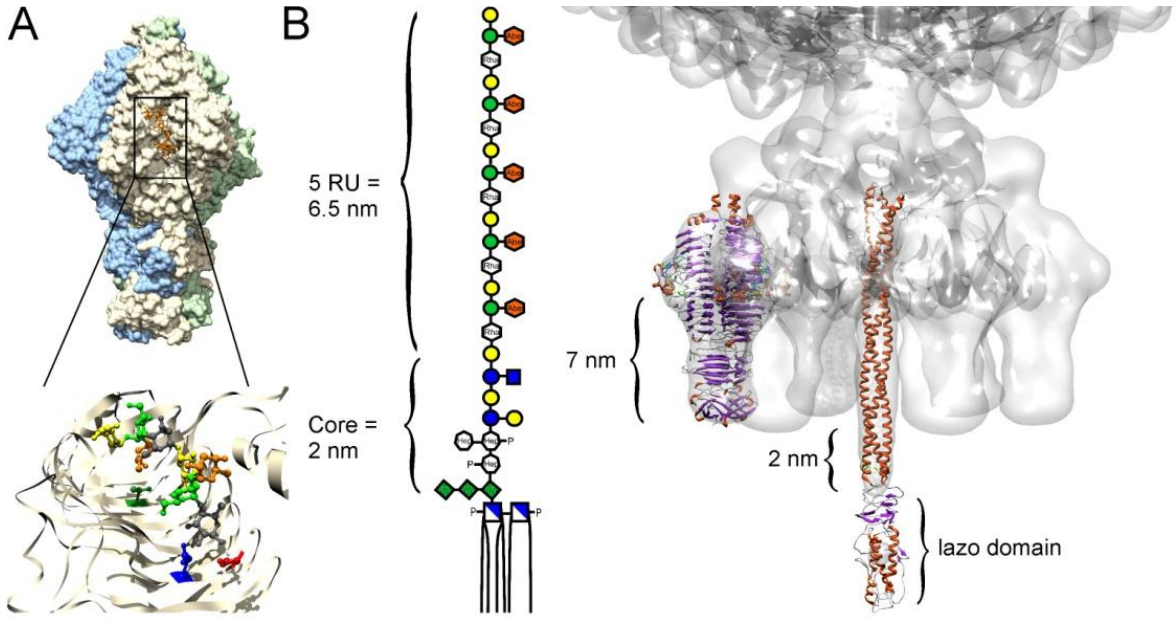

Figure 9.10.1: Putative DNA release mechanism of phage P22 triggered by LPS.
A: Tailspike binding and activity site. Binding cleft in the trimeric protein of P22 TSP (Steinbacher, Baxa et al. 1996). Residues carrying the mutations at T307 (green) and in the active site D392 (red) and D395 (blue) are indicated.
B: The cell-attachment apparatus of phage P22. TSP and gp26 plug crystal structures were modeled into the cryo-EM structure of phage P22 (Steinbacher, Miller et al. 1997; Pettersen, Goddard et al. 2004; Chang, Weigele et al. 2006; Olia, Casjens et al. 2007). Dimensions of the LPS digestion product containing 5 O antigen repeats (Kastowsky, Gutberlet et al. 1992) match the distances in the model and suggest insertion of the gp26 *lazo*-domain into the hydrophobic part of the outer membrane, presumably resulting in its refolding. Sugar icons are according to Varki (Varki, Cummings et al. 2009), an orange symbol was added for the abequose.

More extended conformations may protrude up to 8.5 nm from the outer membrane lipid A layer. The distance between the C-terminal tip of TSP and the O antigen cleavage site also amounts to 7 nm (Figure 9.10.1 B). Hence, phage TSP could cleave and slide down the O antigen until encountering with their tips a barrier made of LPS core and lipid A regions. Indeed, these have been shown to be far more inflexible than the O antigen portion (Kastowsky, Gutberlet et al. 1992). The C-terminal tips of the tailspikes, however, are not the outermost parts of P22 tail machines. It is plug protein gp26 that extends pronouncedly from the bottom of the tail structure (Lander, Khayat et al. 2009) (Olia, Casjens et al. 2007). In a position of the phage particle with TSP attached to the last O antigen repeats susceptible to cleavage, gp26 would certainly penetrate the core structure that has a length of about 2 nm (Kastowsky, Gutberlet et al. 1992).

We propose this gp26-membrane interaction to be the crucial event to trigger the ejection. Driven by the TSP interaction with the inner parts of the O antigen polysaccharide, gp26 would have to insert into the lipid core region, which would then produce a conformational change in the rather flexible *lazo*-domain at the tip of gp26 (Bhardwaj, Olia et al. 2007; Olia, Casjens et al. 2007; Olia, Casjens et al. 2009). Together, TSP and gp26 may serve as a surface pressure sensor to initiate DNA release in analogy to the head-full sensing during DNA packaging into the capsid. Here, a subtle conformational change in the portal protein induces release of DNA terminase and binding of gp4 which initiates the tail assembly, preventing DNA leakage from the phage head (Strauss and King 1984; Lander, Tang et al. 2006; Lander, Khayat et al. 2009). Accordingly, a conformational change in the gp26 plug may lower the binding affinity towards gp10 or the more rigid part of the gp26 plug may be pulled out from the tail hub by the interaction forces exerted on the *lazo*-domain by the lipid parts of the outer membrane. Our model is compatible with the fact that at least three TSP are needed to form an infectious P22 particle, as the fixation at three polysaccharide chains would be minimally required to position the particle with the gp26 needle puncturing the outer membrane surface (Israel 1978; Lander, Tang et al. 2006). The steps following the trigger of ejection of pressurized DNA and ejection proteins remain ill-understood. Here, penetration of all three layers of the cell wall is the prerequisite for successful infection of *Salmonella.*

Once DNA release is triggered in our *in vitro* assay, the complete phage DNA is ejected without addition of external energy. Initially driven by the high pressure of DNA inside the phage head, release of linear double-stranded DNA from the particles is expected to slow down, so that the essentially complete release observed here on the time scale of the experiment may be due to solvent drag acting on the highly viscous DNA and Brownian motion of the particles. Pressure induced ejection was observed for different phages like T5 (Mangenot, Hochrein et al. 2005) and λ (Grayson, Han et al. 2007), although complete DNA translocation during infection is likely driven

by other mechanisms like diffusion, enzyme activity or protein binding, even osmotic gradients might contribute to the intrusion of DNA into the host cell (Chang, Weigele et al. 2006) (Grayson and Molineux 2007), (Inamdar, Gelbart et al. 2006). In the case of phage T7, ejection proteins have been proposed to build an extensible tail that supports the enzyme-driven transport of phage DNA across the two membranes into Gram negative cells (Molineux 2001). DNA in phage P22 is circularly permuted and does not require RNA polymerase binding sites for uptake, as the particles can carry alien transducing DNA (Schmieger 1972; Casjens and Hayden 1988). Together with DNA P22 ejects four different proteins, the role of which remains largely unclear (Israel 1977). From our *in-vitro* ejection experiments a picture emerges where during infection the outer LPS-containing membrane could be overcome initially by DNA ejection forces. Subsequently ejection proteins help in a still unknown way to transport DNA across the peptidoglycan layer and the cytoplasmic membrane (Susskind, Botstein et al. 1974; Israel 1977).

There remains a discrepancy between the time scale of our *in-vitro* ejection experiments and the duration of a lytic cycle of approximately 1 hour (Prevelige 2006). Likely, it is connected to final conformational changes triggering DNA release. When comparing DNA release kinetics of reconstituted phage particles carrying wild-type or hydrolysis defective mutants, it becomes obvious that O antigen hydrolysis alone cannot be rate-limiting. DNA ejection is not blocked completely in particles carrying mutant TSP, although their endorhamnosidase activities are reduced to less than 0.15 % of the wild-type activity. The difference between the rate-limiting step triggering DNA release *in vitro* upon contact with LPS aggregates and the obviously much faster reaction *in vivo* following adsorption onto bacterial cells might be related to the different geometries of the LPS surfaces. The aggregates formed from purified *Salmonella* LPS used here are rather small with an average radius of around 90 nm, as determined by dynamic light scattering. They are thus expected to exhibit significant surface curvature, whereas the surface of the much larger *Salmonella* cells is essentially flat. Although our model described above might predict an effect of the surface geometry on the triggering step, this hypothesis can only be tested in further experiments employing much larger LPS or lipid aggregates or flat bilayers carrying long O antigen polysaccharides.

9.11 Acknowledgements

We thank Wolfgang Rabsch for helpful discussions, Klaus Gast for help with the characterization of LPS aggregates by light scattering, Cameron Haase-Pettingell for initial instructions on phage tailing assays, and Carolin Doering for excellent technical assistance. This work was supported grants from the Deutsche Forschungsgemeinschaft (Se517/16 and Ba4046/1). D. A. is supported by a fellowship of the Leibniz Graduate School of Molecular Biophysics.

9.12 References

1. Prevelige, P. E. J. (2006) Bacteriophage P22. In: Calendar, R. (ed). *The Bacteriophages*, 2 Ed., Oxford University Press, New York
2. Israel, J. V., Anderson, T. F., and Levine, M. (1967) *Proc N A S* **57**, 284-291
3. Teschke, C. M., and Parent, K. N. (2010) *Virology* **401**(2), 119-130
4. Seckler, R. (1998) *J Struct Biol* **122**(1-2), 216-222.
5. Baxa, U., Cooper, A., Weintraub, A., Pfeil, W., and Seckler, R. (2001) *Biochemistry* **40**(17), 5144-5150
6. Steinbacher, S., Seckler, R., Miller, S., Steipe, B., Huber, R., and Reinemer, P. (1994) *Science* **265**(5170), 383-386
7. Steinbacher, S., Miller, S., Baxa, U., Budisa, N., Weintraub, A., Seckler, R., and Huber, R. (1997) *Journal of molecular biology* **267**(4), 865-880
8. Baxa, U., Steinbacher, S., Miller, S., Weintraub, A., Huber, R., and Seckler, R. (1996) *Biophys J* **71**(4), 2040-2048
9. Steinbacher, S., Baxa, U., Miller, S., Weintraub, A., Seckler, R., and Huber, R. (1996) *Proc Natl Acad Sci U S A* **93**(20), 10584-10588
10. Snyder, S., Kim, D., and McIntosh, T. J. (1999) *Biochemistry* **38**(33), 10758-10767
11. Nikaido, H. (2003) *Microbiol. Mol. Biol. Rev.* **67**(4), 593-656
12. Raetz, C. R. H., and Whitfield, C. (2002) *Annual Review of Biochemistry* **71**(1), 635-700
13. Chang, C. Y., Kemp, P., and Molineux, I. J. (2010) *Virology* **398**(2), 176-186
14. Grayson, P., Han, L., Winther, T., and Phillips, R. (2007) *Proceedings of the National Academy of Sciences* **104**(37), 14652-14657
15. Leiman, P. G., Chipman, P. R., Kostyuchenko, V. A., Mesyanzhinov, V. V., and Rossmann, M. G. (2004) *Cell* **118**(4), 419-429
16. Roucourt, B., and Lavigne, R. (2009) *Environ Microbiol* **11**(11), 2789-2805
17. Molineux, I. J. (2006) The T7 group. In: Calendar, R., and Abedon, S. T. (eds). *The Bacteriophages*, 2nd Ed., Oxford University Press, Inc., New York
18. Mangenot, S., Hochrein, M., Radler, J., and Letellier, L. (2005) *Curr Biol* **15**(5), 430-435
19. Winston, F., Botstein, D., and Miller, J. H. (1979) *J Bacteriol* **137**(1), 433-439
20. Daniel, T. K., Chia-li, L., Cameron, H.-P., Jonathan, A. K., Daniel, I. C. W., and Daniel, B. (2002) *Biotechnology and Bioengineering* **78**(2), 190-202
21. Miller, S., Schuler, B., and Seckler, R. (1998) *Protein Sci* **7**(10), 2223-2232
22. Heukeshoven, J., and Dernick, R. (1988) *Electrophoresis* **9**(1), 28-32
23. Darveau, R. P., and Hancock, R. E. (1983) *J. Bacteriol.* **155**(2), 831-838
24. Westphal, O. a. J., K. (1965) Bacterial Lipopolysaccharides: Extraction with phenol:water and further applications of the procedure. In: Whistler, R. L. (ed). *Methods in Carbohydrate Chemistry*, Academic Press, London and New York
25. Freeman, G. G., and Philpot, J. S. L. (1942) *J Biochem* **36**(3-4), 340 - 356
26. Andres, D., Baxa, U., Hanke, C., Seckler, R., and Barbirz, S. (2010) *Biochem Soc Trans* **38**, in press
27. Seckler, R., Fuchs, A., King, J., and Jaenicke, R. (1989) *J Biol Chem* **264**(20), 11750-11753
28. Eriksson, M., Hardelin, M., Larsson, A., Bergenholtz, J., and Akerman, B. (2007) *J Phys Chem B* **111**(5), 1139-1148
29. Mitraki, A., Danner, M., King, J., and Seckler, R. (1993) *J Biol Chem* **268**(27), 20071-20075
30. Iwashita, S., and Kanegasaki, S. (1976) *Eur J Biochem* **65**(1), 87-94
31. Lindberg, A. A. (1977) Bacterial Surface Carbohydrates and Bacteriophage Adsorption. In: Sutherland, I. (ed). *Surface carbohydrates of the procaryotic cell*, Academic Press, London
32. Chang, J., Weigele, P., King, J., Chiu, W., and Jiang, W. (2006) *Structure* **14**(6), 1073-1082

33. Schwarzer, D., Stummeyer, K., Haselhorst, T., Freiberger, F., Rode, B., Grove, M., Scheper, T., von Itzstein, M., Muhlenhoff, M., and Gerardy-Schahn, R. (2009) *J. Biol. Chem.* **284**(14), 9465-9474
34. Liu, C., Eichelberger, M. C., Compans, R. W., and Air, G. M. (1995) *J Virol* **69**(2), 1099-1106
35. Berget, P. B., and Poteete, A. R. (1980) *J Virol* **34**(1), 234-243
36. Chua, J. E., Manning, P. A., and Morona, R. (1999) *Microbiology* **145**(Pt 7), 1649-1659
37. Muller, J. J., Barbirz, S., Heinle, K., Freiberg, A., Seckler, R., and Heinemann, U. (2008) *Structure* **16**(5), 766-775
38. Kastowsky, M., Gutberlet, T., and Bradaczek, H. (1992) *J Bacteriol* **174**(14), 4798-4806
39. Lander, G. C., Khayat, R., Li, R., Prevelige, P. E., Potter, C. S., Carragher, B., and Johnson, J. E. (2009) *Structure* **17**(6), 789-799
40. Olia, A. S., Casjens, S., and Cingolani, G. (2007) *Nat Struct Mol Biol* **14**(12), 1221-1226
41. Bhardwaj, A., Olia, A. S., Walker-Kopp, N., and Cingolani, G. (2007) *Journal of molecular biology* **371**(2), 374-387
42. Olia, A. S., Casjens, S., and Cingolani, G. (2009) *Protein Sci* **18**(3), 537-548
43. Lander, G. C., Tang, L., Casjens, S. R., Gilcrease, E. B., Prevelige, P., Poliakov, A., Potter, C. S., Carragher, B., and Johnson, J. E. (2006) *Science* **312**(5781), 1791-1795
44. Strauss, H., and King, J. (1984) *Journal of molecular biology* **172**(4), 523-543
45. Israel, V. (1978) *J Gen Virol* **40**(3), 669-673
46. Grayson, P., and Molineux, I. J. (2007) *Curr Opin Microbiol* **10**(4), 401-409
47. Inamdar, M. M., Gelbart, W. M., and Phillips, R. (2006) *Biophys J* **91**(2), 411-420
48. Molineux, I. J. (2001) *Mol Microbiol* **40**(1), 1-8
49. Schmieger, H. (1972) *Mol Gen Genet* **119**(1), 75-88
50. Casjens, S., and Hayden, M. (1988) *Journal of molecular biology* **199**(3), 467-474
51. Israel, V. (1977) *J Virol* **23**(1), 91-97
52. Susskind, M. M., Botstein, D., and Wright, A. (1974) *Virology* **62**(2), 350-366
53. Pettersen, E. F., Goddard, T. D., Huang, C. C., Couch, G. S., Greenblatt, D. M., Meng, E. C., and Ferrin, T. E. (2004) *J Comput Chem* **25**(13), 1605-1612
54. Varki, A., Cummings, R. D., Esko, J. D., Freeze, H. H., Stanley, P., Marth, J. D., Bertozzi, C. R., Hart, G. W., and Etzler, M. E. (2009) *Proteomics* **9**(24), 5398-5399

10 Tail morphology controls Lipopolysaccharide triggered DNA release in two *Salmonella* phages

Chapter 10 was originally published as

Tail morphology controls DNA release in two *Salmonella* phages with one lipopolysaccharide receptor recognition system

Dorothee Andres, Yvette Roske, Carolin Doering, Udo Heinemann, Robert Seckler and Stefanie Barbirz;

Molecular Microbiology **83**(6): 1244-53. 2012.

The definitive version is available at

http://onlinelibrary.wiley.com/doi/10.1111/j.1365-2958.2012.08006.x/full

Dorothee Andres designed and performed all shown experiments with exception of the transmission electron microscopy, crystal structure analysis of 9NA tailspike and activity assay of 9NA tailspike mutants. DNA ejection studies were performed together with a supervised technical assistant, Carolin Doering. Dorothee Andres evaluated all data, analyzed them in context and wrote the first manuscript.

10.1 Summary

Bacteriophages recognize host cells with specific tail proteins. It is still not understood to molecular detail how the signal is transmitted over the tail to initiate infection. We have analyzed *in vitro* DNA ejection in long-tailed siphovirus 9NA and short-tailed podovirus P22 upon incubation with *Salmonella* Typhimurium lipopolysaccharide (LPS). We showed for the first time that LPS alone was sufficient to elicit DNA release from a siphovirus *in vitro*. Crystal structure analysis revealed that both phages use similar tailspike proteins (TSP) for LPS recognition. TSP hydrolyze LPS O antigen to position the phage on the cell surface. Thus we were able to compare DNA ejection processes from two phages with different morphologies with the same receptor under identical experimental conditions. Siphovirus 9NA ejected its DNA about 30 times faster than podovirus P22. DNA ejection is under control of the conformational opening of the particle and has a similar activation barrier in 9NA and P22. Our data suggest different efficiencies of signal transduction over the tail in the two morphologies given an identical initial receptor interaction event.

10.2 Introduction

Bacteriophages are widely studied molecular machines which occur with contractile (*Myoviridae*), non-contractile long (*Siphoviridae*) or short tails (*Podoviridae*) (Ackermann 2003). Mechanisms of self-assembly and double stranded DNA packaging have been described for phages of all three morphologies, e.g. for T4, lambda, phi29 or P22 (Smith, Tans et al. 2001; Lander, Tang et al. 2006; Rao and Black 2010; Aksyuk and Rossmann 2011). Cryo electron microscopy or electron tomography structures of phage particles after DNA release have shown that portal complexes undergo structural changes to open DNA ejection channels (Xiang, Morais et al. 2006; Plisson, White et al. 2007; Leiman, Arisaka et al. 2010). How an initial trigger translates into conformational change in the tail during infection, however, is not known in molecular detail.

Generally, tailed phages use specific attachment fibers or spike proteins to establish first host cell surface contacts. The variety of these receptor binding proteins reflects the host adaptation of individual phages (Casjens and Thuman-Commike 2011; Flores, Meyer et al. 2011). Tail fiber or spike proteins were found that bind to lipopolysaccharide (LPS), teichoic acids, capsular polysaccharides or proteins (Young 1967; Schwartz 1975; Yu and Mizushima 1982; Thompson, Pourhossein et al. 2010). Some phages degrade protective outer membrane components prior to recognition of a secondary receptor and irreversible attachment (Lindberg 1977). Podovirus P22 uses its tailspike protein (TSP) to recognize a long *O antigen* chain lipopolysaccharide (LPS) receptor which starts the infection process (Andres, Hanke et al. 2010). *In vitro*, protein receptors have been shown to be sufficient to trigger DNA release from siphoviruses lambda, T5, and SPP-1 (Roa 1981; Böhm, Lambert et al. 2001; São-José, Baptista et al. 2004). However, siphovirus receptors other than proteins have so far not been characterized.

Siphovirus 9NA and podovirus P22 are double stranded DNA bacteriophages that infect the same *Salmonella enterica* spp. host strains (Israel 1978; Wollin, Eriksson et al. 1981). The 9NA genome contains an open reading frame for a TSP with two functional modules (Casjens and Thuman-Commike 2011): An N-terminal capsid binding domain and a C-terminal receptor interacting part (residues 136-673). The latter shares 36% overall identity to the C-terminal receptor interacting part of P22TSP (residues 113-666). By contrast, the N-terminal capsid adaptors of P22TSP and 9NATSP do not show any similarity because they bind to morphologically different phages (Walter, Fiedler et al. 2008; Casjens and Thuman-Commike 2011). In this work, given identical host range and similar TSP we provide experimental evidence that siphovirus 9NA and podovirus P22 use the same TSP-LPS receptor system. With this, we are able for the first time to quantify and compare *in vitro* DNA ejection mechanisms triggered by identical LPS receptors in phages with two different tail morphologies.

10.3 Experimental Procedures

10.3.1 Materials

Fluorescence dye YO-PRO-1 iodide (491/509) was purchased from Invitrogen GmbH (Darmstadt, Germany). Sensor chip CM5, L1 and the Amine Coupling Kit were obtained from GE Healthcare Europe GmbH, Freiburg, Germany. All other chemicals used were of highest purity, and Milli Q water was used throughout. Standard buffer is 50 mM Tris HCl pH 7.6, 4 mM $MgCl_2$ if not otherwise stated. Bacteriophage 9NA was kindly provided by Sherwood Casjens, University of Utah, Salt Lake City, UT. *Salmonella* Typhimurium (*S*. Typhimurium) LPS, TSP digested LPS and octasaccharide preparation has been described (Baxa, Steinbacher et al. 1996; Andres, Hanke et al. 2010). *E. coli* IHE 3042 LPS was obtained from Nina Bröker, Universität Potsdam, Germany.

10.3.2 Phage preparations

Phages 9NA and P22 were propagated, purified and quantified as described previously (Andres, Hanke et al. 2010). Briefly, phages were grown at 37 °C on *S.* Typhimurium DB 7136 LT2 cells (Winston, Botstein et al. 1979). Three hours after infection, cells debris was centrifuged and phages were collected at 35000 *g* for 90 min. Phages were resuspended and further purified in a CsCl gradient at 100000 *g*.

10.3.3 Tailspike protein cloning, purification and carbohydrate interaction

The 9NATSP gene was amplified from guanidinium hydrochloride treated 9NA phage lysates with primers 5'-GGGCGCCATGGCTAATTGCAATGATTATATC-3' (9NATSP M1, amino acids 1-673), 5'-ATCCATGGCGGTATTCA-GAAGCGAAGCTGA-3' (9NATSP ΔN, amino acids 131-673), and 5'-GCGCCG-CGAAGCTTATAATGAGTATGTCACAAA-3'. The amplicons were cloned in vector pET-11d with restriction enzymes HindIII and NcoI and sequenced. 9NA and P22 TSP expression and purification followed standard protocols described previously (Barbirz, Muller et al. 2008). Mutants 9NATSP ΔN E375Q, D408N and D411N were produced using the QuikChange Kit (Agilent, Santa Clara, CA). TSP molar subunit concentrations are given throughout. All experiments were carried out with N-terminally shortenend TSP ΔN lacking capsid adaptor domains. TSP activity towards *S*. Typhimurium *O antigen* polysaccharide was quantified by monitoring reducing end formation with 3,5-dinitrosalicyclic acid (Andres, Hanke et al. 2010). Fluorescently labeled dodecasaccharides were used to probe the activity of 9NATSP mutants as described (Baxa, Steinbacher et al. 1996). LPS and digested LPS were analyzed on 12.5% SDS PAGE and silver-stained.

10.3.4 Crystallization, data collection and structure determination

9NATSP ΔN crystallized in space group 199 ($I2_13$) at room temperature by sitting drop vapor-diffusion mixing 0.4 µl of protein solution (8 mg/ml in 40 mM TrisHCl pH 7.8, 200 mM NaCl, 2 mM EDTA) with equal volumes of precipitant solution (20% polyethylene glycol monomethylether 5000, 0.1 M Bistris pH 6.5). Crystals grew within 1-2 weeks and were shock frozen in liquid nitrogen. Diffraction data to 1.5 Å resolution were collected at 100 K at beamline BL14.1 at the synchrotron-radiation source BESSY, Helmholtz-Centrum Berlin and processed with XDS (Kabsch 2010). Initial phases were obtained by molecular replacement using PHASER with P22TSP (PDB:2VFM) as search model (McCoy, Grosse-Kunstleve et al. 2007). After initial rounds of model building with COOT (Emsley and Cowtan 2004) the structure was refined to an R_{work} of 12.8% and R_{free} of 17.1%. Data collection and refinement statistics are summarized in appendix Table 15.3. Coordinates were deposited at the Protein Data Bank with accession number 3RIQ. Structural alignment of residues of the P22TSP binding site with equivalent positions in 9NATSP is described in appendix Table 15.4. Alignment and figures were generated with PyMOL (The PyMOL Molecular Graphics System, Version 1. 3, Schrödinger, LLC).

10.3.5 Surface Plasmon Resonance (SPR) experiments

P22TSP and 9NATSP were immobilized on sensor chip CM5 in a Biacore 2000 instrument (GE Healthcare, Freiburg, Germany) activated with N-(3-Dimethylaminopropyl)-N′-ethylcarbodiimide (EDC) and N-Hydroxysuccinimide (NHS). *S.* Typhimurium octasaccharides were injected at different concentrations for 2 min at a flow rate of 5 µl/min at 20 °C in 50 mM sodium phosphate, pH 7. Equilibrium signals were used to fit the binding isotherm. LPS surfaces were generated in a Biacore J instrument on an L1 chip activated with 40 mM 3-[(3-cholamidopropyl)dimethylammonio]-1-propanesulfonate (CHAPS) by injecting 190 µl 5 mg/ml *S.* Typhimurium LPS at low flow rate. TSP were injected at different concentrations at medium flow rate. Before each injection LPS surfaces were treated with 10 mM NaOH and 0.1 mg/ml BSA. Standard deviation of responses of consecutive injections on the identical surface without LPS removal was less than 5%. LPS was released from surfaces with 40 mM CHAPS.

10.3.6 Fluorescence DNA ejection assay

DNA ejection was monitored as described previously for phage P22 (Andres, Hanke et al. 2010). Briefly, 8.8×10^8 Pfu/ml 9NA phages were incubated with LPS from *S.* Typhimurium in a stirred, thermostatted plastic cuvette in the presence of 1.1 µM Yo-Pro. Dye fluorescence was excited at 491 nm and detected at 509 nm. Standard deviation was 3%. Fluorescence was corrected for background staining and temperature differences and normalized to the ejected DNA fraction.

Under receptor saturating conditions k_{open} of the conformational opening step was fitted monoexponentially. At lower LPS concentrations, two sequential first order kinetics described DNA release:

$$DNA(t) = A_0 \cdot \left(1 - \frac{1}{k_{open} - k'} \cdot \left(k_{open} \cdot e^{(-k' \cdot t)} - k' \cdot e^{(-k_{open} \cdot t)}\right)\right) \text{ with } k' = k_{bind} \cdot [LPS]$$

10.4 Phage 9NA ejects its DNA upon LPS contact in vitro

Phages 9NA and P22 showed similar efficiencies of plating on the same *S.* Typhimurium strain (Wollin, Eriksson et al. 1981). In the case of P22 purified LPS alone could trigger DNA ejection *in vitro*, showing that LPS interaction alone is sufficient to open the capsid assembly and suggesting that P22 does not use a secondary receptor at the membrane surface (Andres, Hanke et al. 2010). We used the identical *S.* Typhimurium LPS preparations employed for P22 ejection experiments and incubated them with phage 9NA *in vitro* in presence of the DNA staining dye Yo-Pro. We observed increase of dye fluorescence with the half maximum upon binding to DNA released from phage particles (Figure 10.4.1 A). Half of the total fluorescence increase was obtained after 70 seconds.

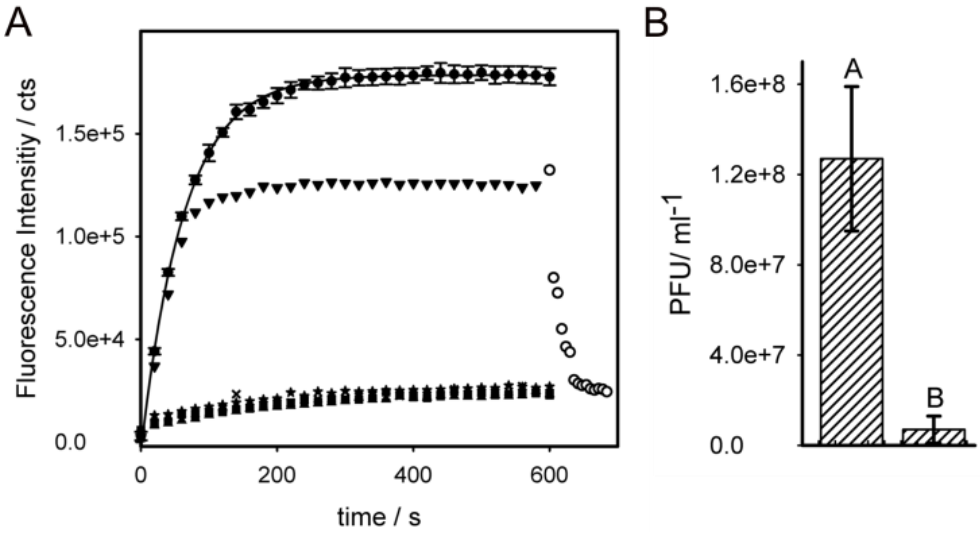

Figure 10.4.1: Incubation of siphovirus 9NA with *Salmonella* Typhimurium lipopolysaccharide
A: DNA ejection kinetics probed with Yo-Pro nucleotide staining dye fluorescence at 37 °C in the presence of 8.8x10^8 pfu/ml 9NA phages with 10 µg/ml *S.* Typhimurium LPS (closed circles), with addition of purified 9NATSP (2 µg/ml) after 55 s (triangles) or with DNase I addition (open circles). Addition of 10 µg/ml TSP digested LPS from *S.* Typhimurium does not increase fluorescence (crosses). Controls contained no LPS (asterisks), 10 µg/ml LPS from an *E. coli* smooth strain (squares). The solid line represents the monoexponential fit with kopen=1.6x10^{-2} s^{-1} for the channel opening step under receptor saturating conditions (cf. Figure 10.7.1 A). Standard deviation from five independent experiments is less than 4 %.
B: Infectivity in presence of LPS. 8.8×10^8 pfu/ml 9NA phages were incubated for 2 h at 37 °C prior to plating on *S.* Typhimurium without (A) or with (B) 10 µg/ml LPS. Clear plaques were quantified after overnight incubation. Standard deviation from three independent experiments.

The signal decreased upon addition of DNase. Hence, upon LPS incubation DNA was released from the phage and was accessible to both dye and nuclease. By contrast, phage particles incubated with polysaccharide or lipid A from *S*. Typhimurium or LPS from an unrelated *E. coli* smooth strain did not elicit any fluorescence increase which indicated that the process was highly specific. DNA obtained from LPS incubated phage particles showed high molecular mass DNA bands on agarose gels and produced restriction patterns identical to those from DNA samples purified from phage (Figure 10.4.2).

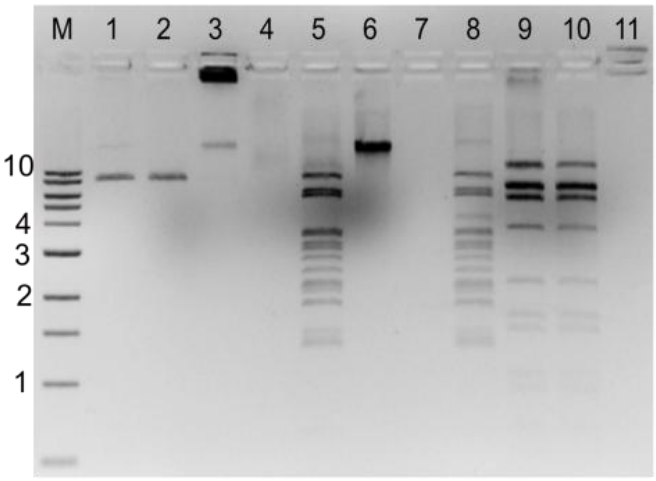

Figure 10.4.2: Agarose gel electrophoresis of whole phage, LPS treated phage or phage DNA preparations
Agarose gel electrophoresis of $6x10^{11}$ pfu/ml 9NA phages (1), incubated with 100 µg/ml DNase (2), 240 µg/ml LPS (3), same amount LPS and DNase (4), 3 U EcoRI (5) or 3 U AccI (9). 300 ng 9NA phage DNA purified from denatured particles without DNase (6) or with 20 µg/ml DNaseI (7), 3 U of EcoRI (8) or 3 U AccI (10). LPS control without phage (11) and kbp marker as indicated (M). Intact 9NA phage particles migrated into the gel as full assemblies with higher mobility and their DNA was not susceptible to nuclease.

From the *in vitro* LPS incubation experiments we therefore conclude that 9NA phage LPS interaction is a crucial step in the infection cycle and triggers DNA release. This result was further supported by the finding that incubation of phage 9NA with LPS prior to infection of *S*. Typhimurium reduced the number of plaque forming units to 5% of the initial value (Figure 10.4.1 B). LPS inactivated phage particles by releasing the DNA and thereby inhibited infection *in vivo*. Hence, 9NA and P22 eject their DNA *in vitro* upon contact with the same, single receptor LPS.

To confirm that LPS contact did not provoque unspecific disassembly of phage particles we analyzed P22 and 9NA with transmission electron microscopy (TEM). Pictures of purified phages showed intact particles filled with DNA (Figure 10.4.3 A-D). After LPS incubation particles kept their overall integrity. However, stain could now diffuse into the capsids showing that they were devoid of DNA (Figure 10.4.3 E-H). LPS preparations form complex aggregates in solution, on the EM grid they were organized in ribbon like structures as described previously (Arrow in Figure 10.4.3 E) (Richter, Vogel et al. 2011). After DNA release 9NA and P22 stayed attached to these structures with their tail machines demonstrating that this was the site crucial for phage LPS interaction (Figure 10.4.3 F,H).

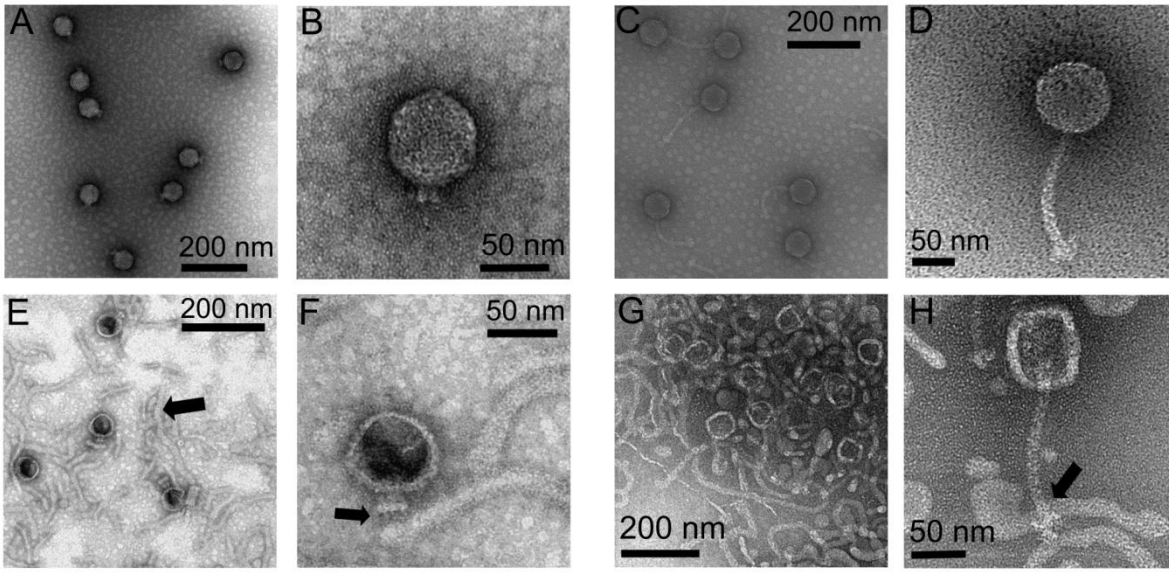

Figure 10.4.3: TEM images of phages 9NA and P22 before and after LPS incubations
6.6x10^8 Pfu/ml P22 (**A**,**B**) or 8.8×10^8 Pfu/ml 9NA (**C**,**D**) particles were stained with 2% (w/v) uranyl acetate and viewed on carbon covered grids. (**E**-**H**): Samples incubated with 10 µg/ml LPS (arrow in **E**). Tail machines of phages attached to LPS are marked by arrows (**F**, **H**).

10.5 Phage 9NA contains a structurally well conserved tailspike protein

Genome sequencing of siphovirus 9NA had unraveled the presence of an open reading frame which was annotated as TSP due to its similarity to the receptor binding domain of P22TSP (Casjens and Thuman-Commike 2011). P22TSP is the LPS interaction protein of phage P22 that triggers DNA release (Andres, Hanke et al. 2010). To check whether infectious 9NA phage particles contain a TSP similar to that of phage P22 we analyzed them in SDS PAGE. We identified a band of approximate molecular mass of 73 kDa corresponding to 9NATSP (Figure 10.5.1 A). Furthermore, we recombinantly expressed and purified 9NATSP. In SDS PAGE it migrated to the same position as the TSP band from the phage particle (Figure 10.5.1 A).

9NATSP is a highly stable, temperature and SDS-resistant native trimer like other homologous TSP (Barbirz, Becker et al. 2009). We also produced an N-terminally truncated protein, 9NATSP ΔN (residues 131-673), which only contained the P22TSP homologous parts. 9NATSP ΔN formed crystals diffracting to 1.5 Å resolution. The diffraction data were phased with molecular replacement using P22TSP as a template (appendix Table 15.3). The 9NATSP polypeptide chain folds into a right-handed parallel β-helix with thirteen consecutive rungs followed by a C-terminal part with intertwining chains in the trimer (Figure 10.5.1 B). Superposition of Cα coordinates of 9NATSP with those of P22TSP showed a root-mean-square deviation of 1.8 Å and confirmed the full fold conservation of both proteins (Figure 10.5.1 C).

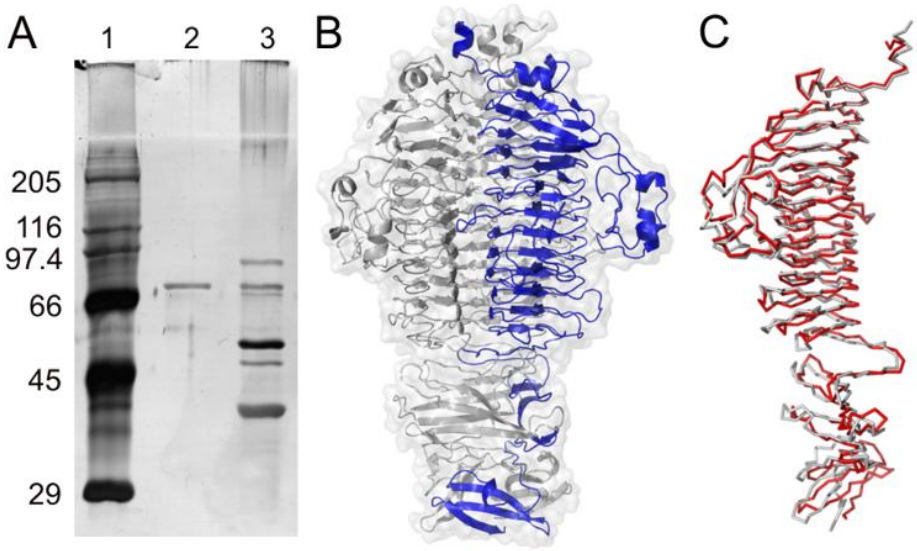

Figure 10.5.1: Characterization of 9NA tailspike protein

A: Analysis of structural proteins in mature 9NA phage particles. 20 ng heat denatured 9NATSP (lane 2) or $8.96x10^9$ Pfu heat denatured 9NA phage (corresponding to 16 ng TSP) (lane 3) applied to 10% SDS-PAGE and silver stained. Molecular mass marker (kDa) (lane 1).
B: Crystal structure of 9NATSP native trimer (residues 131-673) lacking the N-terminal particle attachment domain (ΔN) determined at 1.5 Å resolution. One trimer subunit is shown in blue.
C: 9NA TSPΔN (red) and P22 TSPΔN (gray) Cα positions align with an overall r.m.s.d. of 1.5 Å.

Generally, Cα positions in 9NATSP are less well conserved in the C-terminal part following the β-helix domain consistent with very low (20%) sequence conservation in the C-terminal 122 amino acids. Backbone positions of 9NA and P22TSP superimpose well in the β-helix domain where the polysaccharide binding and cleavage site is located in P22TSP (Steinbacher, Miller et al. 1997). More than 50 % of the 23 residues interacting with the carbohydrate ligand in P22TSP within 5 Å distance are fully conserved in 9NATSP whereas overall sequence identity of the β-helix domain is only 40 % (appendix Table 15.4). Moreover, catalytical site residues which establish the *O antigen* hydrolysis function in P22TSP (E359, D392, D395) are positionally conserved in 9NATSP (E375, D408, D411). Hence, structurally well conserved TSP are present in two morphologically different *Salmonella* phages with either long (9NA) or short (P22) tails.

10.6 9NATSP and P22TSP show similar O antigen receptor binding and cleavage behavior

Given structurally conserved oligosaccharide binding and cleavage sites in 9NA and P22TSP we assayed LPS preparations for degradation by added 9NATSP. In SDS PAGE we found a shift towards shorter chains which indicated that 9NATSP cleaved the O-polysaccharide of LPS in a similar way like P22TSP (Figure 10.6.1 A).

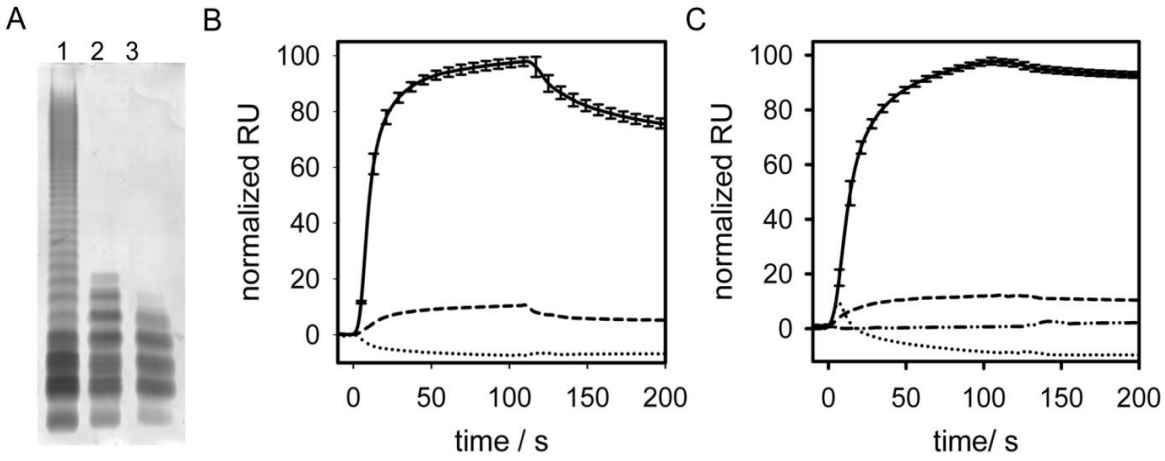

Figure 10.6.1: Interaction of 9NA and P22 tailspike proteins with *Salmonella* Typhimurium LPS

A: 12.5 % SDS PAGE silver stained of purified *S*. Typhimurium LPS (1), digested with P22TSP (2) or with 9NATSP (3). 750 ng LPS were applied to each lane.
B and **C**: Surface plasmon resonance response upon binding of tailspike proteins to immobilized LPS. Normalized response units (RU) are shown for three consecutive injections of 10 µM TSP on the same LPS surface at 20°C of
B: hydrolysis deficient mutant 9NATSPD408N (solid), hydrolysis competent 9NATSP wild type (dotted), hydrolysis deficient mutant 9NATSPD408N (dashed) or
C: hydrolysis deficient mutant P22TSPD392N (solid), hydrolysis competent P22TSP wild type (dotted), hydrolysis deficient mutant P22TSPD392N (dashed), and an unrelated coliphage HK620TSP as control (dashed-dotted). 3 % of data points are shown with standard deviation from three experiments on the same LPS surface. The LPS layer was not removed between injections.

This is in agreement with catalytic residues conserved in both TSP (see above). We generated active site mutants of 9NATSP, i.e. E375Q, D408N and D411N which lacked activity towards *O antigen* (Figure 10.6.2 A). Both, P22 and 9NATSP cleaved O-polysaccharide preparations with similar velocities. 9NATSP released 4.7 µM reducing ends per second per µM TSP, P22TSP 1.8 µM, respectively (Figure 10.6.2 B).

To underpin the role that TSPs play in phage particle attachment we analyzed the interaction of TSP with LPS by surface plasmon resonance. Hydrolysis deficient mutant proteins 9NATSP D408N and P22TSP D392N bound to surface immobilized LPS (Figure 10.6.1 B, C). By contrast, wild type TSP cleaved the *O antigen* chains as shown by the loss of refractive index base line signal. Subsequently, TSP-treated LPS surfaces could not bind any of the hydrolysis defective TSP mutants or wild type TSP. When digested LPS was removed from the surface and analyzed, it contained only short chain lengths of 4-5 repeating units (cf. lane 3 in Figure 10.6.1 A). We conclude that long chains are necessary for correct phage attachment to the LPS receptor and that the attachment is TSP mediated. 9NATSP therefore has the function of an LPS interaction organelle analogous to that of P22TSP with very similar LPS binding and hydrolysis behavior.

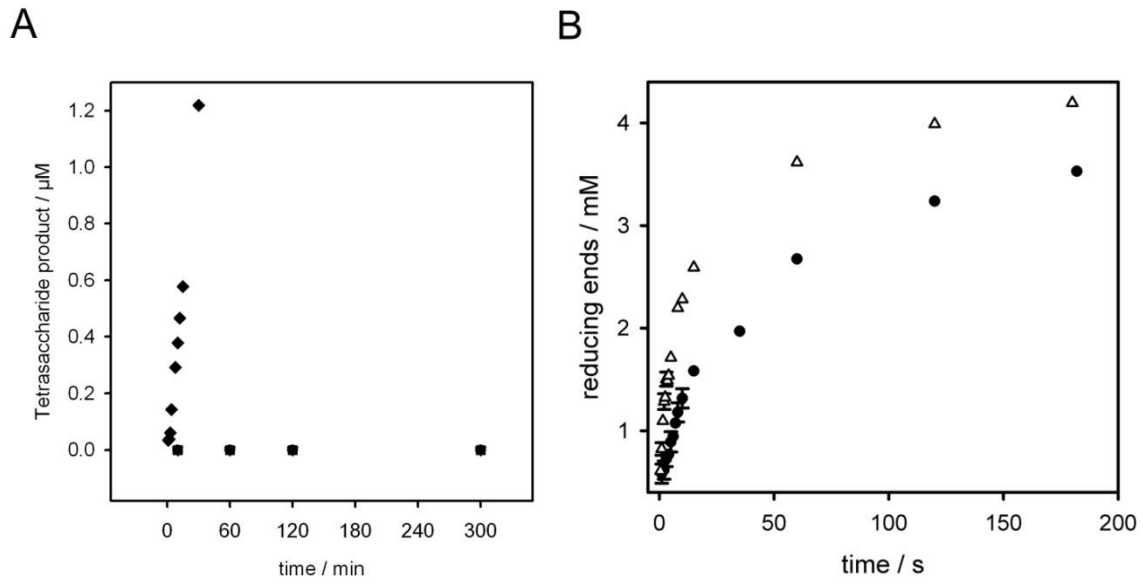

Figure 10.6.2: Hydrolysis activity assays of TSP

A: Kinetics of tetrasaccharide product formation upon incubation of dodecasaccharides with 9NATSP wild type (diamonds), or 9NATSP E375Q (circles), 9NATSP D408N (open triangles), and 9NATSP D411N (squares). The assay was performed as described previously (Baxa, Steinbacher et al. 1996). Briefly, 15 µM 7-amino-4-methylcoumarin labeled *Salmonella* Typhimurium O antigen dodecasaccharides were incubated at 10 °C with 0.5 µM TSP subunits. Aliquots were removed after different time points and the labeled tetrasaccharide cleavage product was quantified by reversed phase HPLC.
B: *Salmonella* Typhimurium O antigen polysaccharide incubated at 20 °C with P22TSPΔN (closed circles) or 9NATSPΔN (open triangles). Reducing ends were quantified with 3,5-dinitrosalicylic acid using a glucose standard. Initial linear slopes yielded v_0 = 4.7 µM s^{-1} per µM 9NATSPΔN or v_0 = 1.8 µM s^{-1} per µM P22TSPΔN. Error bars (SD) from three experiments.

10.7 Ejection kinetics of 9NA and P22 phages depend on tail morphology

As the two phages with very different tail morphologies use a conserved recognition protein for an identical receptor, we were now able to directly compare the *in vitro* mechanisms of the initial DNA release from a podo- and a siphovirus. An LPS-triggered ejection process, as found in 9NA or P22, comprises at least three steps, to which rate coefficients can be assigned:

(1) $$Phage + LPS \xrightarrow{k_{bind}} [PhageLPS] \xrightarrow{k_{conf}} [PhageLPS]^* \xrightarrow{k_{release}} [PhageLPS]_{released} + DNA$$

At first, binding and hydrolysis fix the phage to LPS. Secondly, a conformational change occurs which opens the phage tail machine. Finally, the phage particle releases its DNA. A similar model was described earlier for DNA ejection from siphovirus T5 which uses the membrane protein receptor FhuA (Chiaruttini, de Frutos et al. 2010). In our experimental setup bulk DNA fluorescence was monitored upon incubation of phage particles with LPS, and the fast process of DNA release from individual particles was not resolved (Mangenot, Hochrein et al. 2005). Hence, the conformational change and DNA release steps can be combined and a single rate coefficient

for opening and release can be assigned. With LPS in large molar excess over phage particles, k_{bind} is in the pseudo first order regime, and two sequential first order reactions should well describe DNA ejection *in vitro*:

(2) $$Phage \xrightarrow{k'} [PhageLPS] \xrightarrow{k_{open}} [PhageLPS]_{released} + DNA$$

with $$k' = k_{bind} \cdot c_{LPS}$$

Accordingly, for phage 9NA we observed concentration dependent ejection kinetics until a receptor saturation threshold was reached (Figure 10.7.1 A).

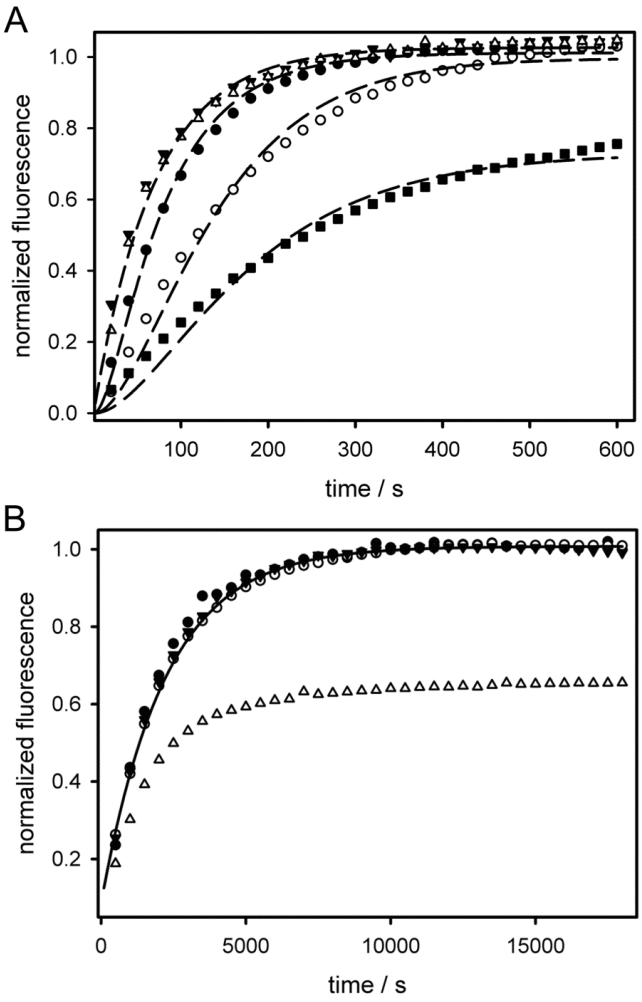

Figure 10.7.1: Lipopolysaccharide concentration dependencies of DNA ejection kinetics in 9NA and P22 phages
Kinetics of Yo-Pro nucleotide staining dye fluorescence at 37 °C in the presence of
A: 8.8x10^8 pfu/ml 9NA phages with *S*. Typhimurium LPS: 15 µg/ml (closed circles), 7.5 µg/ml (open circles), 5 µg/ml (closed triangles) 4 µg/ml (open triangles), 2.5 µg/ml (squares). Lines represent the global fit to two consecutive first order reactions with k_{open}=1.42x10^{-2} s^{-1}.
B: 6.6x10^8 pfu/ml P22 phages incubated with *S*. Typhimurium LPS: 50 µg/ml (closed circles), 10 µg/ml (open circles), 3.3 µg/ml (closed triangles), 1 µg/ml (open triangles). The line represents a monoexponential fit with k_{open}=4.5x10^{-4} s^{-1}.

At LPS concentrations above 7.5 µg/ml velocities of DNA release did not further increase, suggesting that the phage opening step became rate limiting. Under these conditions, the opening step was well described monoexponentially with a k_{open} of 1.6x10^{-2} s^{-1} (Figure 10.7.1 A). A global fit to equation 2 is in good agreement with the data. When LPS concentrations were calculated with

an assumed molecular mass of 10 kDa per chain it also provided an estimate for k_{bind} of about 10^7 M^{-1} s^{-1}. This would well match a fast and irreversible binding step. Thus, considering the sizes of phage particles and LPS aggregates, the initial binding approaches the diffusion limit. By contrast and in agreement with a different tail morphology, phage P22 ejects its DNA more slowly than phage 9NA. LPS amounts less than 3 µg/ml were insufficient to stimulate DNA release from all particles, whereas higher LPS concentrations continuously induced the whole bulk of phages to eject with the same velocity (Figure 10.7.1 B). As a result the opening step under receptor saturation is monoexponential with k_{open} of $4.5x10^{-4}$ s^{-1}.

We analyzed the energy barriers to be overcome during the channel opening step in phages 9NA and P22. To determine activation energies we monitored ejection under receptor saturation conditions, i.e. when the binding step was too fast to be resolved. Both phages showed increasing ejection velocities with increasing temperatures (Figure 10.7.2 A and B). We only fitted initial velocities because slow and unspecific staining processes of the dye Yo-Pro influenced the fluorescence signals at higher temperatures (Figure 10.7.2 C). Yo-Pro has been shown to slowly bind to phage capsids (Eriksson, Hardelin et al. 2007). Despite their different tail morphologies both phages possess parallel Arrhenius plots (Figure 10.7.2 D). Calculated Arrhenius barriers of channel opening are high with 53 kcal/mol for 9NA and 41 kcal/mol for P22, respectively. This is in agreement with similar activation energies for the channel opening step showing that both phages have conserved a similar barrier to DNA ejection.

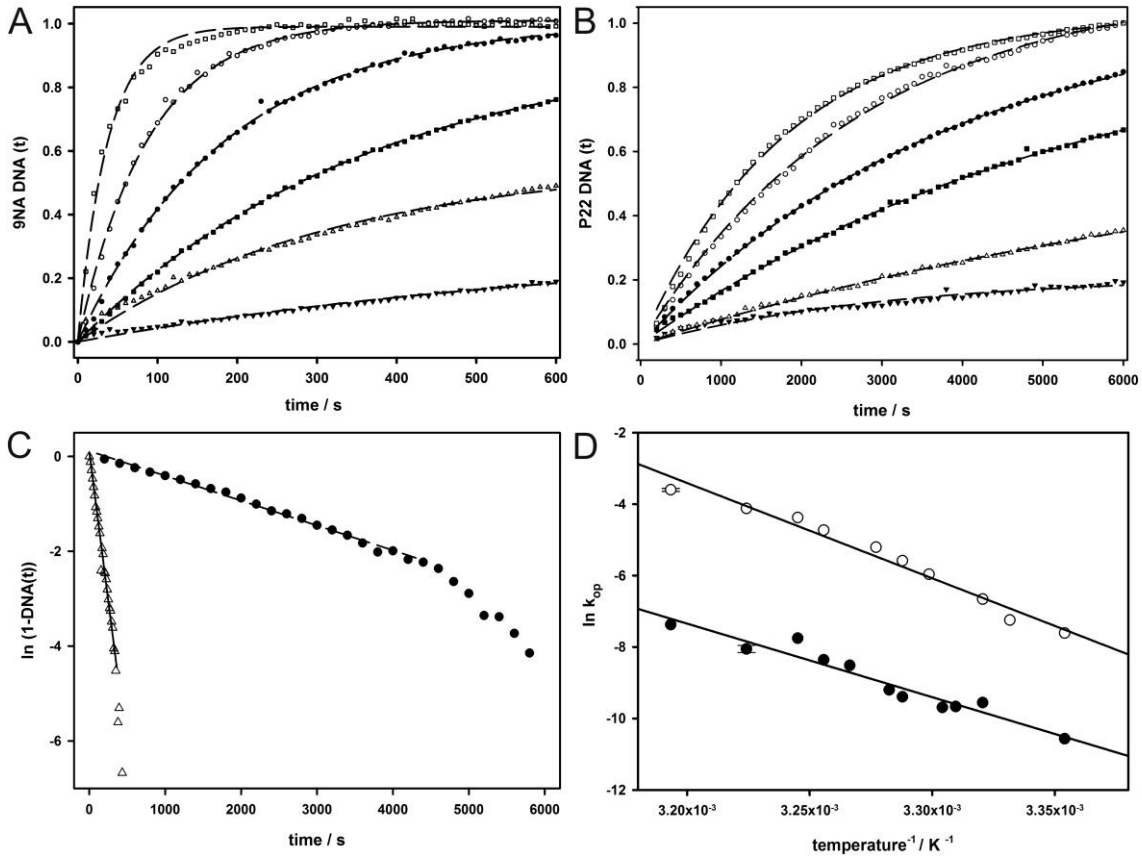

Figure 10.7.2: Temperature dependence of DNA ejection in 9NA and P22 phages

DNA ejection kinetics as probed with Yo-Pro nucleotide staining dye fluorescence were followed at 40 °C (open squares), 35 °C (open circles), 32 °C (closed circles), 30 °C (closed squares), 28 °C (open triangles), 24 °C (closed triangles).
A: 8.8x10^8 pfu/ml 9NA phages or
B: 6.6x10^8 pfu/ml P22 phages with 10 µg/ml *S*. Typhimurium LPS. Solid lines represent monoexponential fits.
C: To correct for staining artifacts after extended dye incubation times, kopen was determined from the slope of the logarithmic unejected DNA fraction as shown exemplarily for measurements at 35 °C with phage P22 (closed circles) or phage 9NA (open triangles).
D: Arrhenius plot of the opening step during DNA ejection from phages 9NA (open triangles) and P22 (closed circles). EA was calculated from a linear fit to 53±3 kcal/mol (9NA) and 41±4 kcal/mol (P22) (standard mean error from linear fit). Error bars show standard deviation of three ejection experiments at a single temperature.

10.8 Discussion

Identical receptor molecules and host attachment organelles that work in identical *in vitro* experiments offer the possibility to investigate phage ejection mechanisms in molecular detail. Opening processes of phage particles upon contact with a receptor are still not well understood. It is therefore necessary to identify underlying principles and distinguish phage species specific from general morphological features that might govern the phage opening process. In this work we have characterized the tailspike protein of Siphovirus 9NA, a structural and functional homolog to

P22TSP, the attachment organelle of Podovirus P22. Despite their overall low sequence homology comparison of structures showed the full conservation of fold and of the active site for both polysaccharide cleaving TSP. *In vitro*, both proteins showed similar enzymatic activities on the identical LPS and polysaccharide substrates, respectively. This is in agreement with the fact that both phages can infect the same *Salmonella* Typhimurium strain. For phage P22 it has been shown that interaction of its TSP with LPS is a sufficient signal *in vitro* to trigger DNA release. We therefore hypothesized that the homologous TSP might also initiate *in vitro* DNA ejection in phage 9NA. Although a number of studies had addressed *in vitro* ejection from Siphoviridae before, they all used purified protein receptors (Roa 1981; Böhm, Lambert et al. 2001; São-José, Baptista et al. 2004). We could now show for the first time for a Siphovirus that purified LPS receptor molecules could trigger DNA release from 9NA particles *in vitro*.

10.8.1 Function of LPS receptor.

Phages in our system recognize and hydrolyze the long *O antigen* chains of LPS and need no further secondary receptor (i.e. protein) for DNA release *in vitro*. We propose a model for this LPS receptor with two functions during infection. At first, it serves to position the phage on the cell surface. Polysaccharide hydrolysis is required during this step as has been shown for P22 which loses infectivity when carrying hydrolysis deficient TSP mutants (Andres, Hanke et al. 2010). Hydrolysis of *O antigen* produces LPS carrying only five to six repeat units which can no longer bind TSP (Figure 10.6.1). Moreover, TSP digested LPS cannot initiate DNA ejection *in vitro* (Figure 10.4.1) and (Andres, Hanke et al. 2010)). This emphasizes that initial attachment must function via long *O antigen* chains that serve as the multivalent receptor for the phage equipped with multiple TSP containing multiple binding sites (Andres, Hanke et al. 2010). Phage LPS interaction therefore is very strong. Accordingly, *O antigen* hydrolysis at a single TSP binding site will not dissociate the phage from the host cell surface but orient the whole phage correctly towards the membrane. For this orientation at least three phage assembled TSP are needed as shown in early infectivity studies with P22 (Israel 1978). By contrast, short *O antigen* chains cannot simultaneously bind and orient the whole phage. However, they are prerequisite for the phage to sufficiently approach the membrane in order to obtain a signal for DNA ejection. The second function of LPS must therefore be a non-specific mechanical contact with lipid A which triggers conformational opening. It is important to note that LPS forms complex aggregates in solution (Richter, Vogel et al. 2011). They might mimic the bacterial outer membrane structure and make it possible for the phage to eject its DNA *in vitro*. This is in agreement with the fact that DNA ejection in our experiments was not stimulated neither by polysaccharide nor lipid A alone: The latter lacks O antigen chains long enough for binding and orientation, polysaccharide lacks the membrane component. Hence, a

simple and unspecific lipid A contact signal is coupled to a highly specific carbohydrate recognition event.

Given the two phages 9NA and P22 with different ejection kinetics the model of a consecutive positioning and triggering function of LPS could now explain the different concentration dependencies observed for both phages. With similar hydrolysis rates for both phages but slower ejection rates for P22, the latter seems to achieve its final position for successful DNA release more slowly than 9NA. This might explain why kinetics of phage P22 DNA ejection, unlike 9NA, do not depend on LPS concentration: During positioning of phage P22 the TSP continue to hydrolyze polysaccharide thus depriving other phages of their receptors. Accordingly, at low LPS concentrations unejected phages remain (Figure 10.7.1 B).

10.8.2 Ejection kinetics depend on tail morphology in phages 9NA and P22

Using the identical LPS receptor system siphovirus 9NA ejects its DNA about 30 fold faster than podovirus P22 under identical experimental conditions *in vitro*. What causes these differences in ejection velocities? Three consecutive steps constitute the process. The receptor binding and hydrolysis step can be considered equal for the two phages given the same tailspike and LPS receptor (see above). The final DNA ejection is a fast process induced by the pressure inside the capsid which can be considered equal given that headful packaging mechanisms were both found for podo- and siphoviruses (Casjens and Hayden 1988; Tavares, Lurz et al. 1996). Rate limiting step monitored *in vitro* under receptor saturation must therefore be the conformational change that leads to opening of the particle. In podovirus P22, the tail is composed of two tail proteins (gp4, gp10) that bind the TSP and attach to the portal protein ring (Tang, Marion et al. 2005). A plug protein (gp26) closes the tail at the bottom (Olia, Casjens et al. 2007). Most likely, contact of the needle like plug with the lipid A moiety of LPS disrupts interactions with gp4 and gp10 (Andres, Hanke et al. 2010). The resulting conformational change in the tail would then transmit the opening signal to the portal protein. DNA protrudes into the tail and is surrounded by ejection proteins gp7, 16 and 20 (Chang, Weigele et al. 2006). Ejection proteins might form an additional channel structure for DNA release in P22, this might slow down ejection compared to siphovirus 9NA. For podoviruses ε15 and T7 an extensible tail was proposed to build up during infection (Kemp, Garcia et al. 2005; Chang, Schmid et al. 2010). For siphovirus 9NA the position of the TSP on the phage has not yet been verified experimentally, but from electron microscopy images it seems most likely that 9NA TSP attach to a baseplate structure at the end of the tail tube (Figure 10.4.3) and (Wollin, Eriksson et al. 1981)). In siphovirus P2 the baseplate has a plug which is removed after opening (Sciara, Bebeacua et al. 2010). 9NA might contain a similar plug which upon mechanical LPS contact would be removed in analogy to the gp26 plug in phage P22. This

would pass a conformational change over the tail tube in a similar way as shown for siphovirus SPP1 to open the portal in a domino like cascade (Plisson, White et al. 2007; Lhuillier, Gallopin et al. 2009). The different kinetics observed for the conformational opening in P22 and 9NA therefore reflect different probabilities for a successful triggering event. It is well conceivable that even less efficient LPS baseplate contacts in 9NA could still provoke particle opening because the domino like transmission over the long repetitive siphovirus tail structure would amplify the signal. By contrast, only fully efficient LPS contacts would stimulate opening via the short tail structure in podovirus P22.

Strikingly, using the identical host LPS receptor recognition system the conformational opening steps have very similar activation barriers, despite the different tail architectures. Moreover, high DNA ejection barriers similar to those of 9NA (53 kcal/mol) and P22 (41 kcal/mol) have also been determined *in vitro* for siphoviruses with various protein receptors, i.e. SPP1 (30 kcal/mol), lambda (26 kcal/mol) and T5 (42 kcal/mol) (Raspaud, Forth et al. 2007). Given these phages with different morphologies and compositions of tails the conformational barrier to overcome during ejection most probably occur at a conserved structure, most likely the portal protein. Structural studies on P22 portal protein suggest that the portal prevents DNA from escape from the capsid after packaging during tail assembly (Tang, Lander et al. 2011). Portal proteins have been found to contain conserved regions in a large number of phages (Casjens 2008; Tadmor, Ottesen et al. 2011). Our findings illustrate that tailed phages have decoupled their individual host receptor systems from the general need of a protective energy barrier which protects them from unspecific DNA release.

10.9 Acknowledgements

We thank Sherwood Casjens and Roger Hendrix for sharing sequence data of 9NA phage. We thank Sibylle Rüstig, Mandy Schietke and Christin Hanke for excellent technical assistance. D.A. is funded by the Leibniz-Gemeinschaft. This work is supported by a grant from the Deutsche Forschungsgemeinschaft [grant number BA 4046/1-1].

10.10 References

Ackermann, H. W., (2003) Bacteriophage observations and evolution. *Res Microbiol* **154**: 245-251.

Aksyuk, A. & M. Rossmann, (2011) Bacteriophage Assembly. *Viruses-Basel* **3**: 172-203.

Andres, D., U. Baxa, C. Hanke, R. Seckler & S. Barbirz, (2010a) Carbohydrate binding of *Salmonella* phage P22 tailspike protein and its role during host cell infection. *Biochem Soc Trans* **38**: 1386-1389.

Andres, D., C. Hanke, U. Baxa, A. Seul, S. Barbirz & R. Seckler, (2010b) Tailspike interactions with lipopolysaccharide effect DNA ejection from phage P22 particles in vitro. *J Biol Chem* **285**: 36768-36775.

Barbirz, S., M. Becker, A. Freiberg & R. Seckler, (2009) Phage Tailspike Proteins with beta-Solenoid Fold as Thermostable Carbohydrate Binding Materials. *Macromol Biosci* **9**: 169-173.

Barbirz, S., J. J. Muller, C. Uetrecht, A. J. Clark, U. Heinemann & R. Seckler, (2008) Crystal structure of Escherichia coli phage HK620 tailspike: podoviral tailspike endoglycosidase modules are evolutionarily related. *Mol Microbiol* **69**: 303-316.

Baxa, U., S. Steinbacher, S. Miller, A. Weintraub, R. Huber & R. Seckler, (1996) Interactions of phage P22 tails with their cellular receptor, *Salmonella* O-antigen polysaccharide. *Biophys J* **71**: 2040-2048.

Böhm, J., O. Lambert, A. S. Frangakis, L. Letellier, W. Baumeister & J. L. Rigaud, (2001) FhuA-mediated phage genome transfer into liposomes: a cryo-electron tomography study. *Curr Biol* **11**: 1168-1175.

Casjens, S. & M. Hayden, (1988) Analysis in vivo of the bacteriophage P22 headful nuclease. *J Mol Biol* **199**: 467-474.

Casjens, S. & P. Thuman-Commike, (2011) Evolution of mosaically related tailed bacteriophage genomes seen through the lens of phage P22 virion assembly. *Virology*: 393-415.

Casjens, S. R., (2008) Diversity among the tailed-bacteriophages that infect the Enterobacteriaceae. *Res Microbiol* **159**: 340-348.

Chang, J., P. Weigele, J. King, W. Chiu & W. Jiang, (2006) Cryo-EM asymmetric reconstruction of bacteriophage P22 reveals organization of its DNA packaging and infecting machinery. *Structure* **14**: 1073-1082.

Chang, J. T., M. F. Schmid, C. Haase-Pettingell, P. R. Weigele, J. A. King & W. Chiu, (2010) Visualizing the structural changes of bacteriophage Epsilon15 and its *Salmonella* host during infection. *J Mol Biol* **402**: 731-740.

Chiaruttini, N., M. de Frutos, E. Augarde, P. Boulanger, L. Letellier & V. Viasnoff, (2010) Is the in vitro ejection of bacteriophage DNA quasistatic? A bulk to single virus study. *Biophys J* **99**: 447-455.

Emsley, P. & K. Cowtan, (2004) Coot: model-building tools for molecular graphics. *Acta Crystallogr D Biol Crystallogr* **60**: 2126-2132.

Flores, C. O., J. R. Meyer, S. Valverde, L. Farr & J. S. Weitz, (2011) Statistical structure of host–phage interactions. *Proc Natl Acad Sci U S A* **108**: E288-E297.

Israel, V., (1978) A model for the adsorption of phage P22 to *Salmonella typhimurium*. *J Gen Virol* **40**: 669-673.

Kabsch, W., (2010) XDS. *Acta Crystallographica Section D-Biological Crystallography*: 125-132.

Kemp, P., L. R. Garcia & I. J. Molineux, (2005) Changes in bacteriophage T7 virion structure at the initiation of infection. *Virology* **340**: 307-317.

Lander, G., L. Tang, S. Casjens, E. Gilcrease, P. Prevelige, A. Poliakov, C. Potter, B. Carragher & J. Johnson, (2006) The structure of an infectious P22 virion shows the signal for headful DNA packaging. *Science* **312**: 1791-1795.

Leiman, P. G., F. Arisaka, M. J. van Raaij, V. A. Kostyuchenko, A. A. Aksyuk, S. Kanamaru & M. G. Rossmann, (2010) Morphogenesis of the T4 tail and tail fibers. *Virol J* **7**: 355.

Lhuillier, S., M. Gallopin, B. Gilquin, S. Brasilès, N. Lancelot, G. Letellier, M. Gilles, G. Dethan, E. V. Orlova, J. Couprie, P. Tavares & S. Zinn-Justin, (2009) Structure of bacteriophage SPP1 head-to-tail connection reveals mechanism for viral DNA gating. *Proc Natl Acad Sci U S A* **106**: 8507-8512.

Lindberg, A. A., (1977) Bacterial Surface Carbohydrates and Bacteriophage Adsorption. In: Surface carbohydrates of the procaryotic cell. I. Sutherland (ed). London: Academic Press, pp. 289 - 356.

Mangenot, S., M. Hochrein, J. Radler & L. Letellier, (2005) Real-time imaging of DNA ejection from single phage particles. *Curr Biol* **15**: 430-435.

McCoy, A. J., R. W. Grosse-Kunstleve, P. D. Adams, M. D. Winn, L. C. Storoni & R. J. Read, (2007) Phaser crystallographic software. *J Appl Crystallogr* **40**: 658-674.

Olia, A. S., S. Casjens & G. Cingolani, (2007) Structure of phage P22 cell envelope–penetrating needle. *Nat Struct Mol Biol* **14**: 1221-1226.

Plisson, C., H. E. White, I. Auzat, A. Zafarani, C. Sao-Jose, S. Lhuillier, P. Tavares & E. V. Orlova, (2007) Structure of bacteriophage SPP1 tail reveals trigger for DNA ejection. *Embo J* **26**: 3720-3728.

Rao, V. B. & L. W. Black, (2010) Structure and assembly of bacteriophage T4 head. *Virol J* **7**: 356.

Raspaud, E., T. Forth, C. São-José, P. Tavares & M. de Frutos, (2007) A kinetic analysis of DNA ejection from tailed phages revealing the prerequisite activation energy. *Biophys J* **93**: 3999-4005.

Richter, W., V. Vogel, J. Howe, F. Steiniger, A. Brauser, M. H. Koch, M. Roessle, T. Gutsmann, P. Garidel, W. Mäntele & K. Brandenburg, (2011) Morphology, size distribution, and aggregate structure of lipopolysaccharide and lipid A dispersions from enterobacterial origin. *Innate Immun* **17**: 427-438.

Roa, M., (1981) Receptor-triggered ejection of DNA and protein in phage lambda. *Fems Microbiology Letters* **11**: 257-262.

Schwartz, M., (1975) Reversible interaction between coliphage lambda and its receptor protein. *J Mol Biol* **99**: 185-201.

Sciara, G., C. Bebeacua, P. Bron, D. Tremblay, M. Ortiz-Lombardia, J. Lichière, M. van Heel, V. Campanacci, S. Moineau & C. Cambillau, (2010) Structure of lactococcal phage p2 baseplate and its mechanism of activation. *Proc Natl Acad Sci U S A* **107**: 6852-6857.

Smith, D., S. Tans, S. Smith, S. Grimes, D. Anderson & C. Bustamante, (2001) The bacteriophage phi 29 portal motor can package DNA against a large internal force. *Nature* **413**: 748-752.

Steinbacher, S., S. Miller, U. Baxa, N. Budisa, A. Weintraub, R. Seckler & R. Huber, (1997) Phage P22 tailspike protein: crystal structure of the head-binding domain at 2.3 A, fully refined structure of the endorhamnosidase at 1.56 A resolution, and the molecular basis of O-antigen recognition and cleavage. *J Mol Biol* **267**: 865-880.

São-José, C., C. Baptista & M. A. Santos, (2004) Bacillus subtilis operon encoding a membrane receptor for bacteriophage SPP1. *J Bacteriol* **186**: 8337-8346.

Tadmor, A. D., E. A. Ottesen, J. R. Leadbetter & R. Phillips, (2011) Probing individual environmental bacteria for viruses by using microfluidic digital PCR. *Science* **333**: 58-62.

Tang, J., G. C. Lander, A. Olia, R. Li, S. Casjens, P. Prevelige, G. Cingolani, T. S. Baker & J. E. Johnson, (2011) Peering down the barrel of a bacteriophage portal: the genome packaging and release valve in p22. *Structure* **19**: 496-502.

Tang, L., W. R. Marion, G. Cingolani, P. E. Prevelige & J. E. Johnson, (2005) Three-dimensional structure of the bacteriophage P22 tail machine. *Embo J* **24**: 2087-2095.

Tavares, P., R. Lurz, A. Stiege, B. Rückert & T. A. Trautner, (1996) Sequential headful packaging and fate of the cleaved DNA ends in bacteriophage SPP1. *J Mol Biol* **264**: 954-967.

Thompson, J. E., M. Pourhossein, A. Waterhouse, T. Hudson, M. Goldrick, J. P. Derrick & I. S. Roberts, (2010) The K5 lyase KflA combines a viral tail spike structure with a bacterial polysaccharide lyase mechanism. *J Biol Chem* **285**: 23963-23969.

Walter, M., C. Fiedler, R. Grassl, M. Biebl, R. Rachel, X. L. Hermo-Parrado, A. L. Llamas-Saiz, R. Seckler, S. Miller & M. J. van Raaij, (2008) Structure of the receptor-binding protein of bacteriophage det7: a podoviral tail spike in a myovirus. *J Virol* **82**: 2265-2273.

Winston, F., D. Botstein & J. H. Miller, (1979) Characterization of amber and ochre suppressors in *Salmonella typhimurium*. *J Bacteriol* **137**: 433-439.

Wollin, R., U. Eriksson & A. A. Lindberg, (1981) *Salmonella* bacteriophage glycanases: endorhamnosidase activity of bacteriophages P27, 9NA, and KB1. *J Virol* **38**: 1025-1033.

Xiang, Y., M. C. Morais, A. J. Battisti, S. Grimes, P. J. Jardine, D. L. Anderson & M. G. Rossmann, (2006) Structural changes of bacteriophage phi29 upon DNA packaging and release. *EMBO J* **25**: 5229-5239.

Young, F. E., (1967) Requirement of glucosylated teichoic acid for adsorption of phage in Bacillus subtilis 168. *Proc Natl Acad Sci U S A* **58**: 2377-2384.

Yu, F. & S. Mizushima, (1982) Roles of lipopolysaccharide and outer membrane protein OmpC of Escherichia coli K-12 in the receptor function for bacteriophage T4. *J Bacteriol* **151**: 718-722.

11 General discussion

11.1 Carbohydrate recognition

The first step during podovirus P22 and siphovirus 9NA infection is specific recognition of their host´s surface – a common principle for many viruses. Both, 9NA and P22, bind to O antigen carbohydrate structures with their tailspikes. Tailspikes contain two modular domains: a major β-helical receptor recognition and an N-terminal phage binding structure.

11.1.1 Carbohydrate specificity

In P22 tailspike β-helical domain binding towards *S*. Typhimurium, *S*. Enteritidis and *S*. Paratyphi O antigen octasaccharides is differently mediated in a 3,6-dideoxyhexose specific pocket. These individual sugar orientations result in distinct binding affinities. The tolerance in P22 tailspike binding site mediates a broader host tropism by allowing different, but specific interactions. The complete octasaccharide is utilized in recognition. Binding studies with smaller O antigen fragments showed reduced affinities whereas larger fragments did not increase affinities [122, 123].

By contrast, many mammalian viruses dock to glycans on eukaryotic cells and primarily involve single terminal sialic acids in binding [124]. For instance, human influenza A hemagglutinin preferably binds to sialic acid in α-2,6-linkage to Gal-2 and is thereby specific for its human host. A single point mutation however results in a different specificity and avian cell surfaces can be recognized that contain sialic acid with an α-2,3-linkage to Gal-2 or vice versa [125]. These rather small but highly specific recognition sites have low affinities in the milli-molar range [126]. Low affinity is overcome by utilizing multiple receptors on the virus and host surface. Multivalent interactions increase affinity towards the carbohydrate ligand and support correct recognition of host cells.

Compared to influenza hemagglutinin, P22 tailspikes are also highly specific and neither bind to O antigen without their 3,6-dideoxyhexose substitution nor to O antigen with different linkages in their main chain [122, 127]. These changes disturb O antigen docking to the tailspike. P22 tailspike is highly selective when binding to three distinct host sugars in different orientations. Three different dideoxyhexose epimers are selected on only one protein. This feature seems to be quite unique so far: Other virus receptors solely bind to saccharide ligands in a single orientation, a one lock, one conformer principle as in lectins [128]. Only viral receptor homologues are described to bind carbohydrate ligands in different orientations [129]. Therefore, tailspikes with their broader recognition abilities offer unique features to understand this biological process in more detail.

11.1.2 Processivity in tailspikes

Multivalent binding and avidity of *Salmonella* lipopolysaccharides (LPS) in P22 tailspike lead to inactivation of P22 phages as assayed *in vivo*. For successful infection, phage P22 is dependent on O antigen cleavage activity located in the central tailspike domain. In assays measuring solely tailspike activity towards O antigen polysaccharide without lipid A moiety they were able to degrade O antigen polysaccharide in an endo- position showing no processivity. But the tailspikes should enable the phage to reach the bacterial surface efficiently and this is clearly dependent on processive cleavage to ensure a straight infection. Here, it is important to distinguish between single tailspikes and tailspikes attached to the phage. During infection at least three tailspikes on the phage have to bind and cleave multiple receptors on the host´s surface [75]. Thereby, six O antigen binding sites are employed by the phage to orient correctly towards the cell membrane. Tailspikes can only cleave LPS if O antigen repeating units (RU) reach with their non-reducing end to the binding site distal of the tailspikes active site. Therefore on a cell or on LPS aggregates, tailspike binding and degrading activity in the phage confers directivity towards the rigid cell surface made up from lipid A molecules: As the phage moves downwards at least one binding site on the phage will stay attached to any LPS receptor and limits diffusion. Meanwhile, other tailspikes degrade their bound O antigen receptor, release cleavage products from the recognition site and rebind to the shortened receptor. Accordingly, phage P22 reaches the outer membrane surface in a directed manner and processivity of P22 tailspikes is induced by their organization in the phage particle. Processivity in cleavage has been shown for tailspikes in podovirus K1F that infects encapsulated *E. coli* K1 [9, 130]. K1F tailspikes (endoNF) bind and cleave α2,8-linked polysialic acid capsules of their hosts. Similar to P22 tailspike and other viral adhesins, endoNF is a β-helical trimer [100, 131]. However, they contain two binding sites on one subunit encompassing the active site which are not present in P22 tailspike. These enable endoNF alone as well as the complete phage to processively degrade capsular polysialic acid [130, 132].

11.1.3 P22-like tailspikes in different phages

P22 tailspike and 9NA tailspike occur in structurally different phages, in a podovirus and a siphovirus, respectively. They only share 36 % sequence identity but nevertheless, apart from the particle binding domain, their overall structure is highly conserved. With their central receptor binding domain, both tailspikes degrade their host´s *S*. Typhimurium O antigen polysaccharide to similar end products employing conserved amino acids. Both proteins bind O antigen octasaccharides with similar thermodynamic parameters. Their Nterminal capsid binding domains are different because they confer attachment to different phage morphologies, in podovirus between gp4 and gp10 and in siphovirus 9NA close to its baseplate [99, 133]. During evolution

9NA and P22 kept their individual N-terminal capsid binding domain, but their receptor binding domain was exchanged between both and enables them to infect *S*. Typhimurium. Other phages use *Salmonella* O antigen receptors as well and recognize them with their tailspike structures. Myovirus Det7 possesses a tailspike structure similar to P22 tailspike with 50 % sequence identity in the overall protein and even 60 % identity in the central receptor binding region [99]. As between 9NA tailspike and P22 tailspike, the virus binding domain at the N-terminus is not conserved between Det7 tailspike and P22 tailspike. In podovirus SP6 that belongs to the T7-like genus in the podoviral family, a P22 like tailspike is responsible for *S*. Typhimurium infection. Interestingly, phage SP6 not only infects *Salmonella* with long O antigen chains but also those without O antigen by employing two distinct tailspikes [134]. These broaden SP6 host specificity because LPS core structures are well conserved between many different *Salmonella* but they are not readily accessible, when covered by O antigen [127]. Obviously, the gene fragment coding for the central β-helical receptor binding domain of P22 tailspike has been exchanged between phages far beyond siphovirus 9NA. The receptor recognition module can be employed on viruses with different origin to adapt their host range to *Salmonella enterica*.

11.1.4 Adaptation in receptor binding domain

But there are noteworthy differences in host specificity between 9NA and P22. Siphovirus 9NA is able to hydrolyze *Salmonella* strains carrying a P22 lysogenic O antigen modification, a α-1,6 glucosylation at galactose in the O antigen main chain [83]. This modification renders *Salmonella* carrying a P22 prophage resistant against multiple infections of P22 [39]. P22 and 9NA, however, compete for the same host range. Because both phages recognize the highly specific O antigen part of LPS, their accessible host range is narrow [127]. By overriding the stop signals of P22, lytic 9NA might overtake lysogenic P22 cells and secure its own survival. Therefore, although we observe a rather recent receptor exchange, phage 9NA adapted its tailspikes to fulfill its own needs.

In a second scenario, tailspikes can conserve their N-terminal tailspike domain, as part of the capsid binding module, and adapt the central receptor binding domain to recognize a different enterobacterial host. Examples are two structurally characterized tailspikes with folds similar to that of P22 tailspike in *E. coli* podovirus HK620 and *Shigella flexneri* podovirus Sf6 [88, 89].

HK620 tailspike is a endo-N-acetylglucosaminidase and cleaves its *E. coli* host O antigen into hexasaccharides [89]. These are bound on the solvent accessible surface in the middle of the β-helix of one subunit. By contrast, the cleavage activity of Sf6 tailspike that hydrolyses its hosts *Shigella flexneri* O antigen into octasaccharides, is allocated on different subunits of the trimer [88]. Thereby, binding occurs in a cleft between two subunits of the trimeric protein. Both

proteins share sequence identity within the N-terminal head binding domain but not in the major receptor binding domain although the overall fold is conserved. In evolution structural conservation of folds is a common principle [5]. The specialty of parallel β-helices is to be very tolerant against insertions, deletions and point mutations and allows rapid adaptation to a new host and bind different complex carbohydrate structures [89].

Therefore, 9NA tailspike is an example of both: It gained a P22 tailspike receptor binding module to its distinct N-terminal baseplate binding domain. The β-helix adapted slightly to accommodate an O antigen with P22 lysogenic modification.

11.2 P22 and 9NA DNA release

11.2.1 Role of lipopolysaccharide receptor

The outer membrane of Gram negative bacteria contains mainly LPS. *In vitro*, purified LPS forms multilamellar aggregates but it is reasonable to assume that their exposed surface resemble those of intact Gram negative bacteria. P22 tailspikes initiate first interaction with host surface by binding to the O antigen. Thereafter, O antigen cleavage activity leads to DNA release from the virus particle *in vitro*. LPS is a two in one receptor: Phage P22 only ejects DNA when LPS carbohydrate structures can be cleaved before lipid A contact occurs. Therefore, LPS outer membrane surface is crucial to trigger a signal in the phage to release its infectious DNA and not a second receptor. *In vitro,* LPS aggregates form a bacterial surface mimic and therefore offer the unique characteristics that are vital for the DNA release process, like multivalent, oriented receptors and polarity [135]. On a bacterial cell, LPS is distributed evenly over the complete outer membrane because it is the only lipid component of the outer leaflet [13]. Thereby, P22 could bind and eject its DNA at any surface site. This is confirmed by the observation that P22 phages are distributed over the complete cell during infection [72]. They do not localize at any specific membrane site. By contrast, other phages like λ were shown to concentrate and inject their DNA at cellular poles [136].

11.2.2 Podoviral DNA release

Tailspike´s multivalent binding and cleavage of O antigen when assembled to podovirus P22 result in a processive movement towards their host membrane. Thereby, the protruding gp26 or plug protein (refer to Figure 9.10.1) initiates opening of the P22 capsid to expel DNA. For that a signal has to be transferred from the outermost C-terminal tip to the portal where gp26 closes the capsid.

As discussed earlier podoviruses P22, Sf6 and HK620 might have diverged from a common ancestor and adapted their tailspike binding domain to a different carbohydrate structure [89]. As

they all belong to the P22-like genus of phages, sharing their overall morphology, DNA sequence similarities and O antigen receptor, it could be considered that they also might share a common DNA release mechanism. They all possess a trimeric gp26 protruding from the phage [137]. Gp26 closes podoviral phage capsids with its N-terminal domain and is likely to be involved in cell penetration at the C-terminal domain. Similar to the N-terminus in P22-like tailspikes, gp26 N-terminus in domain I is conserved between related podoviruses, as they all bind to a well conserved gp10 structure at the tail tube (Figure 5.3.2 D) [70]. Domain II has different length coiled-coil structures and is more diverse [137]. Their very C-terminal domains III and IV, however, have two distinct subfamilies: P22 and HK620 are helical but Sf6 gp26 possesses a knob like structure with a TNF-like fold [138]. These distinct features in the outermost part of the protein could result in different infection mechanisms of Sf6 and HK620 or P22 on their individual hosts. In the light of Sf6 and P22 tailspikes divergence, Sf6 gp26 could act differently than P22 gp26. Sf6 gp26 is more likely to punctuate the *Shigella flexneri* membrane with a rigid knob structure than P22 gp26 with its flexible helical structure at the distal end [138]. Phage HK620 on the other hand, with 60 % gp26 sequence identity to P22 gp26 probably employs a rather similar infection process but adapted to *E. coli* cells.

11.2.3 Efficiency of DNA ejection from different phage morphologies

A second study with siphovirus 9NA showed that its DNA release is in fact very similarly controlled when compared to podovirus P22. 9NA tailspikes attached to the baseplate initiate a mechanism triggered at the LPS surface that opens the phage particle and allows DNA to leave the capsid structure. Likewise, multivalent tailspike binding and enzyme activity in 9NA effect a processive movement towards *Salmonella* membrane. However, DNA release in siphovirus 9NA is about 30 times faster than in podovirus P22.

Bulk ejection kinetics probe the conformational opening step in the phage assembly [108]. Therefore, differences in DNA release kinetics reflect the probability to initiate the opening step. That means the efficiency to open the tail tube for DNA egress mirrors different tail architectures. The tail structure of podoviruses is clearly not long enough to reach the bacterial cytoplasm. However, tomographic snapshots of podovirus ε15 during infection revealed a structure originating from the phage particle and reaching across the *Salmonella* periplasm [81]. This would be in accordance with observations on podovirus T7, where an extensible tail was proposed to be built from ejection proteins to help DNA transportation [80].

Siphoviruses possess a longer tail structure composed of multiple proteins: at one end attached to the phage capsid via a connector, at the other end attached to the baseplate tip where receptor recognition occurs. Overall, they possess more structural proteins that have to be orchestrated to

ensure successful infection.

For example, siphovirus SPP1 recognizes the protein YueB on Gram positive *Bacillus subtilis* to release its DNA [139]. Binding to the receptor at the tail apparatus baseplate initiates opening of the tail cap, as has been shown in cryo EM structures [140]. Thereby, the cap becomes released from tail and a signal is induced in the long tail structure [141]. The tail tube undergoes large structural rearrangements suggesting that the signal is transmitted in a domino cascade to open the DNA stopper at the connector in the capsid [142]. In SPP1 the DNA stopper secures the DNA inside the capsid from which DNA becomes expelled [143]. By contrast, in assembled sipohovirus λ the DNA is thought to penetrate part of the tail structure in the mature particle before contact with the host receptor and DNA ejection [144].

As shown, structural rearrangements for DNA release differ in siphoviruses and podoviruses. The signal transduction mechanism along the tail is more efficient in siphovirus 9NA as indicated from its faster DNA release kinetics. This can be explained when considering a more efficient signal transduction along the tail tube in a domino like cascade as observed for phage SPP1 (Figure 11.2.1 A).

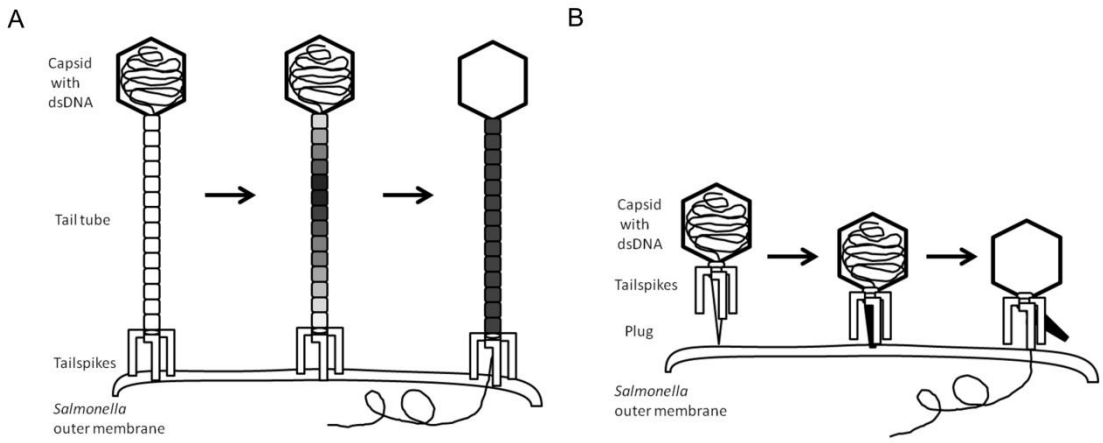

Figure 11.2.1: Efficiency of DNA ejection
A: In siphovirus 9NA, receptor recognition at the *Salmonella* outer membrane might induce a signal that is translated along the long tail in a wave like manner. Thereby, DNA can be released from the phage´s capsid.
B: In podovirus P22, tailspikes induce a signal in the plug protein that can or cannot open the phage capsid for DNA egress.

P22 conformational change for DNA egress seems to be less well started. This is supported by recent observations that P22 mutants with C terminally truncated gp26 get inactivated with *Salmonella* LPS, but do not release their DNA. This suggests that an induced signal along gp26 from the outermost membrane contact site is not transmitted effectively to open the capsid for DNA release (Figure 11.2.1 B) [145].

Large structural rearrangements can be observed in myoviruses that contract over their complete tail structure upon infection. Nevertheless, myoviruses and siphoviruses share high structural similarities in their tail proteins and support a common ancestor for long tailed phages [5, 146]. Myovirus T4 infects *E. coli* by binding to the lipopolysaccharide structures and to outer membrane porin C [147]. During this process the tail baseplate reorganizes and causes the short tail fibers to extend and bind irreversibly [148]. This induces contraction of the outer tail sheath to about half of its initial length and increases its diameter [149]. The contraction of the tail occurs without a major protein conformational change but is based on a more extensive interaction between subunits in the tail propagated in a wave like manner [150]. DNA ejection is triggered when a membrane potential is present and constitutes another signal during infection [151]. Myovirus Det7 possesses P22 like tailspikes but does not release its DNA upon LPS contact (Andres, D., unpublished results). In comparison with siphovirus 9NA and podovirus P22 it confirms that a more regulated mechanism is present in myoviruses to orchestrate their large structural rearrangements for DNA release.

11.2.4 Activation barrier for DNA release

Conformational changes upon DNA release in siphovirus 9NA and podovirus P22 share a similarly high activation enthalpy barrier. Barriers are in a range comparable to activation enthalpies in siphophages analyzed with protein receptors [109]. These barriers protect phages against unspecific DNA release in their environment. Specific receptor recognition initiates a conformational change in the phages for DNA egress. Therefore, lipopolysaccharide recognition acts like a catalyst and lowers the activation enthalpy to allow the conformational transition to occur [152]. Differences in the ejection kinetic in 9NA and P22 can be explained with the activation entropy in the conformational change. The activation entropy has to be smaller in the conformational change for the faster DNA releasing siphovirus 9NA (Figure 11.2.1).

Furthermore, in Poliovirus, a non-enveloped, icosahedral eukaryotic virus, a remarkably similar activation enthalpy of 50 kcal/ mol was measured to ready the virus for infection [152]. It can be speculated if this activation barrier has been conserved in many viruses as have other structural parts of the infection machinery originating from a common ancestor [146]. Once this high activation barrier has been established and proved useful, it could have been kept within different viruses as a functional module in the complete assembly not necessarily connected to a specific protein.

11.2.5 Fate of DNA after release from phage

After the DNA has left the phage through the tail structure it has to reach the bacterial cytoplasm. Myoviruses can reach the cytoplasm directly with their needle like structure, thus, DNA transport can be initiated in the right location. However, this is not the case in siphovirus 9NA and podovirus P22 and it is impossible to deduce DNA transport over cell membranes from DNA ejection experiments *in vitro*. Therefore, one can only speculate on the fate of DNA after release *in vivo*. In both, 9NA and P22, DNA is released upon LPS contact. Accordingly they do not take advantage of outer membrane transporters that are receptors for other phages and could help in DNA transport [15]. However, both phages might eject proteins that help DNA transport in the outer membrane and utilize DNA pressure in the phages head to transport part of the DNA [79, 117]. Additionally, an osmotic gradient from the environment to the periplasm could flush DNA inside [118]. After transport through the periplasm, where DNA could be protected by other ejected proteins, it remains an obstacle how it reaches the cytoplasm without destroying the vital membrane potential. It is tempting to speculate that the bacterial DNA transport machinery present in the inner membrane is employed for this step [153]. A highly conserved membrane channel ComEC is normally used for natural transformation by DNA uptake from the environment and could be utilized for the transport of phage DNA. However, this system has only been investigated in detail for *Bacillus subtilis, Haemophilus influenza, Streptococcus pneumoniae* and *Neisseria gonorrhoeae* but not for other bacteria established in the laboratory [154].

It remains unclear what happens to bacteriophage DNA once it has been transferred inside the bacterial cell: many bacteria possess an immune answer like system based on DNA repeats in the CRISPR locus in their genomes [155]. Upon phage infection they might activate a resistance answer with cas proteins by either cleavage of foreign DNA or in a RNAi like manner [156, 157]. Bacteriophage infection is clearly not a losing game for bacteria: they evolved various strategies to avoid viral infection but these might be of advantage for colonization or avoidance of host responses as well [29]. Furthermore, bacteria utilize bacteriophage DNA fragments to drive their own development either to gain access to a large gene pool from other bacteria or even from the phage itself [4].

11.3 Beyond bacteriophage tail structure research

Bacteriophage long tail structures are likely to resemble bacterial secretion systems [146, 158]. These large molecular machines release material into their environment but the transport mechanism is largely unknown. Further investigation of bacteriophage tail machines and DNA transport processes will help to understand these transporters, that play crucial roles in bacterial

pathogenicity [159].

Furthermore, bacteria evolved parts of long bacteriophage tail structures for their own use. Pyocins are secreted by *Pseudomonas aeroginosa* that kill other *Pseudomonas aeroginosa* strains and resemble myoviral and siphoviral tail structures [160]. R-type pyocins resemble myoviruses and destroy necessary membrane potential in *Pseudomonas aeroginosa* by inserting a hollow tube like structure into bacterial cell membrane. Their specificity can be modified with tailspikes recognizing different O antigen pattern and are therefore highly useful to engineer specific antimicrobial agents [161]. The understanding of different tail structures, their assembly and transport could therefore derive new applications in therapy and preservation [162].

12 Allgemeinverständliche Zusammenfassung

Antibiotika sind immer weniger wirksam bei der Bekämpfung bakterieller Krankheitserreger. Deswegen müssen neue Ansätze erforscht werden, Bakterien unschädlich zu machen. Die Doktorarbeit deutet auf einen möglichen Lösungsweg hin. Auf der Erde gibt es ca. 10^{31} Bakteriophagen. Ein Phage ist ein Virus, das dazu in der Lage ist, ein Bakterium zu infizieren. Täglich werden 1/3 aller Bakterien von Phagen infiziert und getötet –diesen Mechanismus möchte man verstehen und für Therapien nutzen. In der Doktorarbeit werden zwei verschiedene Phagen betrachtet, die P22 und 9NA genannt werden. Beide infizieren Salmonellen, die als Krankheitserreger für Mensch und Tier Bedeutung haben. Beide Phagen bestehen aus einem Kopf, dem so genannten Kapsid, das dicht mit DNS, der Erbsubstanz des Phagen gepackt ist. So dicht, dass das Kapsid fest verschlossen werden muss, um den Austritt der DNS zu verhindern. Diese Aufgabe übernimmt eine Art Schwanz, der sogenannte Tail, der aus dem Kapsid herausragt. Am anderen Ende, das vom Kapsid weg ragt, trägt der Tail sechs stachelförmige Fortsätze, die Tailspikes. Mit diesen Tailspikes können die Phagen ihr Wirtsbakterium *Salmonella* erkennen. Ein gutes Bild zur besseren Vorstellung ist das Aussehen einer Mondlandefähre. Der Phage landet sozusagen auf dem Bakterium, genauer auf der das Bakterium umschließenden Hülle, die aus Lipopolysaccharid (LPS) besteht. LPS hat einen Kohlenhydratanteil, der in die Umgebung reicht, und einen Lipid Anker, mit dem das Molekül in der Zellmembran festgemacht ist. Beide untersuchten Phagen erkennen den richtigen Wirt an der Kohlenhydratstruktur des LPS mithilfe ihrer Tailspikes. Der Phage frisst sich mit ihrer Hilfe durch den LPS-Mantel bis zur Zelloberfläche in der sich das Lipid befindet. Dadurch werden Veränderungen im Phagen initiiert, mit denen er sich auf das bevorstehende Infizieren der Salmonelle vorbereitet. Dazu muss der Phage P22 mittels einer Art Nadel, die sich zwischen den Tailspike-Beinen befindet, an der Zelloberfläche anstoßen. Anschließend wird die unter Druck stehende DNS des Phagen in das Bakterium geschossen. Bei dem Phagen 9NA läuft die Infektion etwas anders ab, da sich seine Struktur vom P22 unterscheidet. Dort, wo bei dem Phagen P22 der Tail direkt an das Kapsid anschließt, befindet sich beim 9NA ein langes Rohr, das die Tailspikes mit dem Kapsid verbindet. Phage 9NA hat daher einen ungefähr viermal so langen Tail. Obwohl dadurch die Strecke, die die DNA aus dem Kapsid zurücklegen muss, sehr viel länger ist, wird die DNA etwa 30x schneller ausgestoßen als bei P22. Vermutlich sind die Veränderungen, die zur Infektion führen, im 9NA Phagen besser aufeinander abgestimmt. Außerdem kann der lange Tail dabei behilflich sein, den 9NA Phagen besser auszurichten, wie ein Gewehr, bei dem das Projektil besser geführt wird. Der 9NA Phage mit seinem langen Tail wäre damit also besser geeignet, Salmonellen unschädlich zu machen.

13 List of publications

1) Andres, D., Baxa, U., Hanke, C., Seckler, R., Barbirz, S.

Carbohydrate binding of *Salmonella* phage P22 tailspike protein and its role during host cell infection.

Biochemical Society Transactions, 2010. 038(5): p. 1386-1389.

Dorothee Andres designed plaque forming assay and performed all shown experiments. She evaluated biophysical and *in vivo* data in context and wrote the manuscript together with Stefanie Barbirz (Physikalische Biochemie, Universität Potsdam).

Chapter 8 in this thesis

2) Andres, D., Hanke, C., Baxa, U., Seul, A., Barbirz, S., Seckler, R.

Tailspike interactions with lipopolysaccharide effect DNA ejection from phage P22 particles in vitro.

Journal of Biological Chemistry, 2010. 285(47): p. 36768-75.

Dorothee Andres designed and performed all shown experiments with exception of the gel filtration analysis. DNA ejection studies were performed together with a supervised undergraduate student, Christin Hanke. Dorothee Andres evaluated all data, analyzed them in context and wrote the first manuscript.

Chapter 9 in this thesis

3) Dorothee Andres, Yvette Roske, Carolin Doering, Udo Heinemann, Robert Seckler and Stefanie Barbirz;

Tail morphology controls DNA release in two *Salmonella* phages with one lipopolysaccharide receptor recognition system

Molecular Microbiology 2012. **83**(6): 1244-53

Dorothee Andres designed and performed all shown experiments with exception of the transmission electron microscopy, crystal structure analysis of 9NA tailspike and activity assay of 9NA tailspike mutants. DNA ejection studies were performed together with a supervised technical assistant, Carolin Doering. Dorothee Andres evaluated all data, analyzed them in context and wrote the first manuscript.

Chapter 10 in this thesis

In prep. 4⋆) Andres, D., Gohlke, U., Bröker, N. K., Rabsch, W., Heinemann, U., Barbirz, S., Seckler, R.

Conserved water on P22 Tailspike surface mediates binding of *Salmonella* Paratyphi O antigen

⋆ to be submitted

Dorothee Andres performed all shown experiments with exception of the heat capacity measurements. *S.* Paratyphi mutants were constructed together with Wolfgang Rabsch at the Robert Koch Institut in Wernigerode. Crystal structure analysis of P22 tailspike complexed with O antigen octasaccharide was performed together with Ulrich Gohlke in Udo Heinemann´s group at the Max Delbrück Centrum in Berlin. Dorothee Andres evaluated all data, analyzed them in context and wrote the first manuscript. The depicted version of the manuscript has not been approved by all co-authors.

Chapter 7 in this thesis

14 References Introduction and General Discussion

1. Bergh, O., et al., *High abundance of viruses found in aquatic environments.* Nature, 1989. **340**(6233): p. 467-468.
2. Ackermann, H.W., *Frequency of morphological phage descriptions in the year 2000. Brief review.* Arch Virol, 2001. **146**(5): p. 843-57.
3. Hendrix, R.W., G.F. Hatfull, and M.C. Smith, *Bacteriophages with tails: chasing their origins and evolution.* Res Microbiol, 2003. **154**(4): p. 253-7.
4. Hendrix, R.W., et al., *Evolutionary relationships among diverse bacteriophages and prophages: All the world´s a phage.* Proc Natl Acad Sci U S A, 1999. **96**(5): p. 2192-2197.
5. Bamford, D.H., J.M. Grimes, and D.I. Stuart, *What does structure tell us about virus evolution?* Current Opinion in Structural Biology, 2005. **15**(6): p. 655-663.
6. Mann, N.H., *The third age of phage.* PLoS Biol, 2005. **3**(5): p. e182.
7. Petty, N.K., et al., *Biotechnological exploitation of bacteriophage research.* Trends in Biotechnology, 2007. **25**(1): p. 7-15.
8. Lindberg, A.A., *Bacteriophage receptors.* Annu Rev Microbiol, 1973. **27**: p. 205-41.
9. Scholl, D., et al., *Bacteriophage K1-5 Encodes Two Different Tail Fiber Proteins, Allowing It To Infect and Replicate on both K1 and K5 Strains of Escherichia coli.* J. Virol., 2001. **75**(6): p. 2509-2515.
10. Schade, S.Z., J. Adler, and H. Ris, *How bacteriophage chi attacks motile bacteria.* J Virol, 1967. **1**(3): p. 599-609.
11. Raimondo, L.M., N.P. Lundh, and R.J. Martinez, *Primary adsorption site of phage PBS1: the flagellum of Bacillus subtilis.* J Virol, 1968. **2**(3): p. 256-64.
12. Boulanger, P., et al., *Purification and Structural and Functional Characterization of FhuA, a Transporter of the Escherichia coli Outer Membrane* Biochemistry, 1996. **35**(45): p. 14216-14224.
13. Silhavy, T.J., D. Kahne, and S. Walker, *The Bacterial Cell Envelope.* Cold Spring Harbor Perspectives in Biology, 2010. **2**(5): p. -.
14. Varki, A., et al., *Symbol nomenclature for glycan representation.* Proteomics, 2009. **9**(24): p. 5398-9.
15. Nikaido, H., *Molecular Basis of Bacterial Outer Membrane Permeability Revisited.* Microbiol. Mol. Biol. Rev., 2003. **67**(4): p. 593-656.
16. Raetz, C.R.H. and C. Whitfield, *Lipopolysaccharide endotoxins.* Annual Review of Biochemistry, 2002. **71**(1): p. 635-700.
17. Holst, O., et al., *Chapter 3 - Core region and lipid A components of lipopolysaccharides*, in *Microbial Glycobiology*, Academic Press: San Diego. p. 29-55.
18. Zahringer, U., B. Lindner, and E.T. Rietschel, *Molecular structure of lipid A, the endotoxic center of bacterial lipopolysaccharides.* Adv Carbohydr Chem Biochem, 1994. **50**: p. 211-76.
19. Snyder, S., D. Kim, and T.J. McIntosh, *Lipopolysaccharide Bilayer Structure: Effect of Chemotype, Core Mutations, Divalent Cations, and Temperature.* Biochemistry, 1999. **38**(33): p. 10758-10767.
20. Raetz, C.R., et al., *Lipid A modification systems in gram-negative bacteria.* Annu Rev Biochem, 2007. **76**: p. 295-329.
21. Holst, O., *The structures of core regions from enterobacterial lipopolysaccharides – an update.* FEMS Microbiology Letters, 2007. **271**(1): p. 3-11.
22. Frank M, U. and R.S.T.a.D. Horton, *The Chemistry and Biological Significance of 3-Deoxy-d-manno-2-Octulosonic Acid (KDO)*, in *Advances in Carbohydrate Chemistry and Biochemistry*. 1981, Academic Press. p. 323-388.
23. Zhang, Y., et al., *Modulation of innate immune responses with synthetic lipid A derivatives.* J Am Chem Soc, 2007. **129**(16): p. 5200-16.

24. Peterson, A.A. and E.J. McGroarty, *High-molecular-weight components in lipopolysaccharides of Salmonella typhimurium, Salmonella minnesota, and Escherichia coli.* J. Bacteriol., 1985. **162**(2): p. 738-745.
25. Allende, D. and T.J. McIntosh, *Lipopolysaccharides in bacterial membranes act like cholesterol in eukaryotic plasma membranes in providing protection against melittin-induced bilayer lysis.* Biochemistry, 2003. **42**(4): p. 1101-8.
26. Roantree, R.J., T.T. Kuo, and D.G. MacPhee, *The effect of defined lipopolysaccharide core defects upon antibiotic resistances of Salmonella typhimurium.* J Gen Microbiol, 1977. **103**(2): p. 223-34.
27. Rietschel, E.T., et al., *Bacterial endotoxin: molecular relationships of structure to activity and function.* FASEB J., 1994. **8**(2): p. 217-225.
28. Popoff, M.Y., *Antigenic formulas of the Salmonella serovars 8th ed. World Health Organization Collaborating Center for Reference and Research on Salmonella.* Res Microbiol, 2001. **152**(10): p. 907-9.
29. Lerouge, I. and J. Vanderleyden, *O-antigen structural variation: mechanisms and possible roles in animal/plant-microbe interactions.* FEMS Microbiology Reviews, 2002. **26**(1): p. 17-47.
30. Aurell, C.A. and A.O. Wistrom, *Critical aggregation concentrations of gram-negative bacterial lipopolysaccharides (LPS).* Biochem Biophys Res Commun, 1998. **253**(1): p. 119-123.
31. Sasaki, H. and S.H. White, *Aggregation Behavior of an Ultra-Pure Lipopolysaccharide that Stimulates TLR-4 Receptors.* Biophys J, 2008. **95**(2): p. 986.
32. Santos, N.C., et al., *Evaluation of Lipopolysaccharide Aggregation by Light Scattering Spectroscopy.* ChemBioChem, 2003. **4**(1): p. 96-100.
33. Brandenburg, K. and U. Seydel, *Investigation into the fluidity of lipopolysaccharide and free lipid A membrane systems by Fourier-transform infrared spectroscopy and differential scanning calorimetry.* Eur J Biochem, 1990. **191**(1): p. 229-36.
34. Schromm, A.B., et al., *Biological activities of lipopolysaccharides are determined by the shape of their lipid A portion.* Eur J Biochem, 2000. **267**(7): p. 2008-13.
35. Brandenburg, K., et al., *Conformation of lipid A, the endotoxic center of bacterial lipopolysaccharide.* Journal of Endotoxin Research, 1996. **3**(3): p. 173-178.
36. Richter, W., et al., *Morphology, size distribution, and aggregate structure of lipopolysaccharide and lipid A dispersions from enterobacterial origin.* Innate Immun, 2010. **17**(5): p. 427-38.
37. Brogden, K.A. and M. Phillips, *The ultrastructural morphology of endotoxins and lipopolysaccharides.* Electron Microsc Rev, 1988. **1**(2): p. 261-78.
38. Shands, J.W., Jr. and P.W. Chun, *The dispersion of gram-negative lipopolysaccharide by deoxycholate. Subunit molecular weight.* J. Biol. Chem., 1980. **255**(3): p. 1221-1226.
39. Luderitz, O., et al., *Structural relationship of Salmonella O and R antigens.* Ann N Y Acad Sci, 1966. **133**(2): p. 349-74.
40. Barksdale, L. and S.B. Arden, *Persisting bacteriophage infections, lysogeny, and phage conversions.* Annu Rev Microbiol, 1974. **28**(0): p. 265-99.
41. Brussow, H., C. Canchaya, and W.D. Hardt, *Phages and the evolution of bacterial pathogens: from genomic rearrangements to lysogenic conversion.* Microbiol Mol Biol Rev, 2004. **68**(3): p. 560-602.
42. Zinder, N.D. and J. Lederberg, *Genetic Exchange in Salmonella.* J. Bacteriol., 1952. **64**(5): p. 679-699.
43. Prevelige Jr, P.E., *Bacteriophage P22*, in *The bacteriophages*, R. Calendar, Editor. 2006, Oxford University Press.
44. Echols, H., *Developmental Pathways for the Temperate Phage: Lysis VS Lysogeny.* Annual Review of Genetics, 1972. **6**(1): p. 157-190.

45. Chang, J., et al., *Cryo-EM Asymmetric Reconstruction of Bacteriophage P22 Reveals Organization of its DNA Packaging and Infecting Machinery.* Structure, 2006. **14**(6): p. 1073-1082.
46. Lander, G.C., et al., *The Structure of an Infectious P22 Virion Shows the Signal for Headful DNA Packaging.* Science, 2006. **312**(5781): p. 1791-1795.
47. Teschke, C.M. and K.N. Parent, *'Let the phage do the work': Using the phage P22 coat protein structures as a framework to understand its folding and assembly mutants.* Virology, 2010.
48. Parent, K.N., et al., *P22 coat protein structures reveal a novel mechanism for capsid maturation: stability without auxiliary proteins or chemical crosslinks.* Structure, 2010. **18**(3): p. 390-401.
49. King, J. and S. Casjens, *Catalytic head assembling protein in virus morphogenesis.* Nature, 1974. **251**(5471): p. 112-9.
50. Olia, A.S., et al., *Three-dimensional structure of a viral genome-delivery portal vertex.* Nat Struct Mol Biol, 2011. **18**(5): p. 597-603.
51. Botstein, D., C.H. Waddell, and J. King, *Mechanism of head assembly and DNA encapsulation in Salmonella phage p22. I. Genes, proteins, structures and DNA maturation.* J Mol Biol, 1973. **80**(4): p. 669-95.
52. Nemecek, D., et al., *Subunit Conformations and Assembly States of a DNA-translocating Motor: The Terminase of Bacteriophage P22.* J Mol Biol, 2007. **374**(3): p. 817-836.
53. Casjens, S., et al., *Bacteriophage P22 portal protein is part of the gauge that regulates packing density of intravirion DNA.* J Mol Biol, 1992. **224**(4): p. 1055-1074.
54. Smith, D.E., et al., *The bacteriophage straight phi29 portal motor can package DNA against a large internal force.* Nature, 2001. **413**(6857): p. 748-52.
55. Casjens, S. and M. Hayden, *Analysis in vivo of the bacteriophage P22 headful nuclease.* Journal of Molecular Biology, 1988. **199**(3): p. 467-474.
56. Jiang, W., et al., *Coat protein fold and maturation transition of bacteriophage P22 seen at subnanometer resolutions.* Nature Structural Biology, 2003. **10**(2): p. 131-135.
57. Lander, G.C., et al., *The P22 tail machine at subnanometer resolution reveals the architecture of an infection conduit.* Structure, 2009. **17**(6): p. 789-99.
58. Lorenzen, K., et al., *Determination of stoichiometry and conformational changes in the first step of the P22 tail assembly.* J Mol Biol, 2008. **379**(2): p. 385-96.
59. Tang, J., et al., *Peering Down the Barrel of a Bacteriophage Portal: The Genome Packaging and Release Valve in P22.* Structure, 2011.
60. Bhardwaj, A., et al., *Domain Organization and Polarity of Tail Needle GP26 in the Portal Vertex Structure of Bacteriophage P22.* J Mol Biol, 2007. **371**(2): p. 374-87.
61. Strauss, H. and J. King, *Steps in the stabilization of newly packaged DNA during phage P22 morphogenesis.* J Mol Biol, 1984. **172**(4): p. 523-43.
62. Olia, A.S., S. Casjens, and G. Cingolani, *Structure of phage P22 cell envelope-penetrating needle.* Nat Struct Mol Biol, 2007. **14**(12): p. 1221-1226.
63. Olia, A.S., S. Casjens, and G. Cingolani, *Structural plasticity of the phage P22 tail needle gp26 probed with xenon gas.* Protein Sci, 2009. **18**(3): p. 537-48.
64. Steinbacher, S., et al., *Crystal structure of P22 tailspike protein: interdigitated subunits in a thermostable trimer.* Science, 1994. **265**(5170): p. 383-6.
65. Pettersen, E.F., et al., *UCSF Chimera--a visualization system for exploratory research and analysis.* J Comput Chem, 2004. **25**(13): p. 1605-12.
66. Seul, A., *Tailspike Interactions in Bacteriophage P22*, in *Physikalische Biochemie*. 2008, Universität Potsdam: Potsdam.
67. Steinbacher, S., et al., *Interaction of Salmonella phage P22 with its O-antigen receptor studied by X-ray crystallography.* Biol Chem, 1997. **378**(3-4): p. 337-43.
68. Baxa, U., et al., *Interactions of phage P22 tails with their cellular receptor, Salmonella O-antigen polysaccharide.* Biophys J, 1996. **71**(4): p. 2040-8.

69. Iwashita, S. and S. Kanegasaki, *Smooth specific phage adsorption: endorhamnosidase activity of tail parts of P22.* Biochem Biophys Res Commun, 1973. **55**(2): p. 403-9.
70. Casjens, S.R. and P.A. Thuman-Commike, *Evolution of mosaically related tailed bacteriophage genomes seen through the lens of phage P22 virion assembly.* Virology, 2011. **411**(2): p. 393-415.
71. Eriksson, U., et al., *Salmonella phage glycanases: substrate specificity of the phage P22 endo-rhamnosidase.* J Gen Virol, 1979. **43**(3): p. 503-11.
72. Crowlesmith, I., M. Schindler, and M.J. Osborn, *Bacteriophage P22 is not a likely probe for zones of adhesion between the inner and outer membranes of Salmonella typhimurium.* J. Bacteriol., 1978. **135**(1): p. 259-269.
73. Israel, V., H. Rosen, and M. Levine, *Binding of Bacteriophage P22 Tail Parts to Cells.* J. Virol., 1972. **10**(6): p. 1152-1158.
74. Eriksson, U. and A.A. Lindberg, *Adsorption of phage P22 to Salmonella typhimurium.* J Gen Virol, 1977. **34**(2): p. 207-21.
75. Israel, V., *A model for the adsorption of phage P22 to Salmonella typhimurium.* J Gen Virol, 1978. **40**(3): p. 669-73.
76. Israel, V., *Role of the bacteriophage P22 tail in the early stages of infection.* J Virol, 1976. **18**(1): p. 361-4.
77. Haywood, A.M., *Virus receptors: binding, adhesion strengthening, and changes in viral structure.* J Virol, 1994. **68**(1): p. 1-5.
78. Israel, V., *E proteins of bacteriophage P22. I. Identification and ejection from wild-type and defective particles.* J Virol, 1977. **23**(1): p. 91-7.
79. Perez, G.L., et al., *Transport of Phage P22 DNA across the Cytoplasmic Membrane.* J. Bacteriol., 2009. **191**(1): p. 135-140.
80. Kemp, P., L.R. Garcia, and I.J. Molineux, *Changes in bacteriophage T7 virion structure at the initiation of infection.* Virology, 2005. **340**(2): p. 307-17.
81. Chang, J.T., et al., *Visualizing the Structural Changes of Bacteriophage Epsilon15 and Its Salmonella Host during Infection.* J Mol Biol, 2010. **402**(4): p. 731-740.
82. Wilkinson.Rg, B.A.D. Stocker, and P. Gemski, *Non-smooth mutants of Salmonella Typhimurium - Differentiation by phage sensitivity and genetic mapping.* Journal of General Microbiology, 1972. **70**(MAY): p. 527.
83. Wollin, R., U. Eriksson, and A.A. Lindberg, *Salmonella Bacteriophage Glycanases: Endorhamnosidase Activity of Bacteriophages P27, 9NA, and KB1.* J. Virol., 1981. **38**(3): p. 1025-1033.
84. Goyal, R. and M. Chakravorty, *Abortive infection of the virulent phage 9NA in a fatty acid auxotroph of Salmonella typhimurium: effect of fatty acid supplementation.* Biochem Biophys Res Commun, 1989. **161**(2): p. 923-30.
85. Murthy, K.G.K. and M. Chakravorty, *Physical mapping and characterization of bacteriophage 9NA genome.* Journal of Biosciences, 1998. **23**(2): p. 143-150.
86. Goyal, R., et al., *Maturarion of bacteriophage 9NA DNA is influenced by the fatty acid composition of the host-cell membrane.* Journal of Biosciences, 1994. **19**(2): p. 183-192.
87. Scholl, D. and C.R. Merril, *Polysaccharide-degrading phages*, in *Phages - their role in bacterial pathogenesis and biotechnology*, M.K. Waldor and D.I. Friedman, Adhya, Sankar L., Editors. 2005, ASM Press: Washington, D.C. p. 400-414.
88. Muller, J.J., et al., *An intersubunit active site between supercoiled parallel beta helices in the trimeric tailspike endorhamnosidase of Shigella flexneri Phage Sf6.* Structure, 2008. **16**(5): p. 766-75.
89. Barbirz, S., et al., *Crystal structure of Escherichia coli phage HK620 tailspike: podoviral tailspike endoglycosidase modules are evolutionarily related.* Mol Microbiol, 2008.
90. Kanegasaki, S. and A. Wright, *Studies on the mechanism of phage adsorption: Interaction between phage epsilon15 and its cellular receptor.* Virology, 1973. **52**(1): p. 160-173.

91. Svenson, S.B., et al., *Salmonella bacteriophage glycanases: endorhamnosidases of Salmonella typhimurium bacteriophages.* J Virol, 1979. **32**(2): p. 583-92.
92. Seckler, R., *Folding and function of repetitive structure in the homotrimeric phage P22 tailspike protein.* J Struct Biol, 1998. **122**(1-2): p. 216-22.
93. Barbirz, S., et al., *Phage Tailspike Proteins with beta-Solenoid Fold as Thermostable Carbohydrate Binding Materials.* Macromol Biosci, 2009.
94. Seckler, R., et al., *Reconstitution of the thermostable trimeric phage P22 tailspike protein from denatured chains in vitro.* J Biol Chem, 1989. **264**(20): p. 11750-3.
95. Steinbacher, S., et al., *Phage P22 tailspike protein: crystal structure of the head-binding domain at 2.3 A, fully refined structure of the endorhamnosidase at 1.56 A resolution, and the molecular basis of O-antigen recognition and cleavage.* J Mol Biol, 1997. **267**(4): p. 865-80.
96. Berget, P.B. and A.R. Poteete, *Structure and Functions of the Bacteriophage P22 Tail Protein.* J. Virol., 1980. **34**(1): p. 234-243.
97. Weintraub, A., et al., *Heterogeneity in Oligosaccharides from the O-Polysaccharide Chain of the Lipopolysaccharide from Salmonella Typhi 253Ty Determined by Fast Atom Bombardment Mass Spectrometry.* Glycoconjugate J, 1988. **5**: p. 207 - 13.
98. Steinbacher, S., et al., *Crystal structure of phage P22 tailspike protein complexed with Salmonella sp. O-antigen receptors.* Proc Natl Acad Sci U S A, 1996. **93**(20): p. 10584-8.
99. Walter, M., et al., *Structure of the receptor-binding protein of bacteriophage det7: a podoviral tail spike in a myovirus.* J Virol, 2008. **82**(5): p. 2265-73.
100. Weigele, P.R., E. Scanlon, and J. King, *Homotrimeric, beta-stranded viral adhesins and tail proteins.* J Bacteriol, 2003. **185**(14): p. 4022-30.
101. Dupont, K., et al., *Identification of Lactococcus lactis genes required for bacteriophage adsorption.* Appl Environ Microbiol, 2004. **70**(10): p. 5825-32.
102. Bartual, S.G., et al., *Structure of the bacteriophage T4 long tail fiber receptor-binding tip.* Proc Natl Acad Sci U S A, 2010. **107**(47): p. 20287-92.
103. Liu, X., et al., *Structural changes in a marine podovirus associated with release of its genome into Prochlorococcus.* Nat Struct Mol Biol, 2010. **17**(7): p. 830-836.
104. Spinelli, S., et al., *Lactococcal bacteriophage p2 receptor-binding protein structure suggests a common ancestor gene with bacterial and mammalian viruses.* Nat Struct Mol Biol, 2006. **13**(1): p. 85.
105. Tavares, P., Zinn-Justin, S and Orlova, E.V., *Genome Gating in Tailed Bacteriophage Capsids*, in *Viral Molecular Machines*, M.G. Rossmann and V. Rao, Editors. 2012, Springer Science and Business Media
106. de Frutos, M., L. Letellier, and E. Raspaud, *DNA Ejection from Bacteriophage T5: Analysis of the Kinetics and Energetics.* Biophys. J., 2005. **88**(2): p. 1364-1370.
107. Inamdar, M.M., W.M. Gelbart, and R. Phillips, *Dynamics of DNA ejection from bacteriophage.* Biophys J, 2006. **91**(2): p. 411-20.
108. Chiaruttini, N., et al., *Is the In Vitro Ejection of Bacteriophage DNA Quasistatic? A Bulk to Single Virus Study.* Biophys J, 2010. **99**(2): p. 447-455.
109. Raspaud, E., et al., *A Kinetic Analysis of DNA Ejection from Tailed Phages Revealing the Prerequisite Activation Energy.* Biophysical Journal, 2007. **93**(11): p. 3999-4005.
110. Gelbart, W.M. and C.M. Knobler, *Virology. Pressurized viruses.* Science, 2009. **323**(5922): p. 1682-3.
111. Evilevitch, A., et al., *Osmotic pressure inhibition of DNA ejection from phage.* Proc Natl Acad Sci U S A, 2003. **100**(16): p. 9292-5.
112. Evilevitch, A., et al., *Effects of salt concentrations and bending energy on the extent of ejection of phage genomes.* Biophys J, 2008. **94**(3): p. 1110-20.
113. Mangenot, S., et al., *Real-time imaging of DNA ejection from single phage particles.* Curr Biol, 2005. **15**(5): p. 430-5.

114. Leforestier, A. and F. Livolant, *The Bacteriophage Genome Undergoes a Succession of Intracapsid Phase Transitions upon DNA Ejection.* J Mol Biol, 2010. **396**(2): p. 384-395.
115. Grayson, P., et al., *Real-time observations of single bacteriophage lambda DNA ejections in vitro.* Proc Natl Acad Sci U S A, 2007. **104**(37): p. 14652-7.
116. Knobler, C.M. and W.M. Gelbart, *Physical Chemistry of DNA Viruses.* Annual Review of Physical Chemistry, 2009. **60**(1): p. 367-383.
117. São-José, C., et al., *Pressure Built by DNA Packing Inside Virions: Enough to Drive DNA Ejection in Vitro, Largely Insufficient for Delivery into the Bacterial Cytoplasm.* J Mol Biol, 2007. **374**(2): p. 346-355.
118. Grayson, P. and I.J. Molineux, *Is phage DNA 'injected' into cells--biologists and physicists can agree.* Curr Opin Microbiol, 2007. **10**(4): p. 401-9.
119. Molineux, I.J., *No syringes please, ejection of phage T7 DNA from the virion is enzyme driven.* Mol Microbiol, 2001. **40**(1): p. 1-8.
120. Kemp, P., M. Gupta, and I.J. Molineux, *Bacteriophage T7 DNA ejection into cells is initiated by an enzyme-like mechanism.* Mol Microbiol, 2004. **53**(4): p. 1251-65.
121. González-Huici, V., M. Salas, and J.M. Hermoso, *The push–pull mechanism of bacteriophage Ø29 DNA injection.* Mol Microbiol, 2004. **52**(2): p. 529-540.
122. Baxa, U., et al., *Enthalpic Barriers to the Hydrophobic Binding of Oligosaccharides to Phage P22 Tailspike Protein.* Biochemistry, 2001. **40**(17): p. 5144-5150.
123. Baxa, U., *Lipopolysaccharid-Erkennung durch das P22 Tailspikeprotein*, in *Biologie und Vorklinische Medizin*. 1998, Universität Regensburg: Regensburg. p. 123.
124. Neu, U., J. Bauer, and T. Stehle, *Viruses and sialic acids: rules of engagement.* Curr Opin Struct Biol, 2011. **21**(5): p. 610-8.
125. de Vries, R.P., et al., *Only two residues are responsible for the dramatic difference in receptor binding between swine and new pandemic H1 hemagglutinin.* J Biol Chem, 2010. **286**(7): p. 5868-75.
126. Gamblin, S.J. and J.J. Skehel, *Influenza hemagglutinin and neuraminidase membrane glycoproteins.* J Biol Chem, 2010. **285**(37): p. 28403-9.
127. Lindberg, A.A., *Bacterial Surface Carbohydrates and Bacteriophage Adsorption*, in *Surface carbohydrates of the procaryotic cell*, I. Sutherland, Editor. 1977, Academic Press: London. p. 289 - 356.
128. Gabius, H.J., et al., *From lectin structure to functional glycomics: principles of the sugar code.* Trends Biochem Sci, 2011. **36**(6): p. 298-313.
129. Stehle, T. and J.M. Casasnovas, *Specificity switching in virus-receptor complexes.* Curr Opin Struct Biol, 2009. **19**(2): p. 181-8.
130. Schwarzer, D., et al., *Proteolytic Release of the Intramolecular Chaperone Domain Confers Processivity to Endosialidase F.* J. Biol. Chem., 2009. **284**(14): p. 9465-9474.
131. Stummeyer, K., et al., *Crystal structure of the polysialic acid-degrading endosialidase of bacteriophage K1F.* Nat Struct Mol Biol, 2005. **12**(1): p. 90-6.
132. Leiman, P.G., et al., *The Structures of Bacteriophages K1E and K1-5 Explain Processive Degradation of Polysaccharide Capsules and Evolution of New Host Specificities.* J Mol Biol, 2007. **371**(3): p. 836-849.
133. Casjens, S.R., *Diversity among the tailed-bacteriophages that infect the Enterobacteriaceae.* Res Microbiol, 2008. **159**(5): p. 340-8.
134. Scholl, D., et al., *Genomic analysis of bacteriophages SP6 and K1-5, an estranged subgroup of the T7 supergroup.* J Mol Biol, 2004. **335**(5): p. 1151-71.
135. Evans, S.V. and C. Roger MacKenzie, *Characterization of protein-glycolipid recognition at the membrane bilayer.* J Mol Recognit, 1999. **12**(3): p. 155-68.
136. Edgar, R., et al., *Bacteriophage infection is targeted to cellular poles.* Mol Microbiol, 2008. **68**(5): p. 1107-16.

137. Bhardwaj, A., et al., *An evolutionarily conserved family of virion tail needles related to bacteriophage P22 gp26: correlation between structural stability and length of the alpha-helical trimeric coiled coil.* J Mol Biol, 2009. **391**(1): p. 227-45.
138. Bhardwaj, A., et al., *Atomic structure of bacteriophage Sf6 tail needle knob.* J Biol Chem, 2011. **286**(35): p. 30867-77.
139. Sao-Jose, C., et al., *The ectodomain of the viral receptor YueB forms a fiber that triggers ejection of bacteriophage SPP1 DNA.* J Biol Chem, 2006. **281**(17): p. 11464-70.
140. Goulet, A., et al., *The opening of the SPP1 bacteriophage tail, a prevalent mechanism in Gram-positive-infecting siphophages.* J Biol Chem, 2011. **286**(28): p. 25397-405.
141. Plisson, C., et al., *Structure of bacteriophage SPP1 tail reveals trigger for DNA ejection.* Embo J, 2007. **26**(15): p. 3720-8.
142. Lhuillier, S., et al., *Structure of bacteriophage SPP1 head-to-tail connection reveals mechanism for viral DNA gating*. 2009. p. 8507-8512.
143. Tavares, P., et al., *Sequential headful packaging and fate of the cleaved DNA ends in bacteriophage SPP1.* J Mol Biol, 1996. **264**(5): p. 954-67.
144. Thomas, J.O., *Chemical linkage of the tail to the right-hand end of bacteriophage lambda DNA.* J Mol Biol, 1974. **87**(1): p. 1-9.
145. Hanke, C., *Die Rolle des Plug Proteins gp26 im Infektionsmechanismus des Salmonella Bakteriophagen P22*, in *Physikalische Biochemie*. 2011, Universität Potsdam: Potsdam.
146. Pell, L.G., et al., *The phage lambda major tail protein structure reveals a common evolution for long-tailed phages and the type VI bacterial secretion system.* Proc Natl Acad Sci U S A, 2009. **106**(11): p. 4160-5.
147. Yu, F. and S. Mizushima, *Roles of lipopolysaccharide and outer membrane protein OmpC of Escherichia coli K-12 in the receptor function for bacteriophage T4.* J. Bacteriol., 1982. **151**(2): p. 718-722.
148. Rossmann, M.G., et al., *The bacteriophage T4 DNA injection machine.* Current Opinion in Structural Biology, 2004. **14**(2): p. 171-180.
149. Leiman, P.G., et al., *Three-Dimensional Rearrangement of Proteins in the Tail of Bacteriophage T4 on Infection of Its Host.* Cell, 2004. **118**(4): p. 419-429.
150. Aksyuk, A.A., et al., *The tail sheath structure of bacteriophage T4: a molecular machine for infecting bacteria.* Embo J, 2009. **28**(7): p. 821-9.
151. Labedan, B. and E.B. Goldberg, *Requirement for membrane potential in injection of phage T4 DNA.* Proc Natl Acad Sci U S A, 1979. **76**(9): p. 4669-4673.
152. Tsang, S.K., et al., *Kinetic analysis of the effect of poliovirus receptor on viral uncoating: the receptor as a catalyst.* J Virol, 2001. **75**(11): p. 4984-9.
153. Krüger, N.J. and K. Stingl, *Two steps away from novelty--principles of bacterial DNA uptake.* Mol Microbiol, 2011. **80**(4): p. 860-7.
154. Chen, I., P.J. Christie, and D. Dubnau, *The ins and outs of DNA transfer in bacteria.* Science, 2005. **310**(5753): p. 1456-60.
155. Barrangou, R., et al., *CRISPR provides acquired resistance against viruses in prokaryotes.* Science, 2007. **315**(5819): p. 1709-12.
156. Garneau, J.E., et al., *The CRISPR/Cas bacterial immune system cleaves bacteriophage and plasmid DNA.* Nature, 2010. **468**(7320): p. 67-71.
157. Perez-Rodriguez, R., et al., *Envelope stress is a trigger of CRISPR RNA-mediated DNA silencing in Escherichia coli.* Mol Microbiol, 2011. **79**(3): p. 584-99.
158. Leiman, P.G., et al., *Type VI secretion apparatus and phage tail-associated protein complexes share a common evolutionary origin.* Proc Natl Acad Sci U S A, 2009. **106**(11): p. 4154-9.
159. Worrall, L.J., E. Lameignere, and N.C. Strynadka, *Structural overview of the bacterial injectisome.* Curr Opin Microbiol, 2011. **14**(1): p. 3-8.
160. Nakayama, K., et al., *The R-type pyocin of Pseudomonas aeruginosa is related to P2 phage, and the F-type is related to lambda phage.* Mol Microbiol, 2000. **38**(2): p. 213-31.

161. Scholl, D., et al., *An engineered R-type pyocin is a highly specific and sensitive bactericidal agent for the food-borne pathogen Escherichia coli O157:H7.* Antimicrob Agents Chemother, 2009. **53**(7): p. 3074-80.
162. Clark, J.R. and J.B. March, *Bacteriophages and biotechnology: vaccines, gene therapy and antibacterials.* Trends in Biotechnology, 2006. **24**(5): p. 212-218.

15 Appendix

15.1 Supplement for Recognition of *Salmonella* O antigens in P22 tailspike protein

Table 15.1: P22 TSP co-crystallized with *S*. Paratyphi octasaccharide diffraction data collection and refinement statistics

Data Collection	
Wavelength [Å]	0.91841
Temperature [K]	100
Space group	P 2_1 3
Unit Cell Parameters a, b, c [Å] α, β, γ [°]	 119.94, 119.94, 119.94 90.0, 90.0, 90.0
Resolution range [Å][a]	33.27 - 1.75 (1.80-1.75)
Reflections[a] Unique Completeness [%] Multiplicity	 58030 (4247) 99.9 (99.9) 5.7 (5.2)
Data quality[a] Intensity [I/σ(I)] R_{meas} Wilson B value [Å^2]	 16.1 (3.2) 10.7 (62.7) 11.55
Refinement	
Resolution range [Å][a]	33.27-1.75 (1.80-1.75)
Reflections[a] Number Completeness [%] Test Set (5%)	 55128 (4227) 99.9 (99.2) 2902 (211)
R_{work} R_{free}	0.137 (0.169) 0.156 (0.220)
Contents of the Asymmetric Unit Protein Molecules, Residues, Atoms Octasaccharide, Molecules, Atoms Glycerol, Molecules, Atoms Water, Molecules	 1, 552, 4271 1, 83 3, 18 661
Mean Temperature factors [Å^2][b] All Atoms Protein Octasaccharide Ligand Glyerol Molecules Water Oxygens	 14.33 12.31 21.35 36.55 25.96
RMSD from Target Geometry Bond Lengths [Å] Bond Angles [°] RMSD Temperature Factors [Å^2]	 0.010 1.372

Main-chain Bonds	0.566
Main-chain Angles	1.028
Side-chain Bonds	1.719
Side-chain Bonds	2.814
Estimated Coordinate Error [Å]	
Based on R_{free}	0.018
Based on Maximum Likelihood	0.032
Validation Statistics[c]	
Ramachandran Plot	
Residues in Allowed Regions [%, No.]	99.8, 574
Residues in Favoured Regions [%, No.]	96.9, 557
Outliers [%, No.]	0.18, 1 (Ile504)
MOLPROBITY Clashscore[d]	4.02

Table 15.2: Interactions between octasaccharides, TSP and water molecules.
Distances were calculated with LigandExplorer

3THO 1.75 Å				
***S*. Paratyphi/ Sugar**	Atom 1	Atom 2	Distance	Type
Galactose 1	A:701:GLA:O2	A:1524:HOH:O	2.77	Bridged H-Bond
	A:701:GLA:O3	A:1469:HOH:O	2.89	Bridged H-Bond
	A:701:GLA:O3	A:1520:HOH:O	2.32	Bridged H-Bond
Mannose 2	A:702:MAN:O2	A:1524:HOH:O	3.26	Bridged H-Bond
	A:702:MAN:O3	A:1524:HOH:O	2.72	Bridged H-Bond
	A:702:MAN:O4	A:1458:HOH:O	2.85	Bridged H-Bond
	A:702:MAN:O6	A:1459:HOH:O	2.54	Bridged H-Bond
	A:702:MAN:O6	A:1496:HOH:O	2.74	Bridged H-Bond
	A:702:MAN:O6	A:1528:HOH:O	3.22	Bridged H-Bond
	A:702:MAN:O4	A:303:ASP:OD1	2.71	Hydrogen Bond
Paratose 3	A:703:PAR:O2	A:1447:HOH:O	2.54	Bridged H-Bond
	A:703:PAR:O2	A:1468:HOH:O	2.6	Bridged H-Bond
	A:1468:HOH:O	A:304:GLY:N	2.98	Bridged H-Bond
	A:703:PAR:C6	A:309:GLU:CG	3.81	Hydrophobic
	A:703:PAR:C6	A:311:LEU:CD1	3.68	Hydrophobic
	A:703:PAR:C4	A:309:GLU:CG	3.82	Hydrophobic
	A:703:PAR:O4	A:285:ARG:NH1	3.08	Hydrogen Bond
	A:703:PAR:O4	A:309:GLU:OE1	2.56	Hydrogen Bond
	A:703:PAR:C3	A:283:LEU:CD1	3.75	Hydrophobic
Rhamnose 4	A:704:RAM:O5	A:1467:HOH:O	3.04	Bridged H-Bond
	A:704:RAM:C6	A:369:VAL:CG1	3.76	Hydrophobic
Galactose 5	A:705:GLA:O3	A:1459:HOH:O	3.19	Bridged H-Bond
	A:705:GLA:O2	A:1456:HOH:O	2.98	Bridged H-Bond
	A:705:GLA:O2	A:1482:HOH:O	2.72	Bridged H-Bond
	A:705:GLA:O4	A:1448:HOH:O	3.05	Bridged H-Bond

	A:705:GLA:O4	A:1458:HOH:O	2.83	Bridged H-Bond
	A:705:GLA:O4	A:1459:HOH:O	2.84	Bridged H-Bond
	A:705:GLA:O6	A:928:HOH:O	2.8	Bridged H-Bond
	A:705:GLA:O5	A:1448:HOH:O	3.04	Bridged H-Bond
	A:705:GLA:C4	A:365:TRP:CH2	3.69	Hydrophobic
	A:705:GLA:C5	A:365:TRP:CH2	3.67	Hydrophobic
	A:705:GLA:C6	A:365:TRP:CH2	3.85	Hydrophobic
	A:705:GLA:C6	A:365:TRP:CZ2	3.69	Hydrophobic
	A:705:GLA:O6	A:359:GLU:OE1	2.55	Hydrogen Bond
	A:705:GLA:O6	A:359:GLU:OE2	3.21	Hydrogen Bond
	A:705:GLA:O6	A:363:LYS:NZ	2.87	Hydrogen Bond
Mannose 6	A:706:MAN:O4	A:1452:HOH:O	2.73	Bridged H-Bond
	A:706:MAN:O3	A:1456:HOH:O	2.99	Bridged H-Bond
	A:706:MAN:O5	A:363:LYS:NZ	2.8	Hydrogen Bond
	A:706:MAN:O6	A:363:LYS:NZ	3.03	Hydrogen Bond
	A:706:MAN:O6	A:366:GLN:OE1	2.83	Hydrogen Bond
Paratose 7	A:707:PAR:O5	A:1341:HOH:O	3.03	Bridged H-Bond
	A:707:PAR:O4	A:1144:HOH:O	2.78	Bridged H-Bond
	A:707:PAR:O4	A:1478:HOH:O	2.86	Bridged H-Bond
	A:707:PAR:O2	A:1270:HOH:O	2.62	Bridged H-Bond
	A:707:PAR:O2	A:1456:HOH:O	2.89	Bridged H-Bond
Rhamnose 8	A:708:RAM:O2	A:1067:HOH:O	2.93	Bridged H-Bond
	A:708:RAM:O2	A:1196:HOH:O	2.85	Bridged H-Bond
	A:708:RAM:C4	A:359:GLU:CD	3.76	Hydrophobic
	A:708:RAM:C6	A:237:SER:CB	3.85	Hydrophobic
	A:708:RAM:C6	A:391:TRP:CE2	3.77	Hydrophobic
	A:708:RAM:C6	A:391:TRP:CD2	3.76	Hydrophobic
	A:708:RAM:C6	A:391:TRP:CE3	3.85	Hydrophobic
	A:708:RAM:C6	A:391:TRP:CZ2	3.86	Hydrophobic
	A:708:RAM:C1	A:391:TRP:CE3	3.78	Hydrophobic
	A:708:RAM:O2	A:395:ASP:OD2	2.49	Hydrogen Bond
	A:708:RAM:O3	A:363:LYS:NZ	2.99	Hydrogen Bond
	A:708:RAM:O3	A:366:GLN:OE1	2.73	Hydrogen Bond
	A:708:RAM:O3	A:395:ASP:OD2	3.26	Hydrogen Bond

1TYX, 1.80 Å

***S*. Typhimurium/ sugar**	Atom 1	Atom 2	Distance	Type
Galactose 1	A:1:GLA:C2	A:309:GLU:CD	3.79	Hydrophobic
	A:1:GLA:C2	A:311:LEU:CD1	3.87	Hydrophobic
	A:1:GLA:C6	A:370:GLY:CA	3.71	Hydrophobic
	A:1:GLA:O2	A:285:ARG:NH2	2.77	Hydrogen Bond
	A:1:GLA:O2	A:309:GLU:OE1	2.46	Hydrogen Bond

	A:1:GLA:O2	A:309:GLU:OE2	3.29	Hydrogen Bond
Mannose				
Abequose 3	A:3:ABE:O4	A:726:HOH:O	2.74	Bridged H-Bond
	A:3:ABE:O4	A:875:HOH:O	2.92	Bridged H-Bond
	A:875:HOH:O	A:304:GLY:N	2.81	Bridged H-Bond
	A:3:ABE:C2	A:303:ASP:CG	3.66	Hydrophobic
	A:3:ABE:O2	A:303:ASP:OD2	3.13	Hydrogen Bond
Rhamnose 4	A:4:RAM:C6	A:365:TRP:CZ3	3.71	Hydrophobic
	A:4:RAM:C6	A:365:TRP:CH2	3.86	Hydrophobic
Galactose 5	A:5:GLA:O4	A:787:HOH:O	3.06	Bridged H-Bond
	A:5:GLA:O5	A:787:HOH:O	3.26	Bridged H-Bond
	A:5:GLA:O6	A:767:HOH:O	2.79	Bridged H-Bond
	A:5:GLA:C4	A:365:TRP:CH2	3.81	Hydrophobic
	A:5:GLA:C5	A:365:TRP:CH2	3.69	Hydrophobic
	A:5:GLA:C6	A:365:TRP:CZ2	3.75	Hydrophobic
	A:5:GLA:C6	A:365:TRP:CH2	3.75	Hydrophobic
	A:5:GLA:O6	A:359:GLU:OE1	2.59	Hydrogen Bond
	A:5:GLA:O6	A:359:GLU:OE2	3.22	Hydrogen Bond
	A:5:GLA:O6	A:363:LYS:NZ	2.75	Hydrogen Bond
Mannose 6	A:6:MAN:O5	A:363:LYS:NZ	2.84	Hydrogen Bond
	A:6:MAN:O6	A:363:LYS:NZ	3.14	Hydrogen Bond
	A:6:MAN:O6	A:366:GLN:OE1	2.95	Hydrogen Bond
Abequose 7				
Rhamnose 8	A:8:RAM:O3	A:874:HOH:O	2.84	Bridged H-Bond
	A:8:RAM:O5	A:874:HOH:O	3.1	Bridged H-Bond
	A:8:RAM:C4	A:359:GLU:CD	3.74	Hydrophobic
	A:8:RAM:C6	A:359:GLU:CG	3.83	Hydrophobic
	A:8:RAM:C6	A:359:GLU:CD	3.74	Hydrophobic
	A:8:RAM:C6	A:391:TRP:CD2	3.7	Hydrophobic
	A:8:RAM:C6	A:391:TRP:CE2	3.76	Hydrophobic
	A:8:RAM:C6	A:391:TRP:CE3	3.82	Hydrophobic
	A:8:RAM:O1	A:392:ASP:OD2	2.68	Hydrogen Bond
	A:8:RAM:O2	A:395:ASP:OD2	2.9	Hydrogen Bond
	A:8:RAM:O3	A:363:LYS:NZ	3.22	Hydrogen Bond
	A:8:RAM:O3	A:366:GLN:OE1	3.16	Hydrogen Bond
	A:8:RAM:O3	A:395:ASP:OD2	2.68	Hydrogen Bond

1TYU, 1.80 Å				
***S*. Enteritidis/ Sugar**	Atom 1	Atom 2	Distance	Type
Galactose 1	A:1:GLA:O3	A:758:HOH:O	2.9	Bridged H-Bond
	A:1:GLA:O2	A:285:ARG:NH2	2.82	Hydrogen Bond
	A:1:GLA:O2	A:309:GLU:OE2	2.67	Hydrogen Bond
Mannose 2	A:2:MAN:O4	A:777:HOH:O	2.89	Bridged H-Bond
Tyvelose 3	A:3:TYV:O2	A:744:HOH:O	2.8	Bridged H-Bond
	A:3:TYV:O2	A:751:HOH:O	2.65	Bridged H-Bond
	A:744:HOH:O	A:304:GLY:N	2.85	Bridged H-Bond
	A:3:TYV:C4	A:307:THR:CG2	3.88	Hydrophobic
	A:3:TYV:C6	A:337:LEU:CD2	3.86	Hydrophobic
	A:3:TYV:C6	A:365:TRP:CZ2	3.6	Hydrophobic
	A:3:TYV:C6	A:365:TRP:CH2	3.86	Hydrophobic
	A:3:TYV:O4	A:309:GLU:OE2	2.52	Hydrogen Bond
Rhamnose 4	A:4:RAM:C6	A:365:TRP:CZ3	3.84	Hydrophobic
	A:4:RAM:C6	A:365:TRP:CH2	3.82	Hydrophobic
Galactose 5	A:5:GLA:O4	A:792:HOH:O	3.02	Bridged H-Bond
	A:5:GLA:O5	A:792:HOH:O	3.15	Bridged H-Bond
	A:5:GLA:O6	A:771:HOH:O	2.8	Bridged H-Bond
	A:5:GLA:C4	A:365:TRP:CH2	3.82	Hydrophobic
	A:5:GLA:C5	A:365:TRP:CH2	3.7	Hydrophobic
	A:5:GLA:C6	A:365:TRP:CZ2	3.75	Hydrophobic
	A:5:GLA:C6	A:365:TRP:CH2	3.85	Hydrophobic
	A:5:GLA:O6	A:359:GLU:OE1	2.59	Hydrogen Bond
	A:5:GLA:O6	A:359:GLU:OE2	3.22	Hydrogen Bond
	A:5:GLA:O6	A:363:LYS:NZ	2.76	Hydrogen Bond
Mannose 6	A:6:MAN:C6	A:365:TRP:CE3	3.81	Hydrophobic
	A:6:MAN:O5	A:363:LYS:NZ	2.83	Hydrogen Bond
	A:6:MAN:O6	A:363:LYS:NZ	3.02	Hydrogen Bond
	A:6:MAN:O6	A:366:GLN:OE1	3.05	Hydrogen Bond
Tyvelose 7				
Rhamnose 8	A:8:RAM:O3	A:880:HOH:O	2.89	Bridged H-Bond
	A:8:RAM:C4	A:359:GLU:CD	3.81	Hydrophobic
	A:8:RAM:C6	A:391:TRP:CD2	3.78	Hydrophobic
	A:8:RAM:C6	A:391:TRP:CE2	3.79	Hydrophobic
	A:8:RAM:C6	A:391:TRP:CE3	3.8	Hydrophobic
	A:8:RAM:C6	A:391:TRP:CZ2	3.86	Hydrophobic
	A:8:RAM:C6	A:391:TRP:CZ3	3.84	Hydrophobic

	A:8:RAM:C6	A:391:TRP:CH2	3.87	Hydrophobic
	A:8:RAM:O1	A:392:ASP:OD2	2.63	Hydrogen Bond
	A:8:RAM:O2	A:395:ASP:OD2	2.67	Hydrogen Bond
	A:8:RAM:O3	A:363:LYS:NZ	3.17	Hydrogen Bond
	A:8:RAM:O3	A:366:GLN:OE1	3.14	Hydrogen Bond
	A:8:RAM:O3	A:395:ASP:OD2	2.75	Hydrogen Bond

Figure 15.1.1: Electron density for *S*. Paratyphi Paratose3 in the binding site at one σ electron density. The sugar is well resolved.

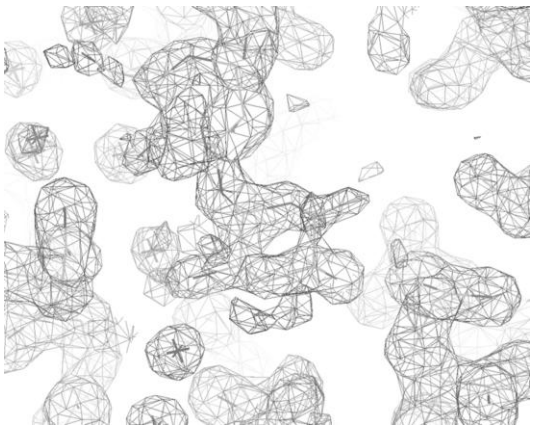

15.2 Supplement for Tail morphology controls Lipopolysaccharide triggered DNA release

Table 15.3: 9NA TSP Diffraction data collection and refinement statistics

	9NATSP ΔN[a]
Data collection	
Space group	$I2_13$
Unit cell / Å	a = 149.1
Resolution / Å	33.3 – 1.50 (1.54 – 1.50)
$R_{r.i.m.}$ [%][b]	7.1(75.5)
Completeness / %	99.7 (99.9)
<I/σ(I)>	15.6 (2.6)
Redundancy	4.6 (1.1)
Unique reflections	87485 (6455)
Solvent content / %	47.6
Monomers in asymmetric unit	1
Model refinement	

R_{work} / R_{free} / %[c]	12.8 / 17.1
Water molecules	722
Average *B* / Å²	19.4
R.m.s.d. bonds / Å	0.015
R.m.s.d. angles / Å	1.47
Ramachandran statistics	
Favored (%)	96.8
Allowed (%)	3.2
Outlier (%)	0

[a]Values in parentheses are for the outer resolution shell.

[b]$R_{r.i.m.} = 100\Sigma_h [n / [n\text{-}1)]^{1/2} \Sigma_i |I_i(h) - \langle I(h)\rangle| / \Sigma_h \Sigma_i I_i(h)$, where *n* is the multiplicity of observations.

[c]$R_{work} = \Sigma ||F_o| - |F_c|| / \Sigma |F_o|$, where F_o and F_c are the structure factor amplitudes from the data and the model, respectively. R_{free} is R_{work} using a 5% test set of structure factors.

Table 15.4: Comparison of oligosaccharide interacting residues in 9NA and P22TSP
Residues within 5 Å distance of the *Salmonella* Typhimurium octasaccharide bound to P22TSP (pdb code 1tyx) compared to structurally equivalent positions in 9NATSP (pdb code 3riq) after superimposition of Cα positions. Major changes are boxed.

Residue in P22TSP (1TYX)	Residue in 9NATSP (3RIQ)	Remarks
Val 236	Val 256	
Val 240	His 259	
Leu 283	Leu 299	
Arg 285	Thr 301	H-bond missing
Asp 303	Glu 318	
Gly 304	Gly 320	
Thr 307	Thr 323	
Glu 309	Glu 324	
Leu 311	His 326	
Val 331	Gly 347	Hydrophobic contact missing
Ser 332	Ser 348	
Gln 335	Leu 351	H-bond missing
Leu 337	Ile 353	
Glu 359	Glu 375	Catalytic site
Lys 363	Lys 379	

Trp 365	Tyr 381	
Gln 366	Gln 382	
Val 369	Ile 385	
Gly 370	Gly 386	
Trp 391	Tyr 407	
Asp 392	Asp 408	Catalytic site
Asp 395	Asp 411	Catalytic site
Thr 400	Thr 416	Different side chain rotamer

So long, farewell, auf Wiedersehen, good bye!

Thank you –

Robert Seckler for his support during this project, for the possibility to attend many international conferences and for giving me scientific freedom.

Stefanie Barbirz for introducing me into the international scientific community, for your advice, feedback and many valuable discussions.

Wolfgang Rabsch for opening a new perspective on microbiology and for access to the impressive microbe collection at the Robert Koch Institute.

Ulrich Gohlke for the introduction and help in crystallography.

The FASEB Conference on Microbial Polysaccharides of Medical/Agricultural and Industrial Importance 2008 for sparking an endless source of lipopolysaccharide enthusiasm. Especially Prof. Otto Holst whom I met on many conferences and always taught me something new.

Likewise, the Phage and Virus Assembly meeting community for doing so with bacteriophages. Especially Prof. Ian Molineux and Prof. Roger Hendrix for discussing new aspects in this work.

All funding agencies that supported to travel to conferences: Federation of European Microbiological Societies, Potsdam Graduate School and The Biochemical Society.

The Leibniz Graduate School of Molecular Biophysics for a lot of great meetings.

Christin Hanke for taking challenges and for your delight in working.

Carolin Doering for standing as solid as a rock.

Nina Kristin Bröker for clear scientific discussions and for open words.

Karolin Heinle for many crucial discussions especially at the beginning of my thesis.

Roland Knorr for not giving up on lipopolysaccharide GUVs.

Sabine Kaltofen for balancing everything.

Simone Brockman, Mandy Schietke, Sibylle Rüstig and Jana Kramer for reliable and solid technical assistance.

All my recent and past colleagues for advice and support and for countless coffees (and cakes).

Ingolf Behr for his lack of understanding for too long science nights, for too many worked through weekends and license number plates imprinted with P-BC-22: it always kept me down-to-earth.

My parents for supporting and encouraging me, my brother for spurring me and my grandparents for their trust in my scientific outcome.

Erklärung

Hiermit versichere ich, dass ich die vorliegende Arbeit selbstständig angefertigt und keine anderen als die angegebenen Quellen und Hilfsmittel verwendet habe. Ich versichere weiterhin, dass alle anderen Werken wörtlich oder inhaltlich entnommenen Stellen als solche gekennzeichnet wurden.
Die Arbeit wurde bisher keiner anderen Prüfungsbehörde vorgelegt.

Potsdam, den 15. November 2011

(Dorothee Andres)